

Energy Performance Modeling of Buildings with Directional Reflective Roofs

Hamid Reza Hooshangi

A Thesis
in
The Department
of
Building, Civil, and Environmental Engineering

Presented in Partial Fulfillments of the Requirements
for the Degree of Master of Applied Science at
Concordia University
Montreal, Quebec, Canada

July, 2015

© Hamid Reza Hooshangi, 2015

CONCORDIA UNIVERSITY

School of Graduate Studies

This is to certify that the thesis prepared

By: Hamid Reza Hooshangi

Entitled: Energy Performance Modeling of Buildings with Directional Reflective Roofs

and submitted in partial fulfillment of the requirements for the degree of:

Master of Applied Science (Building Engineering)

Complies with the regulations of the University and meets the accepted standards with respect to originality and quality.

Signed by the final examining committee:

<u>Dr. Fariborz Haghighat</u>	Chair
<u>Dr. Ali Dolatabadi</u>	Examiner
<u>Dr. Leon Wang</u>	Examiner
<u>Dr. Hashem Akbari</u>	Supervisor

Approved by _____
Chair of Department or Graduate Program Director

_____ 2015 _____
Dean of Faculty

Title: Building Energy Modeling of Directional Reflective Materials (DRMs) Using DOE-2.1E

Author: Hamid Reza Hooshangi

Abstract

Solar reflectance of most diffused flat surfaces is fairly constant for all daylight hours except early in the morning and late in the afternoon. Hence, most standards rate and label the reflectance of roofing surfaces with a single value. However, some newly developed roofing materials, called directional reflective materials (DRMs), are designed to have dependent reflectance on incident sunlight angle.

The Cool Roof Rating Council (CRRC) has investigated several approaches to label DRMs and have selected a single reflectance. However, the performance of the labelling approaches to estimate HVAC energy consumption of buildings has not been investigated yet.

In this study, an algorithm to simulate the mean hourly reflectance of DRM roof is developed using DOE-2.1E program. Afterwards, the HVAC energy consumption of building is simulated based on the calculated hourly solar reflectance. In addition, DOE-2 simulations were performed using the reflectance calculated by several labeling approaches, and their effects in predicting cooling, heating and total HVAC energy consumption of a building with DRM roof is assessed.

The results indicated that the selected approach by CRRC (M2) is the most accurate model to represent the reflectance of DRMs. It has the most accuracy in estimating annual space cooling energy by an estimation difference of 1.7% (0.92 kWh/m²) in Houston, 1.1% (0.32 kWh/m²) in Sacramento and 1.8% (0.2 kWh/m²) in Montréal. M2 overestimates the space heating energy by overestimating reflectance of DRMs during winter. It tends to overestimate the annual space heating energy by as much as 1.8% (0.12 kWh/m²) in Houston, 0.5% (0.1 kWh/m²) in Sacramento and 0.3% (0.38 kWh/m²) in Montréal.

Acknowledgement

I would like to express my sincere gratitude to my supervisor, Professor Hashem Akbari, for his guidance and valuable advices and constant support during this research.

This research was in part funded by a grant from the Cool Roof Rating Council (CRRC) and a scholarship from the Huntsman Corporation. The authors appreciate their support throughout this project.

I also thank my colleagues Dr. Ali G. Touchaei, Dr. Hatef Aria, Mr. Mir Ata Hosseini, Mr. Farhad Mofidi and Mrs. Zahra Jandaghian for their help along the way.

Contents

List of Figures	VII
List of Tables	IX
List of Symbols	XII
List of Acronyms	XIII
1 Introduction.....	1
1.1 Benefits and impacts of cool roofs.....	1
1.2 Standards for measuring solar reflectance of roofing materials.....	2
1.3 Objectives of this research	3
1.4 Approach	3
2 Literature review	5
2.1 Cool roofs; advantages and impacts.....	5
2.2 Standards for measuring solar reflectance and labelling cool roof materials	8
2.2.1 Homogenous and variegated cool roof materials.....	8
2.2.2 Directional reflective roofing materials	9
2.3 Summary	15
3 Methodology	17
3.1 Building energy simulation programs	17
3.1.1 DOE-2.1E.....	17
3.1.2 TRNSYS	18
3.1.3 EnergyPlus	18
3.2 Selected simulation program.....	19
3.2.1 Algorithm of heat transfer in DOE-2	20
3.2.2 Solar calculations in DOE-2	22
3.3 Properties of simulated DRM sample	26
3.3.1 Reflectance variation of DRM as a function of incident solar radiation angle.....	26
3.3.2 Applying labelling approaches	28
3.4 Simulating DRM reflectance in DOE-2.1E	30
3.5 Outdoor climates	33
3.6 Prototypical building characteristics	36
3.6.1 HVAC sizing procedure.....	40
3.7 Summary	40
4 Simulated heating and cooling energy use.....	42
4.1 Building HVAC energy consumption in Houston	43

4.2	Building HVAC energy consumption in Sacramento	54
4.3	Building HVAC energy consumption in Montréal	64
4.4	Peak demand estimation.....	72
4.5	Discussion	73
5	Summary and conclusion.....	78
5.1	Future work	80
5.2	Contribution	81
5.3	Publications	81
	Bibliography	83
	Appendix A: Requirements of standards for cool roofs	88
	Appendix A.1: ASHRAE Standard 90.1	88
	Appendix A.2: ASHRAE Standard 90.2	89
	Appendix A.3: International energy conservative code.....	89
	Appendix A.4: California energy commission's Title 24.....	90
	Appendix A.5: Energy Star for roof products.....	91
	Appendix A.6: Cool-roof provisions in other standards and programmes	92
	Appendix B. Cool roof solar reflectance measurement process	94
	Appendix C. Monthly result of HVAC energy consumption	96
	Appendix D. The FORTRAN code for finding hourly projected incident solar angle on the roofing surface	121

List of Figures

Fig. 2-1. Image of a DRM sample from two opposite angles, (a) sky view and (b) street view.	7
Fig. 2-2. Reflectance of variegated asphalt shingle for different zenith angles (Hooshangi et al., 2015).	9
Fig. 2-3. Effect of materials properties on solar reflectance distribution of DRM ($R_{ref}=0.9$ and $R_{abs}=0.04$). (a) corrugation angle of 120 and 140 degrees, (b) reflectance of reflective or absorptive sides (Akbari & Touchaei, 2014).	10
Fig. 2-4. Symmetric solar reflectance distribution of DRMs under AM1GH condition. The y axis represents the surface azimuth, x axis shows the light source zenith angle, and, z axis is amount of solar reflectance (Akbari & Touchaei, 2014).	12
Fig. 2-5. labeling approaches and metrics	14
Fig. 3-1. DOE-2 flowchart (DOE-2 official website).	20
Fig. 3-2. DOE-2.1E Cartesian coordinate systems to calculate solar incident angle.....	24
Fig. 3-3. Defined coordinate systems; “xz” plane is vertically perpendicular to the DRM surface	25
Fig. 3-4. Variation of solar reflectance and projected incident angle for DRM with $R_{abs}=0.15$, $R_{ref}=0.80$ and corrugation angle = 120° (AM1GH solar spectral irradiance) (Akbari & Touchaei, 2014)	27
Fig. 3-5. The method of defining projected incident angle. $\alpha=0^\circ$ while the absorptive side is toward a light source and $\alpha=180^\circ$ represents a light source pointing to the reflective side of DRM.	27
Fig.3-6. The maximum, minimum and R20 of considered DRM sample reflectances (Akbari & Touchaei, 2014)	29
Fig.3-7. Reflectance values regarding to the labelling approached for simulated DRM sample .	30
Fig.3-8. Variation of projected incident angle and solar reflectance for 45° tilted surface, 21st of January, Houston. Surfaces toward (a) South, (b) East, (c) North and (d) West.....	32
Fig.3-9. Variation of projected incident angle and solar reflectance for 45° tilted surface, 21st of July, Houston. Surfaces toward (a) South, (b) East, (c) North and (d) West.....	33
Fig.3-10. Houston meteorological data from TMY3, (a) temperature range in degrees, (b) mean hourly solar radiation (Wh/m ²) (Ligget & Milne, 2008).....	34
Fig. 3-11. Sacramento meteorological data from TMY3, (a) temperature range in degrees, (b) mean hourly solar radiation (Wh/m ²) (Ligget & Milne, 2008).....	35
Fig. 3-12. The flowchart regarding to processes through DOE-2.1E to consider hourly solar reflectance of DRM sample	41

Fig. 4-1: Annual HVAC energy consumption and annually estimation difference of the labeling approaches (M1 to M5) to estimate $Q_{\text{Hourly R}}$. The building is located in Houston with tilt angle of 26.6° ; building azimuth of (a) zero degree, (b) 45° and (c) 90°	48
Fig. 4-2: Annual HVAC energy consumption and annually estimation difference of the labeling approaches (M1 to M5) to estimate $Q_{\text{Hourly R}}$. The building is located in Houston with tilt angle of 45° ; building azimuth of (a) zero degree, (b) 45° and (c) 90°	49
Fig. 4-3: The estimation difference of the labelling approaches in estimating annual HVAC energy consumption of (a) space cooling, (b) space heating and (c) total HVAC energy consumption in Houston. Minimum, 1st quartile, median, 3rd quartile and maximum amount of the percent error of the labelling approaches. The mean is shown as the circle marker.....	53
Fig. 4-4: Annual HVAC energy consumption and estimation difference between simulations with hourly reflectance and labeling approach reflectances (M1 to M5), for prototype in Sacramento with tilt angle of 26.6° ; building azimuth of (a) zero degree, (b) 45° and (c) 90°	59
Fig. 4-5: Annual HVAC energy consumption and estimation difference between simulations with hourly reflectance and labeling approach reflectances (M1 to M5), for prototype in Sacramento with tilt angle of 45° ; building azimuth of (a) zero degree, (b) 45° and (c) 90°	60
Fig. 4-6: The estimation difference of labeling approaches in estimating annual HVAC energy consumption of (a) space cooling and (b) space heating and (c) total HVAC energy consumption in Sacramento. Minimum, 1st quartile, median, 3rd quartile and maximum amount of percent error of each approach. The mean is shown as circle marker.....	62
Fig. 4-7: Annual HVAC energy consumption and estimation difference between simulations with hourly reflectance and labeling approach reflectances (M1 to M5), for prototype in Montréal with tilt angle of 26.6° ; building azimuth of (a) zero degree, (b) 45° and (c) 90°	68
Fig. 4-8: Annual HVAC energy consumption and estimation difference between simulations with hourly reflectance and labeling approach reflectances (M1 to M5), for prototype in Montréal with tilt angle of 45° ; building azimuth of (a) zero degree, (b) 45° and (c) 90°	69
Fig. 4-9: The estimation difference of labeling approaches in predicting annual HVAC energy consumption of (a) space cooling and (b) space heating and (c) total HVAC energy consumption in Montréal. Minimum, 1st quartile, median, 3rd quartile and maximum amount of percent error of each approach. The mean is shown as circle marker.....	71
Fig. 4-10: Estimation difference of labeling approaches in estimating annual HVAC energy consumption of (a) space cooling and (b) space heating and (c) total HVAC energy consumption in all the considered locations. Minimum, 1st quartile, median, 3rd quartile and maximum amount of estimation difference of each approach. The mean is shown as circle marker.	75

List of Tables

Table 3-1. New and old single-family residential prototype characteristics	37
Table 3-2. Size of HVAC systems	40
Table 4-1: The simulated cases of residential building	42
Table 4-2: Annual energy consumption of HVAC system (kWh) in Houston, roof tilt angle of 26.6° and building azimuth of zero degree.....	44
Table 4-3: Annual energy consumption of HVAC system (kWh) in Houston, roof tilt angle of 26.6° and building azimuth of 45°	44
Table 4-4: Annual energy consumption of HVAC system (kWh) in Houston, roof tilt angle of 26.6° and building azimuth of 90°	45
Table 4-5: Annual energy consumption of HVAC system (kWh) in Houston, roof tilt angle of 45° and building azimuth of zero degree.....	45
Table 4-6: Annual energy consumption of HVAC system (kWh) in Houston, roof tilt angle of 45° and building azimuth of 45°	46
Table 4-7: Annual energy consumption of HVAC system (kWh) in Houston, roof tilt angle of 45° and building azimuth of 90°	46
Table 4-8: Monthly cooling and heating energy consumption of HVAC system (kWh), New vintage in Houston, roof tilt angle of 26.6° and building azimuth of zero degree.....	47
Table 4-9: Maximum estimation difference of the labeling approaches in estimating mean (hourly average) cooling and heating energy consumption in Houston	51
Table 4-10: Annual energy consumption of HVAC system (kWh) in Sacramento, roof tilt angle of 26.6° and building azimuth of zero degree	55
Table 4-11: Annual energy consumption of HVAC system (kWh) in Sacramento, roof tilt angle of 26.6° and building azimuth of 45°	56
Table 4-12: Annual energy consumption of HVAC system (kWh) in Sacramento, roof tilt angle of 26.6° and building azimuth of 90°	56
Table 4-13: Annual energy consumption of HVAC system (kWh) in Sacramento, roof tilt angle of 45° and building azimuth of zero degree	57
Table 4-14: Annual energy consumption of HVAC system (kWh) in Sacramento, roof tilt angle of 45° and building azimuth of 45°	57
Table 4-15: Annual energy consumption of HVAC system (kWh) in Sacramento, roof tilt angle of 45° and building azimuth of 90°	58

Table 4-16: Maximum estimation differences of the labeling approaches in estimating mean (hourly average) cooling and heating energy consumption in Sacramento	63
Table 4-17: Annual energy consumption of HVAC system (kWh) in Montréal, roof tilt angle of 26.6° and building azimuth of zero degree	64
Table 4-18: Annual energy consumption of HVAC system (kWh) in Montréal, roof tilt angle of 26.6° and building azimuth of 45°	65
Table 4-19: Annual energy consumption of HVAC system (kWh) in Montréal, roof tilt angle of 26.6° and building azimuth of 90°	65
Table 4-20: Annual energy consumption of HVAC system (kWh) in Montréal, roof tilt angle of 45° and building azimuth of zero degree	66
Table 4-21: Annual energy consumption of HVAC system (kWh) in Montréal, roof tilt angle of 45° and building azimuth of 45°	66
Table 4-22: Annual energy consumption of HVAC system (kWh) in Montréal, roof tilt angle of 45° and building azimuth of 45°	67
Table 4-23: Maximum estimation difference of the labeling approaches in estimating mean (hourly average) cooling and heating energy consumption in Sacramento	70
Table 4-24: Building electricity peak demand (kW) for new vintage in Houston with azimuth of zero degree and tilt angle of 45°	73
Table A-1. Typical minimum cool roof requirements assumed by Title 24	91
Table A-2. ENERGY STAR for roof products (Version 2.0) qualifying criteria (Islands, 2008)	92
Table A- 3. Typical minimum cool roof requirements	93
Table B-1. Summary of standards for measuring solar reflectance	95
Table C-1: Monthly cooling and heating energy consumption of HVAC system (kWh), old vintage in Houston, roof tilt angle of 26.6°	97
Table C-2: Monthly cooling and heating energy consumption of HVAC system (kWh), old vintage in Houston, roof tilt angle of 45°	99
Table C-3: Monthly cooling and heating energy consumption of HVAC system (kWh), new vintage in Houston, roof tilt angle of 26.6°	101
Table C-4: Monthly cooling and heating energy consumption of HVAC system (kWh), new vintage in Houston, roof tilt angle of 45°	103
Table C-5: Monthly cooling and heating energy consumption of HVAC system (kWh), old vintage in Sacramento, roof tilt angle of 26.6°	105

Table C-6: Monthly cooling and heating energy consumption of HVAC system (kWh), old vintage in Sacramento, roof tilt angle of 45°	107
Table C-7: Monthly cooling and heating energy consumption of HVAC system (kWh), New vintage in Sacramento, roof tilt angle of 26.6°	109
Table C-8: Monthly cooling and heating energy consumption of HVAC system (kWh), New vintage in Sacramento, roof tilt angle of 45°	111
Table C-9: Monthly cooling and heating energy consumption of HVAC system (kWh), Old vintage in Montréal, roof tilt angle of 26.6°	113
Table C-10: Monthly cooling and heating energy consumption of HVAC system (kWh), Old vintage in Montréal, roof tilt angle of 45°	115
Table C-11: Monthly cooling and heating energy consumption of HVAC system (kWh), New vintage in Montréal, roof tilt angle of 26.6°	117
Table C-12: Monthly cooling and heating energy consumption of HVAC system (kWh), New vintage in Montréal, roof tilt angle of 45°	119

List of Symbols

Symbol	Unit	Definition
q_{out}	$\frac{Btu}{hr}$	Heat flow through the inside roof surface
q_1	$\frac{Btu}{hr}$	Hourly solar energy absorbed by the surface
q_2	$\frac{Btu}{hr}$	Hourly combined convective heat transfer and radiation heat exchange between the surface and outside air
q_3	$\frac{Btu}{hr}$	Net radiation heat exchange between roof and sky
SOLI	-	Solar radiation incident on outside roof surface from direct, diffuse, and reflected radiation
SURABSO	-	Solar absorptance of wall or roof outside surface
FILMU	-	Combined radiative and convective film coefficient
DBRT	°F	Outside air temperature
β	degree	Solar altitude angle (above the horizontal)
ϕ	degree	Solar azimuth angle
L_{st}	degree	Standard meridian
L_{loc}	degree	Longitude
E	-	Equation of time
H	degree	Hour angle
δ	degree	Solar declination angle
SAZM	degree	Solar azimuth angle (measured clockwise from south)
SALT	degree	Solar altitude
THSNHR	degree	Solar azimuth angle (measured clockwise from north)
PHSUND	degree	Solar altitude angle (above horizon)
ψ	degree	Surface azimuth angle (measured clockwise from north)
Σ	degree	Tilt angle

List of Acronyms

Abb.	Full name
AM1GH	Air Mass 1, Global Horizontal standard solar irradiance condition
ASHRAE	American Society of Heating, Refrigerating and Air Conditioning Engineers
COP	Coefficient Of Performance
CRRC	Cool Roof Rating Council
DOE	Department OF Energy
DRM	Directional Reflective Materials
Emittance	Thermal Emittance
GHG	Greenhouse Gas
Hourly R	Hourly Solar Reflectance
HVAC	Heating, Ventilation and Air Conditioning
M1, M2 ... M5	Metrics, labeling approaches
NREL	National Renewable Energy Laboratory
PNNL	Pacific Northwest National Laboratory
Reflectance	Solar Reflectance
TMY	Typical Meteorological Year

1 Introduction

1.1 Benefits and impacts of cool roofs

Roofing surfaces with a high thermal emittance (surface emissivity averaged over the thermal spectrum, about 10 micron) and low solar absorptance (surface absorptivity over the solar spectrum, 250-2500 nm) are called 'cool roofs'. Because of high solar reflectance, cool roofs experience lower daytime temperature compared to dark roofs. The roof temperature reduction by 10-13°C was measured by Konopacki et al. (1998) after installing cool roofs on several buildings in California.

Consequently, cool roofs offer energy savings during cooling season by reducing the heat flux through the roof. Akbari et al. (1992) found that high albedo-coated roofs can reduce cooling energy by 40-50%, and peak power cooling energy by 30-40% in a school in Sacramento, CA.

In addition to power demand reduction, cool roofs have many environmental benefits. They can lead to local air temperature decrease, urban heat island mitigation, air quality improvement and smog reduction (Akbari & Levinson, 2008; Synnefa et al., 2008). For instance, increasing the albedo of roofs in Montréal from 0.2 to 0.8 reduces the average temperature of urban areas by 0.3°C (Akbari & Touchaei, 2013). Also, slowing climate change can be achieved with reflecting more sunlight to the space by cool roofs (Levinson & Akbari, 2010). Additionally, less thermal stress in cool roofs can lessen the maintenance and increase lifetime of roofing products (Akbari et al., 2001).

On the other hand, cool roofs can induce heating penalty during the wintertime. Hosseini & Akbari (2014) used DOE-2.1E to simulate the energy consumption of office and retail buildings in four cold cities in North America. Their results showed annual heating penalties of up to 23 MJ/m² for cool roof versus dark roof in Anchorage, Synnefa et al. (2007), through simulation studies for various climatic conditions, demonstrated that increasing roof reflectance by 0.45 causes heating penalty by 0.2-17 kWh/m².

A major portion of solar irradiance belongs to visible (42%) and invisible near-infrared (52%) spectrums. Light surfaces, particularly white homogeneous roofing materials, have a high solar reflectance in visible and NIR bands. Nevertheless, using white roofs may adversely affect the aesthetical appeal of buildings. So most of the owners of pitched roofs prefer non-white roofing materials (Synnefa et al., 2007) (Levinson et al., 2007)

These impacts can be addressed by a new innovative technology, called directional reflective materials (DRMs). These products have two sides: light (reflective) side toward the sky and absorptive (dark) side directed towards the ground level. Therefore, DRMs have high solar reflectances throughout summer when sun is high, and high solar absorptance during winter while sun is low. Not only will DRMs eliminate the negative effect of homogenous cool roofs during winter, but they potentially can reduce heating load. Further investigation of the effect of DRMs on heating energy is desirable. In addition, issues regarding to aesthetical appearance of buildings are addressed by using dark colors on absorptive side of DRMs.

1.2 Standards for measuring solar reflectance of roofing materials

There are several codes and standards that suggest methods for measuring solar reflectance of homogenous and colored (variegated) cool roofs (Appendix A). The solar reflectance of homogeneous or variegated roofing materials is approximately uniform in all directions of light source, i.e. sun. In other words, reflectance of homogeneous or variegated roofing materials is not a function of sun zenith angle. As a result, only one initial solar reflectance for each roofing surface is assigned by current standards.

The reflectance of DRMs is strongly dependent on incident sunlight angle. Consequently a method needs to be defined to estimate the optical performance of DRMs accurately. This method should have following characteristics: (1) accurate estimation of heat absorption of the roof, (2) easy to label by manufacturers, (3) intuitive for customers to choose, and (4) simple for modelers to utilize.

Akbari & Touchaei (2014) investigated five labeling approaches. Three of these labeling approaches assigned one reflectance for DRMs for a whole year. Other approaches considered the seasonal reflectance (one reflectance for summer, one reflectance for winter and the mean value of these numbers for the other seasons). Akbari & Touchaei (2014) analyzed the accuracy of each approach in estimating the mean hourly and peak heat absorption of DRM samples.

Cool Roof Rating Council (CRRC) investigated the proposed labeling approaches. CRRC accepted one of the labeling approaches as a method for labeling DRMs. However, Akbari & Touchaei (2014) did not explore the accuracy of the labeling approaches on estimating HVAC energy consumption of buildings.

1.3 Objectives of this research

The first objective of this research is to model DRMs incorporated with DOE-2.1E building energy analysis program. In this model the energy consumption of building HVAC system can be simulated while the reflectance of roof (DRM surface) is changed hourly.

Comparing the labeling approaches investigated by Akbari & Touchaei (2014) with hourly solar reflectance model, based on the heating and cooling energy consumption of HVAC system is the second goal of this work. The comparisons on single family residential building prototypes located in Houston (TX), Sacramento (CA) and Montréal (QC) are performed.

1.4 Approach

This thesis is organized in four chapters in addition to this introduction (chapter 1). Chapter 2 presents a review of related literature on cool roof products and their benefits and impacts. This is followed by the methods for measuring solar reflectance of different types of cool roofs (i.e. homogenous and heterogeneous variegated materials). Then an innovative cool roof technology, called directional reflective materials (DRMs), and its advantageous compared to other cool roof products is

introduced. The papers relevant to DRMs and their optical properties are reviewed. Finally, methods for labeling solar reflectance of DRMs are discussed.

Chapter 3 discusses the methodology applied to achieve the research objectives. The first part is a summary of the three widely used building energy simulation software. The second section of chapter 3 discusses the particular simulation software (DOE-2.1E) that was used to reach to our first goal. A discussion of the algorithm that developed to obtain mean hourly solar reflectance of roof incorporated with simulation software is presented. Then, the optical properties and the method of labeling DRMs is discussed. Chapter 3 also highlights the characteristics of simulated building prototypes.

Chapter 4 provides the complete results of monthly and annual energy consumption of HVAC system. The first three sections explain the results of each location based on the simulations with mean hourly solar reflectance and annual or seasonal reflectances. This chapter concludes with a discussion about the accuracy of labeling approaches in estimating thermal performance of DRMs.

Chapter 5 consists of a summary and conclusion continued by references and two appendices. It provides a brief overview of simulation results and a comparison of the accuracy of the different labeling approaches.

2 Literature review

2.1 Cool roofs; advantages and impacts

High solar reflection and high thermal emittance are the principal characteristics of cool roof surfaces. These features reduce the heat transfer through the roof. Consequently it decreases cooling energy use, and increases comfort in unconditioned buildings (Akbari H. , 2005) (Levinson & Akbari, 2010). Akbari et al. (1992) found that high albedo coated roofs can reduce cooling energy (40-50%) and peak power cooling energy (30-40%) in Sacramento, CA. A simulation study was carried out by Synnefa et al. (2007) to evaluate the effect of cool roofs on cooling and heating energy demand of residential buildings for various climate conditions. The results showed that increasing solar reflectance of a roof by 0.65 (from base case of 0.2), reduced cooling load by 8-48 kWh/m², depending on the location of building. The simulation study by Taha et al. (1996) also indicated 20-40% saving during peak cooling times in residential area of Los Angeles Basin.

Moreover, less thermal stress in cool roofs can lessen the maintenance and increase lifetime of products (Akbari et al., 2001). Cool roofs also have many environmental benefits, such as lowering local air temperature, leading to better air quality and reducing smog. Also, they are slowing climate change by reflecting more sunlight to the space (Levinson & Akbari, 2010).

Most of the cool roof materials have high solar emissivity (above or near 0.9). Therefore increasing the solar reflectance of roofing materials is the major part of current researches in this field. Major portion of solar irradiance belongs to visible (42%) and invisible near-infrared (52%) spectrums. So white surfaces with high NIR reflected basecoats are the coolest type of roofing surfaces. There are currently a variety of homogeneous roof surfaces with cool white or light colors in market including metal roofs, conventional asphalt shingles with white granules, reflective clay tiles and coated concrete tiles (Synnefa, et al., 2007). However, because of aesthetic appeal of buildings, most of homeowners prefer not to have white roofs. So it limits the application of white roofing surfaces (Levinson, et al., 2007).

Furthermore, lower surface temperature of cool roof surfaces may increase the potential of moisture accumulation in roofing assembly (Ahrab & Akbari, 2013). Rose (2007) measured the surface temperature of a white roof assembly which was defected because of moisture accumulation. The surface temperature was measured 5-7°C colder than outdoor air. In cold climates, the low temperature on the underside of cool roofs reduce the drying potential. Moreover, clear skies during the night may lead the temperature to drop below the dew point. Thus, high moisture accumulation and mold growth problems are caused by higher solar reflectance and thermal emittance of cool roofs (Ahrab & Akbari, 2013).

Also, because of lower solar absorption, higher heating energy may be expected (Akbari et al., 2001). Akbari and Taha (1992) studied the impacts of white surfaces on walls and roof on cooling and heating energy consumption of buildings in four Canadian cities (Montréal, Edmonton, Toronto and Vancouver). They increased the reflectance of walls and roofs from albedo of 0.3 to 0.5 to evaluate the effect of whitening on energy consumption. Their results indicated that heating penalty caused by cool exterior surfaces is 0.2% or 0.1GJ/year. Synnefa et al. (2007), through simulation studies for various climatic conditions, demonstrated that increasing roof reflectance by 0.45 causes heating penalties by 0.2-17 kWh/m². Also, they estimated the annual heating load increment of 4% (0.7 kWh/m²) for the insulated buildings. Hosseini & Akbari (2014) used DOE-2.1E to simulate the energy consumption of office and retail buildings in four cold cities in North America. Their results showed heating penalty of up to 2300 MJ/100 m² for cool roof versus dark roof in Anchorage, AK.

Final concern of applying reflective surfaces on roofs (or walls) is related to the closely packed building areas. The reflected sunlight from roof can be absorbed by other buildings and increase their cooling energy (Sakai et al., 2012).

Research has been performed to investigate and solve the disadvantages of cool roofs. Levinson et al. (2007) recommend a novel technique to produce variegated surfaces with dark appearance and high solar reflectance. They proposed materials with

two layers of spray coatings for producing non-white cool concrete tile and asphalt shingle. First layer is consist of a thin white basecoat with high absorption in wavelengths shorter than 500 nm, strongly scattering in 500-2000 nm, and moderately absorbing at wavelengths higher than 2000 nm. The second layer is a colored topcoat with weak NIR absorption.

Recently, a new technology called directional reflective materials (DRMs) is introduced that can solve most of the concerns regarding to cool roofs. First of all, these materials (Fig. 2-1) have different appearance from the sky and the street. They have absorptive side toward the street and reflective side toward the sky. So, the issue regarding to aesthetic view of building is addressed by using dark colors in absorptive side. Secondly, the reflective side has high solar reflectance so it reflects the sunlight during summer while the sun is high in the sky. In addition, during winter that sun is low in the sky, most of the sunlight is absorbed by the absorptive side of DRMs. Hence, this characteristic can reduce the heating energy penalty during winter.

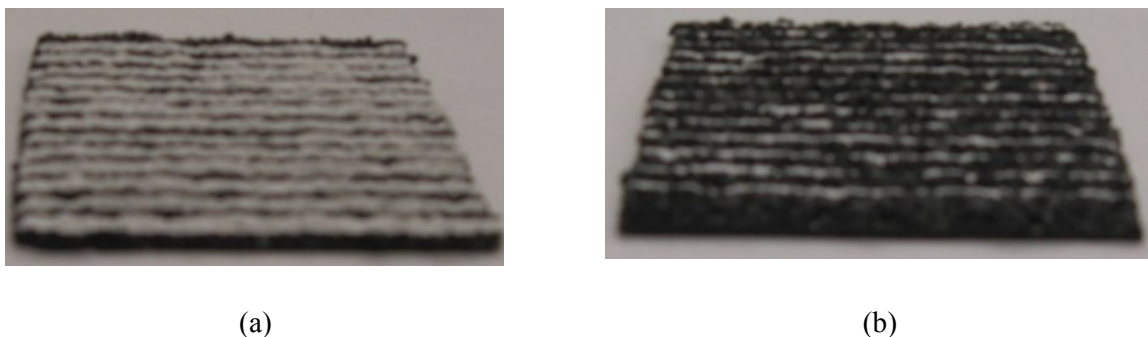


Fig. 2-1. Image of a DRM sample from two opposite angles, (a) sky view and (b) street view.

Recently, using retro-reflective materials on cool roofs are being suggested by several studies (Sakai et al. (2012), Masatoshi et al. (2013) and Yuan et al. (2012)). The retro-reflective materials are specially engineered surfaces that reflect the incident light back towards its source (sun). Applying retro-reflective materials on reflective side of DRMs can significantly reduce the diffuse reflection toward the surrounding buildings.

2.2 Standards for measuring solar reflectance and labelling cool roof materials

2.2.1 Homogenous and variegated cool roof materials

The advantages of cool roofs on energy saving, peak power demand decrease, air quality improvement, GHG emission reduction, and heat island effect mitigation lead to prescribing them in many standards of buildings (Akbari & Levinson, 2008). There are several instruments and standards for measuring and labelling solar reflectance and thermal emittance of roofing materials (Appendix A). To measure solar reflectance of roofing materials, pyranometer, portable solar reflectometer and spectrophotometer are widely used (Appendix B).

ASTM E903: Standard Test Method for Solar Absorptance, Reflectance, and Transmittance of Materials Using Integrating Spheres (2012), provides a procedure for measuring near-normal beam-hemispherical spectral reflectance using a spectrophotometer equipped with an integrating sphere.

ASTM E1918-06: Standard Test Method for Measuring Solar Reflectance of Horizontal and Low-Sloped Surfaces in the Field (2006), uses a pyranometer for measuring global solar reflectance of flat or rough horizontal and low sloped surfaces with area of at least 10 m².

Solar reflectance of roofing products are also measured by portable solar reflectometer. Measurements by solar reflectometer can be conducted based on ASTM C1549-09: Standard Test Method for Determination of Solar Reflectance Near Ambient Temperature Using a Portable Solar Reflectometer (2009).

ASTM C1549-09 is applicable for homogeneous samples. Solar reflectance of non-uniform or variegated surfaces cannot be estimated by measuring one spot. Statistical methods are required to apply for estimating solar reflectance, or solar absorptance of variegated roofing materials (Santamouris et al., 2011). CRRC has developed a method, CRRC-1 standard (2012), to measure the solar reflectance of flat (or nearly-flat) variegated roofing materials using C1549-09.

All of the current standards presumed that the solar reflectance of a roofing sample is a function of the material's properties. Therefore, the solar reflectance is uniform in all the directions; in other words, the solar reflectance is constant for different positions of sun. This assumption is practical for homogeneous and variegated surfaces. Fig. 2-2 shows that for different zenith angles the solar reflectance of Santa Fe variegated asphalt shingle is almost constant (Hooshangi et al., 2015).

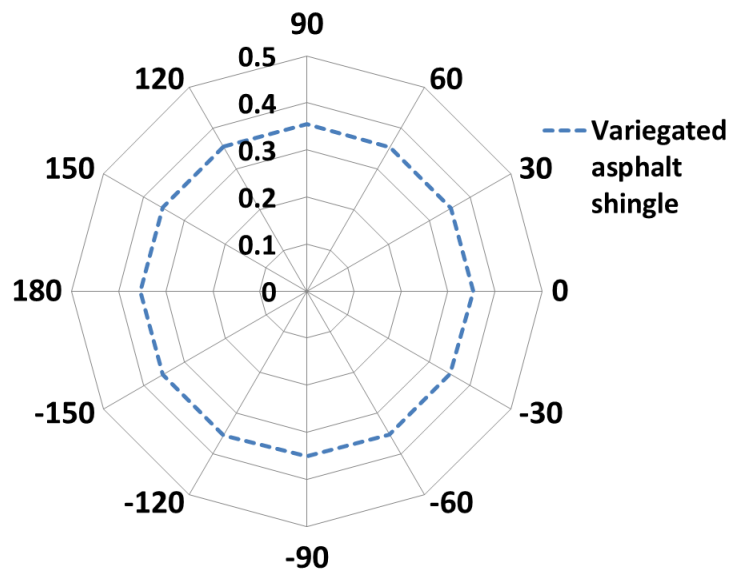
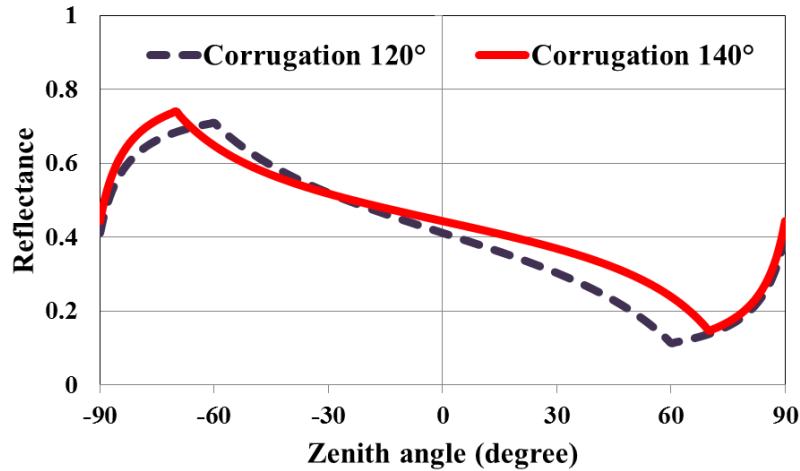


Fig. 2-2. Reflectance of variegated asphalt shingle for different zenith angles (Hooshangi et al., 2015).

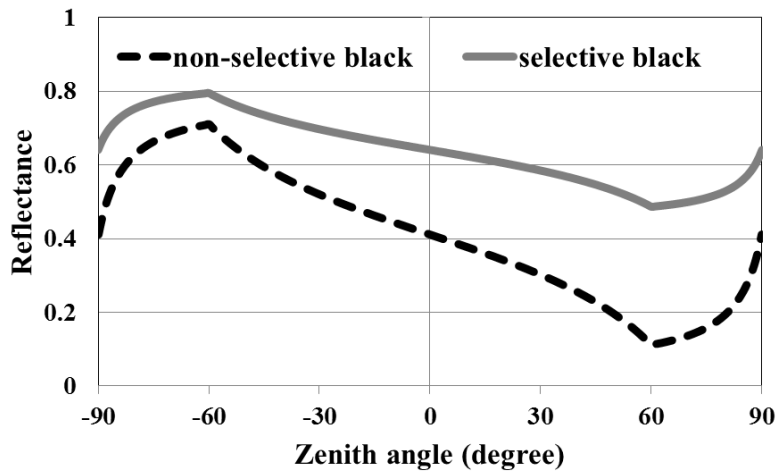
2.2.2 Directional reflective roofing materials

Assuming uniform solar reflectance for DRMs that developed to have high solar reflectance toward the sky but appear dark from streets, is inaccurate. Reflectance of DRMs is not only a function of material properties, it also is a function of solar position with respect to the surface. One class of developed DRMs uses a corrugated surface that has a reflective side and an absorptive side. The material properties of this class of DRMs can be categorized to corrugation angle, reflectance of reflective and absorptive sides and the area of each side. Fig. 2-3 shows the effect of corrugation angle on the DRM with non-selective white ($R=0.9$) on reflective side and non-

selective black ($R=0.04$) on absorptive side. Fig. 2-3 also demonstrates the effect of reflectance of each side on reflectance variation of DRM sample (Akbari & Touchaei, 2014). It can be observed that replacing non-selective black of absorptive side with selective black ($R=0.46$) can significantly increase the solar reflectance distribution of DRM sample.



(a)



(b)

Fig. 2-3. Effect of materials properties on solar reflectance distribution of DRM ($R_{ref}=0.9$ and $R_{abs}=0.04$). (a) corrugation angle of 120 and 140 degrees, (b) reflectance of reflective or absorptive sides (Akbari & Touchaei, 2014).

Akbari and Touchaei (2014) developed a model to calculate the reflectance distribution of DRMs based on their material's properties (i.e. corrugation angle,

reflectance of absorptive and reflective sides and area of each side). First, they calculated the absorptance through dividing the amount of absorbed energy from irradiance (on reflective and absorptive sides) by the amount of global irradiance strikes on the DRM. The summation of absorptance and reflectance for opaque surface must be one. So reflectance can be calculated by applying this principal. Also, they prepared a simulation tool to calculate the reflectance distribution of DRMs with respect to the sun positions.

Absence of the measured data for reflectance of DRMs reasons the authors to estimate the optical performance of DRMs. They assumed that the reflectance distribution of DRM samples under Air Mass 1, Global Horizontal (AM1GH) standard solar irradiance condition can represent the measured data in a laboratory. According to AM1GH condition on clear sky, 89% and 11% of global solar radiation is beam and diffuse solar radiation, respectively (Levinson, Akbari, & Berdahl, 2010).

In addition, they develop a simulation tool to calculate hourly mean solar reflectance and heat absorptance through DRMs. This simulation tool is capable of applying different standard solar irradiances.

The reflectance of DRMs at zenith angle of 20° (towards reflective side) (R_{20}) and average of reflectance distribution (R_{ave}) were being employed for further investigations. R_{ave} is computed as the mean of reflectances (zenith of 0° to 180°). Due to simulating DRM optical performances under AM1GH condition using a tool developed by Akbari & Touchaei (2014) the reflectance is axisymmetric (Fig. 2-4). Therefore, R_{ave} is equal to the average of maximum and minimum of reflectance for zenith angles of 0° to 180° .

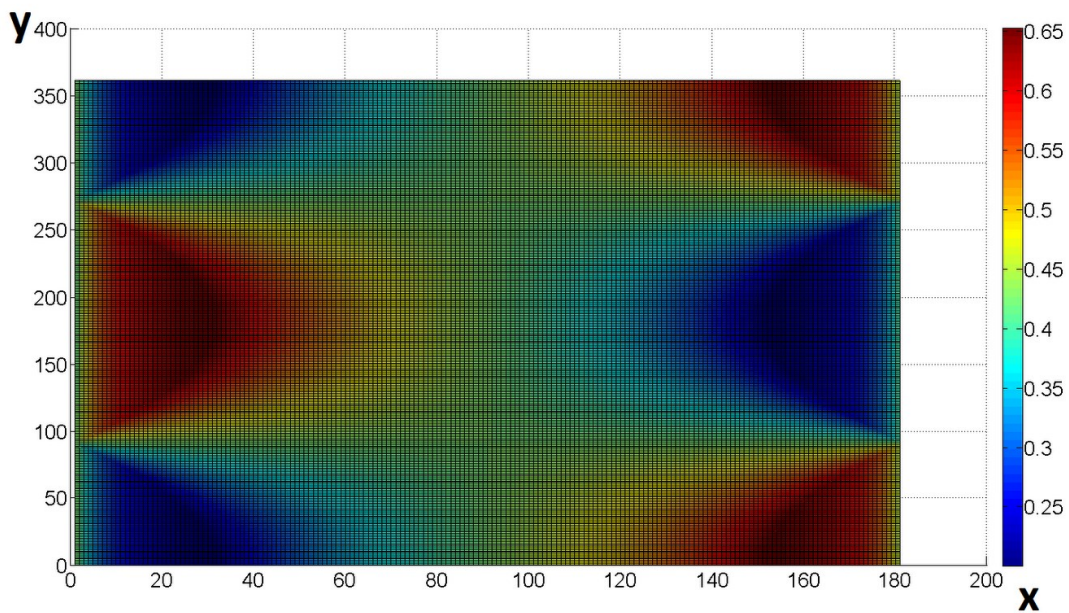
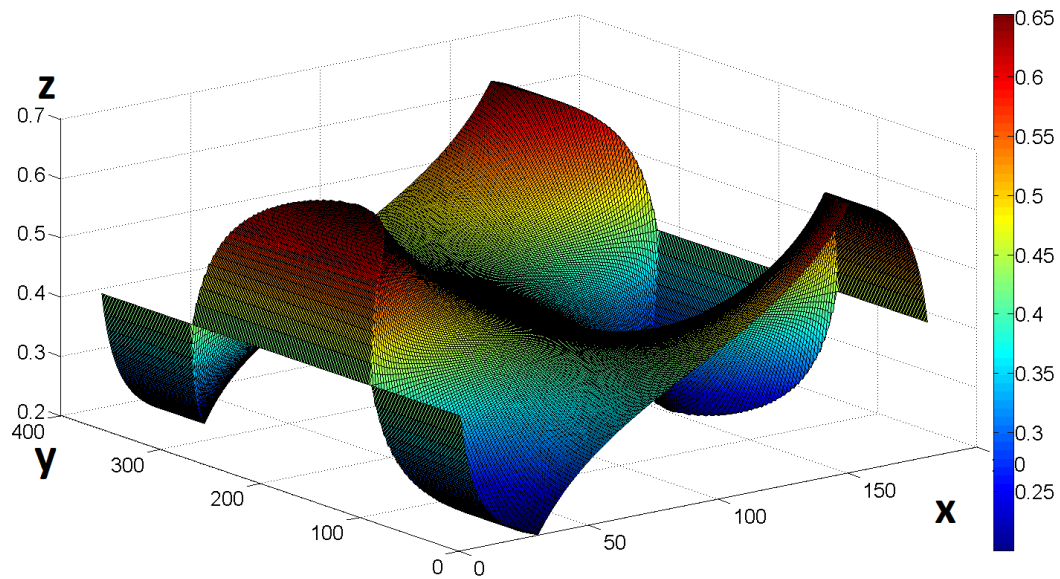


Fig. 2-4. Symmetric solar reflectance distribution of DRMs under AMIGH condition. The y axis represents the surface azimuth, x axis shows the light source zenith angle, and, z axis is amount of solar reflectance (Akbari & Touchaei, 2014).

In addition to this algorithm, i.e. constant proportion of beam to diffuse, we can apply more accurate methods of estimating beam and diffuse solar intensity. To calculate the amount of total, beam and diffuse irradiance that reach to the surface on

the ground, ASHRAE (2007) recommends a method. It proposes using monthly proportions of beam and diffuse irradiances.

Akbari & Touchaei (2014) investigated the performance of DRMs by estimating the hourly mean solar reflectance (or hourly mean solar absorptance) and peak heat absorptance of DRM samples, with respect to the sun position. Based on their results, they proposed two options for labelling approaches. In the *first* option, a simple approach, they assigned a single value to the solar reflectance of DRM for entire of the year.

It is worth to note that the base case for defining and investigating the approaches is related to the 37° latitude (i.e. mid-US mainland). However, Akbari & Touchaei (2014) state that the labelling approaches are applicable for DRMs located in 25° and 49° latitudes, too. According to their analysis, R_{ave} can accurately represent the winter mean reflectance and R_{20} can characterize the summer mean reflectance. They define approach M1 as the single reflectance for the entire year and equal to R_{ave} . Consequently, M1 underestimates the reflectance of DRM during summertime. M2 is designated to represent summer reflectance or R_{20} . Therefore, approach M2 should overestimate the reflectance in wintertime. The approach M3 is defined by a correlation of the annual mean of solar reflectance to R_{ave} .

In the *second* option, they assigned a summer reflectance (R_s), a winter reflectance (R_w), and the average of them for swing seasons reflectance (R_{swing}). M4 is based on the correlation of winter and summer reflectances to R_{ave} . Fig. 2-5 demonstrates the summary of all the investigated and proposed labelling approaches by Akbari & Touchaei (2014).

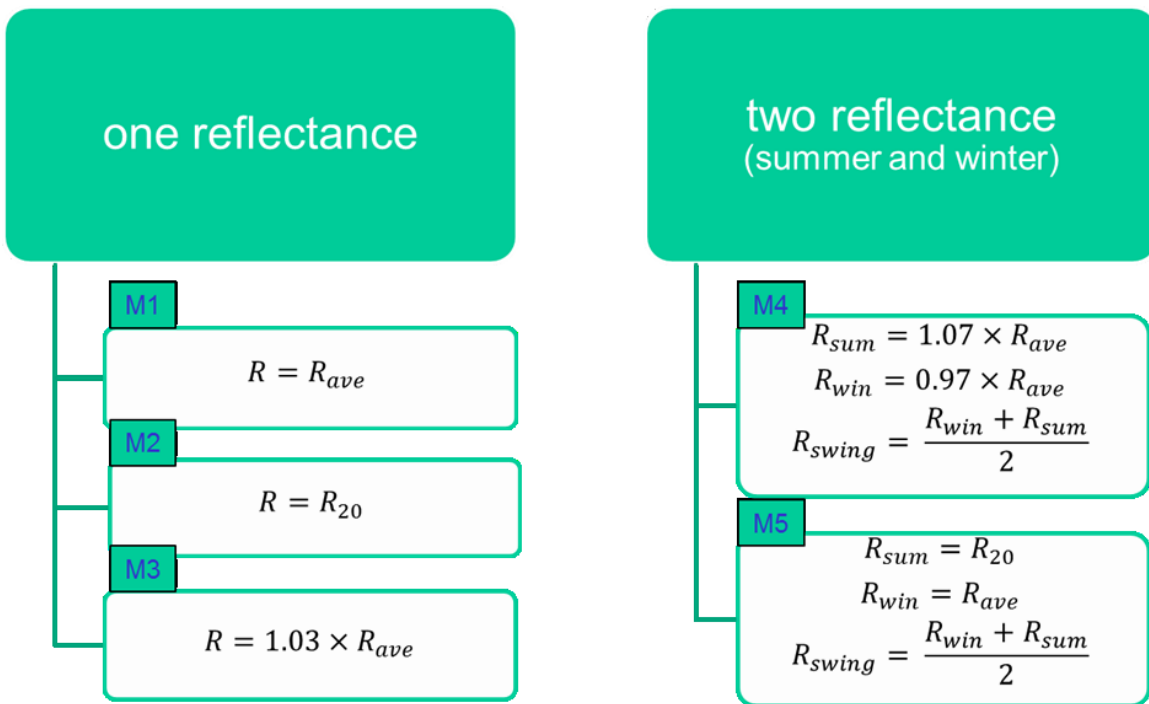


Fig. 2-5. labeling approaches and metrics

The appropriate approach is the one that has the least error in predicting mean hourly and peak heat absorption. Sizing of HVAC systems depends on peak cooling load or peak heat absorption in summer.

Akbari & Touchaei (2014) investigated a variety of DRM samples for different locations (latitudes), roof tilt angles and sky conditions (hazy and clear). However, they published only the results related to approaches M1, M2 and M5. They concluded that M5 has the minimum difference in estimating mean and peak heat absorption. However, M2 has the same performance as M5 during summer; so both metrics predict the peak heat absorption identically.

The initial reflectance of roofing materials are assigned by one value in all the current standards (Appendix A). Therefore, Akbari & Touchaei (2014) propose the approach M2 for labelling DRMs. Then, this method (i.e. M2) is accepted by Cool Roof Rating Council (CRRC) as the standard of labelling DRMs. However, neither

Akbari & Touchaei (2014) nor CRRC investigate the performance accuracy of the labelling approaches on the HVAC energy consumption of buildings. Akbari & Touchaei (2014) explore the heat absorption of DRM surfaces with simple method. This method cannot consider the longwave heat radiation from surface, heat convection of roof and ambient air, heat storage in building envelope and heat conduction through different layers of roofing assembly.

2.3 Summary

The white homogenous materials have high solar reflectance in visible and NIR bands. Hence, they can lower the cooling energy demand and increase the thermal comfort in unconditioned buildings. However, they might increase the heating energy during winter. Moreover, because of aesthetical reasons, some homeowners may prefer to have non-white roofs. In order to address these issues, new innovative technology called directional reflective materials (DRMs) is introduced to the roofing market.

DRMs are manufactured with two sides: reflective and absorptive. During summer when sun is high in the sky the reflective side is toward the sky, therefore, most of incident solar irradiance is reflected. During the winter when sun angle is low, the absorptive side absorbs the sunlight. From aesthetical point of view, the roof looks dark from the street.

All the current standards related to the building materials presumed that the solar reflectance of a roofing is only a function of the material's properties and it is constant for different positions of the sun. This assumption is incorrect for DRMs since their reflectance is a function of light source position (i.e. zenith angle).

Akbari & Touchaei (2014) analysed options with one or two reflectances to represent the annual reflectance of DRMs. These options are as follows; (1) M1: single reflectance for the entire year and equal to winter reflectance (R_{ave}); (2) M2: single reflectance for the entire year and equal to summer reflectance (R_{20}); (3) M5: using R_{ave} , R_{20} and $\frac{R_{20}+R_{avg}}{2}$ as winter, summer and swing seasons reflectances, respectively. (4) M3: single reflectance for the entire year and based on the correlation of winter,

summer and annual average reflectance to the R_{ave} of many DRM products. (5) M4: using a regression model to find the best correlation of winter and summer (swing season reflectance is the mean of winter and summer reflectances).

The approach M2 is accepted by CRRC as the standard of labeling the DRMs. However, neither Akbari & Touchaei (2014) nor CRRC investigate the accuracy of the labeling approaches for estimating the HVAC energy consumption of buildings. Akbari & Touchaei (2014) explored the heat absorption of DRM surfaces with simple method. This method cannot consider the longwave heat radiation from surface, heat convection of roof to ambient air, heat storage in building envelope and heat conduction through different layers of roofing assembly.

3 Methodology

In this chapter, steps to model DRMs incorporated with DOE-2.1E will be explained. In the first section, three major building-energy simulation tools and their capabilities are discussed. Then, steps to calculate the hourly solar reflectance of DRMs in DOE-2.1E simulation tool are presented, followed by a discussion of a developed algorithm to extract required data from DOE-2. Then based on the calculated solar angles with respect to the surface, the algorithm looks up the relevant solar reflectance from input data (measured or simulated) of reflectance distribution of DRM roof. Finally, the characteristics of building prototypes used in simulations to investigate the performance of the labelling approaches are presented.

3.1 Building energy simulation programs

A wide variety of building energy performance simulation programs are in use for the past 60 years. DOE-2.1E, TRNSYS and EnergyPlus are extensively used by building-energy researchers. In this section, we first briefly introduce these three simulation programs. Then, the reasons for selected simulation program is described.

3.1.1 DOE-2.1E

DOE-2.1E has been used widely for more than thirty years for building design analyses. Also its reliability persuade building standard associations to use DOE-2.1E for testing and developing requirements of building standards in the US and around the world. It can be used to simulate the energy efficiency of existing or new buildings, and efficiency of new technologies.

Given hourly weather data, building location, building envelope's material and geometric, HVAC description and utility rate structure, DOE-2.1E predicts the hourly energy consumption and energy cost (Crawley et al., 2008). According to DOE-2.1E official website "The source code as well as engineering manual are offered. Therefore, the users can add or modify components which are not considered in regular runs; that's why it is highly used by the researchers" (DOE2 official website).

3.1.2 TRNSYS

TRNSYS (Transient System Simulation Program) is one of the most flexible simulation software available in the market with a graphical interface (known as the TRNSYS Simulation Studio), a simulation engine, and a library of components that ranges from various building models to standard HVAC equipment to renewable energy and emerging technologies. This program can consider buildings equipped with photovoltaics, solar thermal, fuel cells, etc.

By entering the input data, the simulation engine solves the energy system. The HVAC system is represented by a set of algebraic and differential equations. TRNSYS solves HVAC-system components, envelope thermal balance and air network simultaneously at each time step (Crawley et al., 2008).

Source code and documentation are offered, so users can modify or add components do not exist in the standard library (TRNSYS official website); however, there is no assumptions about the building or HVAC system (although default information is available); hence, the user must enter detailed information about the building and system into the TRNSYS interface based on his or her knowledge.

Finally, the modular nature of TRNSYS lets modifications to the mathematical model of program. New components can be developed and export from other software into the TRNSYS (Crawley et al., 2008).

3.1.3 EnergyPlus

EnergyPlus is a modular, structured code supported by US Department of Energy (DOE) that contains most of the popular features and capabilities of BLAST and DOE-2. The inputs and outputs of this program are text files. However it might increase the time of modelling process (DOE official website-EnergyPlus).

Load calculation steps can be defined by user (15-min default). It simulates the building based on the integrated solution, i.e. calculating cooling, heating and electrical response of system and plant with a variable time step. This feature allows to evaluate realistic system controls, interzone air flow, moisture adsorption and desorption in

building elements, etc. Additionally, integrated solution provides more accurate estimation of the space temperature of zones compared to DOE-2. Therefore, it provides more reliable information for choosing HVAC system and plant sizing. (Crawley et al., 2008).

3.2 Selected simulation program

In order to demonstrate the energy performance of DRMs we select DOE-2.1E. It has following reasons. First of all, DOE-2.1E is capable of adding or modifying components by accessing to the source code of the program. In addition, predefined functions let the user to insert components to each subprogram which are not considered in normal runs so straightforwardly.

DOE-2.1E also uses simple but accurate assumptions to reduce the running time of simulations. This program also known as one of the accurate building energy simulation tools which is being used by researchers and building industry. Sullivan & Winkelmann (1998) validate the accuracy of DOE-2.1E in predicting heating energy, room air temperature and incident solar angle on the windows with measured data. Carriere et al. (1999) compared the estimated amounts of energy consumption of HVAC system by DOE-2.1E and experimental data. It is concluded that this software can estimate the total HVAC energy consumption (i.e. electrical heat pump) within 5.8%. Finally DOE-2.1E is free for public and its complete guide books (such as DOE-2.1 Basics (1991), DOE-2 Engineers Manual (1982) and DOE-2 Reference Manual (1980)) provide a lot of information for users.

As shown in (Fig. 3-1), DOE-2 has subprogram (BDL Processor) for translation of input to the language of the program. Then translated input is being considered as input in four subprograms (LOADS, SYSTEMS, PLANT and ECON). LOADS, HVAC (including SYSTEMS and PLANT) and ECON, are executed in sequence, e.g. the output of LOADS becomes the input of HVAC, etc. Also, we have access to the report results of each subprogram calculations.

The required input data consists of the following components:

- The geometry and composition of building envelop, i.e. Building materials and their properties
- Internal zones characteristic
- Schedules
- Weather data
- HVAC characteristics
- Energy prices

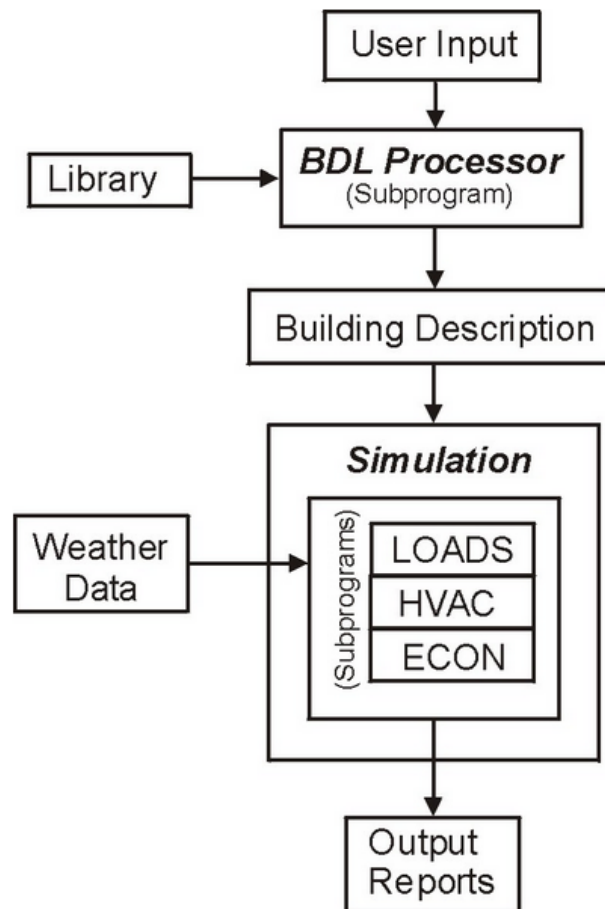


Fig. 3-1. DOE-2 flowchart (DOE-2 official website).

3.2.1 Algorithm of heat transfer in DOE-2

According to DOE-2 Engineers Manual (DOE-2, 1982) and Hosseini (2014) heat balance equation at the outside surfaces is as Eq. 3-1:

$$q_{out} = q_1 + q_2 + q_3 \quad \text{Eq. 3-1}$$

where q_1 is the hourly solar energy absorbed by the surface (Eq. 3-2).

$$q_1 = SOLI \times SURABSO \quad \text{Eq. 3-2}$$

where *SOLI* represents the summation of direct solar radiation, diffuse sky radiation, and ground reflection (short wave radiation). *SURABSO* represents the solar absorptance of wall or roof outside surface.

q_2 is the convective heat transfer between the roof or wall and outside air. It also contains the long wave interchange with the air (Eq. 3-3). DOE-2 uses combined radiative and convective film coefficient (*FILMU*) in heat calculations of surface with temperature of T and outside air with temperature of *DBRT*.

$$q_2 = FILMU \times (DBRT - T) \quad \text{Eq. 3-3}$$

q_3 indicates long wave re-radiation (Eq. 3-1). That is the difference between the long wave radiation from the sky and the radiation from ground which is reach to the surface, and the radiation emitted by a black body at the outdoor air temperature.

DOE-2 can consider heat flow through wall and roofs with and without considering heat capacity. In this research we consider the wall and roof with finite heat capacity (delayed mode). This algorithm simulates the heat transfer through building envelop more accurately by considering a set of response factors, rather than U-value. The response factor technique characterize heat flow in building assembly as a time series of thermal responses with a heat flux (Kreider, 2000) or temperature pulses (DOE-2, 1982). According to DOE-2 Engineers Manual (1982) response factor technique can consider the effect of thermal mass, placement of insulation, and architectural features.

The heat transfer is affected by wind speed, surface roughness, re-radiation from other surfaces, the absorptivity of the surface of wall or roof, wall area and temperature difference between inside and outside thorough simulations in DOE-2

(DOE-2, 1982). Engineers Manual (1982) explains steps of calculating the surface temperature and amount of heat through roof and walls in details.

DOE-2 let the user to define one value as the input for solar absorptance of the roof outside surface. But as it mentioned in the literature review, the solar reflectance (1 – solar absorptance) of DRMs are changing based on the solar incident angle (Akbari & Touchaei, 2014). So the solar absorptance in Eq. 3-2 should be change hourly basis (i.e. simulation time steps of DOE-2). In this study we use the function capability of DOE-2 to add hourly solar absorptance to the simulation algorithm. For this modification, we initially need to find out the incident solar sunray angle on the DRM surface, which is placed on the roof of a building.

3.2.2 Solar calculations in DOE-2

The position of the sun can be found in terms of solar altitude β above the horizontal and solar azimuth ϕ . These angles are a function of time and geographic latitude and longitude of considered surface. Sun-angle relationships are in terms of solar time rather than standard time. Converting standard time to solar time is conducted by using Eq. 3- 4:

$$\text{solar time} - \text{standard time} = 4(L_{st} - L_{loc}) + E \quad \text{Eq. 3- 4}$$

where L_{st} and L_{loc} represent the standard meridian and longitude of the location, respectively. The equation of time E , is determined in DOE-2 by applying Duffie & Beckman algorithm (2006):

$$E = 229.2(0.000075 + 0.001868 \cos B - 0.032077 \sin B - 0.014615 \cos 2B - 0.04089 \sin 2B) \quad \text{Eq. 3- 5}$$

Where,

$$B = (n - 1) \frac{360}{365} \quad \text{Eq. 3- 6}$$

and n =day of the year. Time in sun angle equations is expressed as the hour angle H . Hour angle is equal to 0.25 times the number of minutes from time and solar noon.

The declination δ is calculated from (Duffie & Beckman, 2006).

$$\delta = 23.45 \sin\left(360 \frac{284 + n}{365}\right) \quad \text{Eq. 3-7}$$

Finally, solar altitude angle and solar azimuth angle is estimated using Eq. 3- 8 and Eq. 3- 9, respectively.

$$\beta = \arcsin(\cos L \cos\delta \cos H + \sin L \sin\delta) \quad \text{Eq. 3-8}$$

$$\phi = \arcsin \frac{\cos \delta \sin H}{\cos \beta} \quad \text{Eq. 3-9}$$

According to DOE-2 Engineers Manual (1982), solar azimuth and solar altitude are named as *SAZM* (measured clockwise from south) and *SALT*, respectively. However, for printing the reports from hourly values of these angles one should follow the variables which are defined in FORTRAN code of DOE-2. DOE-2 Supplement, Version 2.1E (Winkelmann, et al., 1993) use *THSNHR* (solar azimuth, degrees measured clockwise from north) and *PHSUND* (solar altitude, degrees above horizon).

As it was mentioned in the literature review (Akbari & Touchaei, 2014), the solar reflectance of DRMs is a function of material properties, and solar radiation with respect to a surface. The solar radiation with respect to a surface is a function of the surface orientation and the sun's position. Surface azimuth angle (ψ) and tilt angle (Σ) represent the surface orientation (Fig. 3-2). ψ is measured clockwise from north in DOE-2. So the next step is to find the projected angle of sunray, while we know the solar azimuth and solar altitude angles, on the DRM sample which is placed in the roof with known building azimuth and roof tilt angles.

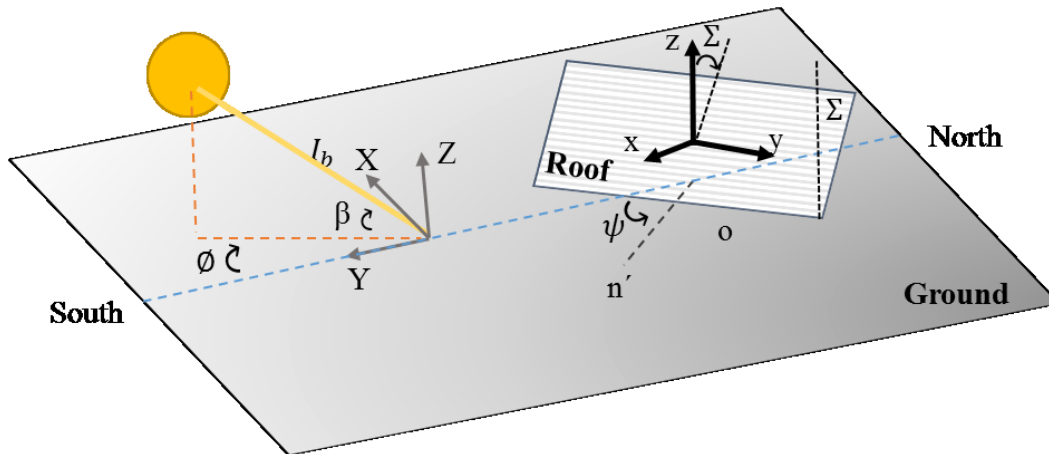


Fig. 3-2. DOE-2.1E Cartesian coordinate systems to calculate solar incident angle

DOE-2.1E computes the solar incident angle, the angle at which the beam radiation of sun (I_b) reaches the surface, and it is called *ETA*. This program initially project the sunray on XYZ coordinate system in the directions of “ X ”, “ Y ” and “ Z ”. This coordinate system is defined with “ X ” pointing west, “ Y ” pointing south and “ Z ” as vertical to the XY plane (DOE-2, 1982) (Fig. 3-2). Eq. 3- 10 to Eq. 3- 12, give the vectors of sunray or beam irradiance in XYZ coordinate system.

$$RAYCOS(1) = \sin\phi \cos\beta \quad \text{Eq. 3- 10}$$

$$RAYCOS(2) = \cos\beta \cos\phi \quad \text{Eq. 3- 11}$$

$$RAYCOS(3) = \sin\beta \quad \text{Eq. 3- 12}$$

According to Engineers Manual (1982), primarily coordinate system in DOE-2.1E has “ x ” pointing east and “ y ” pointing north. It is equivalent to rotate XYZ for 180° around “ z ” axis. Therefore:

$$RAYCOS(1) = -\sin\phi \cos\beta \quad \text{Eq. 3- 13}$$

$$RAYCOS(2) = -\cos\beta \cos\phi \quad \text{Eq. 3- 14}$$

Then, DOE-2.1E defines the third coordinate system to consider the building azimuth, too. So it rotates the “ xyz ” coordinate system around z axis equal to building azimuth (ψ) to produce new “ xyz ” Cartesian coordinate system. It projects the vectors of sunray in XYZ as below:

$$RAYCOS(1)_{new} = RAYCOS(1)_{old} \cos \psi - RAYCOS(2)_{old} \sin \psi \quad Eq. 3-15$$

$$RAYCOS(2)_{new} = RAYCOS(2)_{old} \cos \psi + RAYCOS(1)_{old} \sin \psi \quad Eq. 3-16$$

$$RAYCOS(3)_{new} = \sin \beta \quad Eq. 3-17$$

Finally, solar incident angle is obtained by considering tilt angle of surface (DOE-2, 1982). *ETA* is used as the cosine of incident angle in DOE-2 program.

$$ETA = (RAYCOS(1)_{new} \sin \psi + RAYCOS(2)_{new} \cos \psi) \sin \Sigma + RAYCOS(3)_{new} \times \cos \Sigma \quad Eq. 3-18$$

However, we are looking for projected of incident angle on the plane which is vertically perpendicular to the tilted surface. This angle can represent the zenith angle of light source which is illuminates the DRM surface in plane perpendicular to the corrugation surfaces of DRMs (Fig.3-5).

The projected incident angle (α), can be calculated in the Cartesian coordinate system which has another rotation around “y” axis equal to tilt angle (Σ). The new “xyz” coordinate system is shown in Fig. 3-3.

In other words, we initially rotate the *XYZ* coordinate system around “z” axis equal to ψ . Then we do the rotation around “y” axis as the same as tilt angle. I use the transform matrix to apply both rotations and find the sunray vectors in new coordinate system (*xyz*).

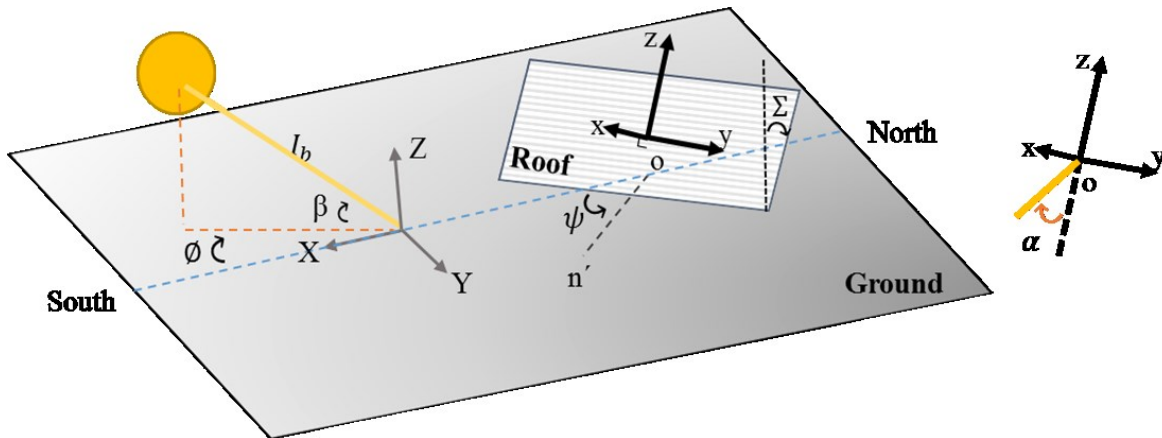


Fig. 3-3. Defined coordinate systems; “xz” plane is vertically perpendicular to the DRM surface

The rotation matrices about z and y axes are shown in Eq. 3- 19 and Eq. 3- 20. Based on the right hand rule the clockwise rotation around y axis (Fig. 3-3), should contain negative sign.

$$R_z(\psi) = \begin{bmatrix} \cos \psi & -\sin \psi & 0 \\ \sin \psi & \cos \psi & 0 \\ 0 & 0 & 1 \end{bmatrix} \quad \text{Eq. 3- 19}$$

$$R_y(\Sigma) = \begin{bmatrix} \cos(-\Sigma) & 0 & \sin(-\Sigma) \\ 0 & 1 & 0 \\ -\sin(-\Sigma) & 0 & \cos(-\Sigma) \end{bmatrix} \quad \text{Eq. 3- 20}$$

The transform matrix will be the multiple of $R_z(\psi)$ and $R_y(\Sigma)$, in sequence (Eq. 3- 21).

$$R_t = R_z(\psi) \times R_y(\Sigma) = \begin{bmatrix} \cos \psi \cos \Sigma & -\sin \psi & -\cos \psi \sin \Sigma \\ \sin \psi \cos \Sigma & \cos \psi & -\sin \psi \sin \Sigma \\ \sin \Sigma & 0 & \cos \Sigma \end{bmatrix} \quad \text{Eq. 3- 21}$$

Eventually, if we multiple the vectors of sunray in XYZ system by R_t , the projected sunray on xz plane can be achieved and it is the same as ETA .

DOE-2 reads the solar radiation data from weather data (if are on the weather file). In our simulations, DOE-2 obtains total horizontal solar radiation ($SOLRAD$), direct normal solar radiation (RDN or $DIRSOL$) and diffuse solar radiation ($BSUN$ or $DIFSOL$) from weather data, e.g. TMY3 or CTMY2.

3.3 Properties of simulated DRM sample

3.3.1 Reflectance variation of DRM as a function of incident solar radiation angle

The DRM sample with corrugation angle of 120° and cool black surface on absorptive side, and white surface on reflective side is considered. The reflectances of absorptive and reflective sides is assumed to be 0.15 (R_a) and 0.8 (R_r). The variation of DRM reflectance regarding to the zenith angle (the same as projected incident angle) is shown in Fig. 3-4. The reflectance distribution is generated using a tool developed by Akbari & Touchaei (2014).

Fig. 3-5 shows how we define the projected incident angles. α is equal to zero degree when the absorptive side is toward light source, and, $\alpha = 180^\circ$ represents that the light source is completely pointing to the reflective side of DRM.

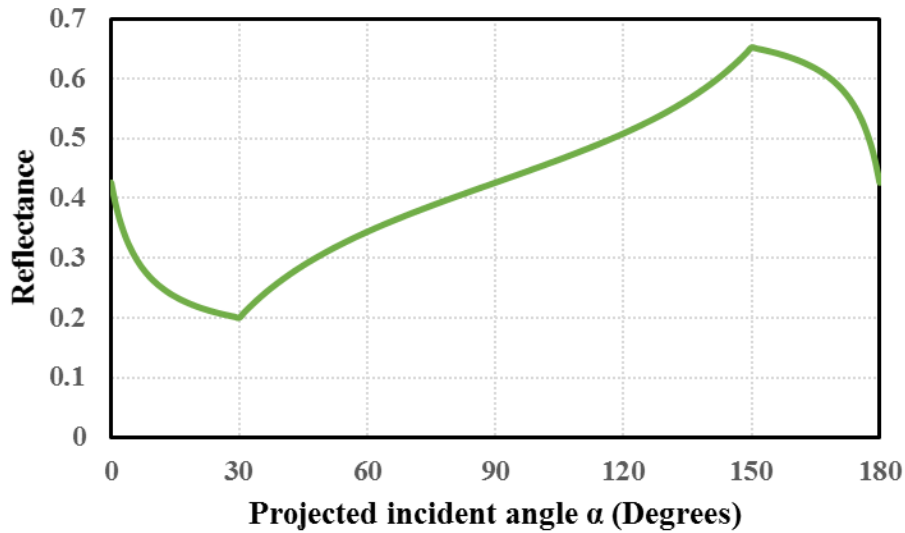


Fig. 3-4. Variation of solar reflectance and projected incident angle for DRM with $R_{abs}= 0.15$, $R_{ref}= 0.80$ and corrugation angle = 120° (AM1GH solar spectral irradiance) (Akbari & Touchaei, 2014)

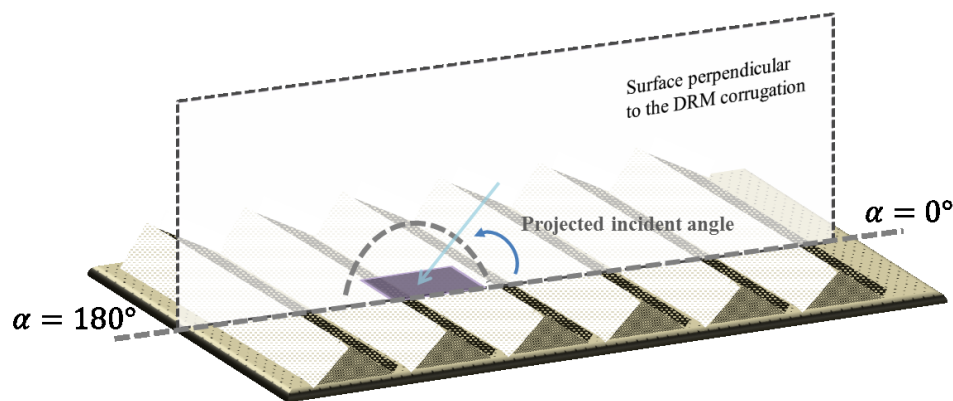


Fig. 3-5. The method of defining projected incident angle. $\alpha=0^\circ$ while the absorptive side is toward a light source and $\alpha=180^\circ$ represents a light source pointing to the reflective side of DRM.

The illumination of light source which is reached to the DRM is completely diffuse when the incident angles are zero degree or 180° . Because of the equal area of

absorptive and reflective side, the diffuse reflectance of DRM is equal to the average of R_r and R_a .

Fig. 3-4 illustrates that the DRM sample has lower reflectance once the projected incident angle is in the direction of street and the minimum reflectance occurs at the angle of 30° . Corrugation angle of selected DRM is 120° that's why the minimum reflectance occurs at the angle of 30° . In this angle, the beam radiation from light source, or sun, can only reach to the absorptive side of DRM. However, diffuse radiation can see the both side of reflective and absorptive sides. So total reflectance (i.e. diffuse and beam reflectances) of DRM at $\alpha = 30^\circ$ is higher than R_a . DRM samples have higher reflectance when the sun is high in the sky. The maximum reflectance is occurred when reflective side can only see the sunlight (e.g. $\alpha = 150^\circ$ when corrugation angle is 120°).

3.3.2 Applying labelling approaches

Deriving reflectance of DRM according to the amounts assigned by the labelling approaches is the object of this section. A simulation tool developed by Akbari & Touchaei (2014) is used to generate solar reflectance variation of DRM sample with respect to the zenith angle. As shown in Fig.3-6, R_{max} , R_{min} and R_{20} are 0.65, 0.2 and 0.48, respectively. The mean solar reflectance R_{ave} (average of maximum and minimum reflectance) is calculated as 0.43.

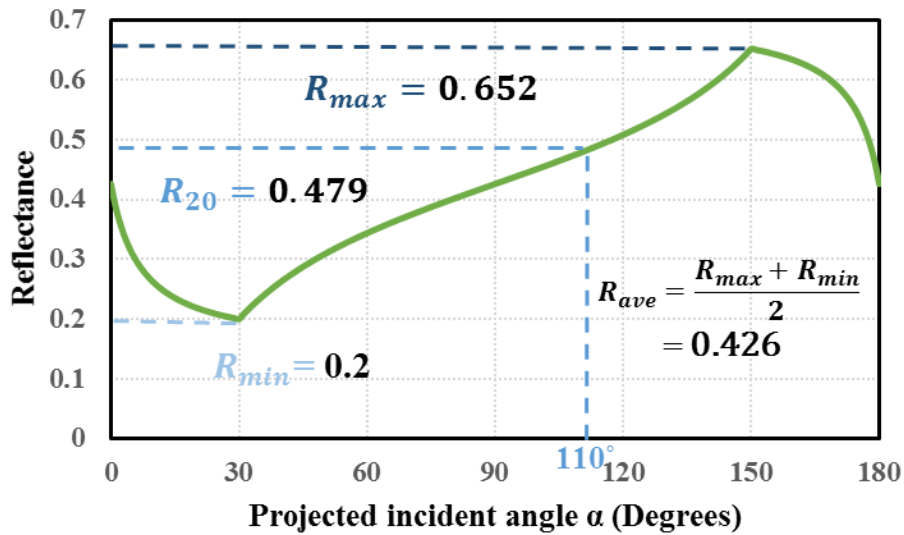


Fig.3-6. The maximum, minimum and R_{20} of considered DRM sample reflectances (Akbari & Touchaei, 2014)

The first three approaches assigned a single value to the reflectance of DRM. According to Akbari & Touchaei (2014) analysis, R_{ave} is near to the winter mean reflectance and R_{20} can characterize the summer mean reflectance. Akbari & Touchaei (2014) consider summer months as May, Jun and July. Also, winter period includes November, December and January.

The approach M3 was defined by the correlation of annual mean of solar reflectance to R_{ave} . The calculated solar reflectance of each approaches is shown in Fig.3-7.

In more accurate approaches, Akbari & Touchaei (2014) decomposed the reflectance to summer reflectance (R_s), winter reflectance (R_w) and the average of them for swing season reflectance (R_{swing}). The approach M4 is based on the correlation of winter and summer reflectances to R_{ave} .

The approach M5 is based on the combination of M1 and M2 approaches. M5 is accurate for both summer and winter periods by considering R_{20} as R_s and R_{ave} as R_w . Fig.3-7 shows the values of reflectance which is calculated based on the extracted data of DRM solar reflectance variation with respect to the projected incident angle.

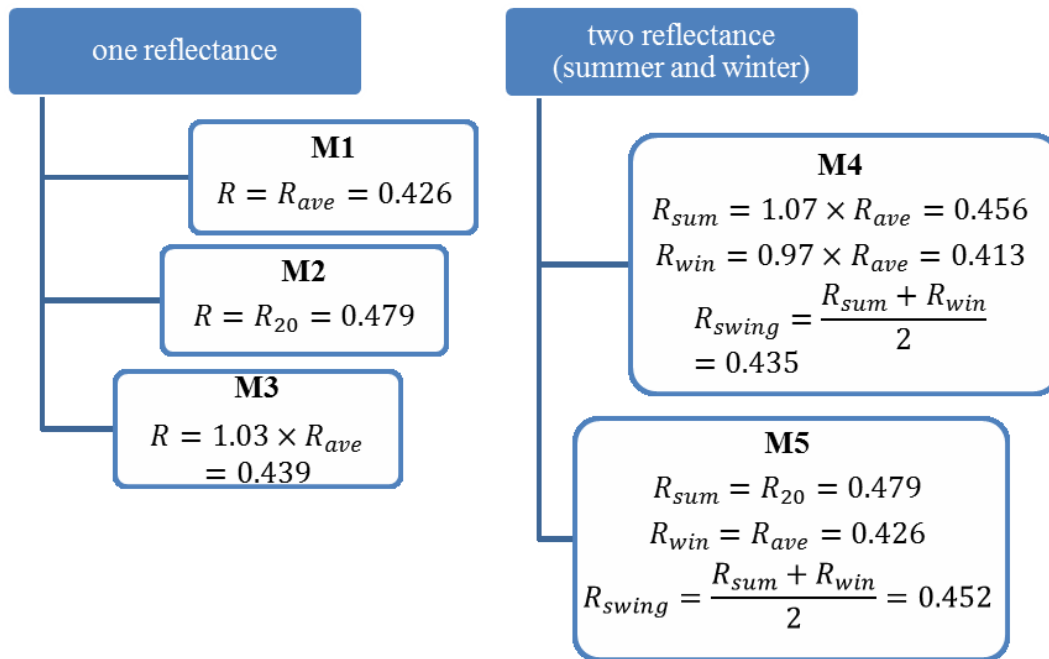


Fig.3-7. Reflectance values regarding to the labelling approached for simulated DRM sample

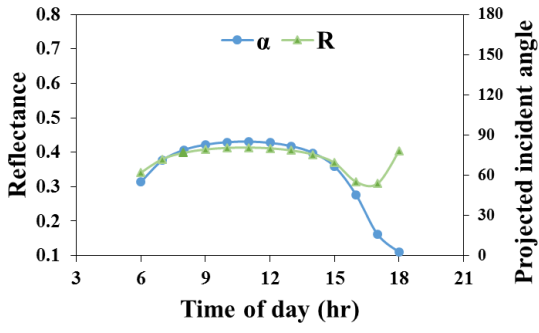
3.4 Simulating DRM reflectance in DOE-2.1E

As it was explained in section 3.2, we can derive the hourly projected incident angle through DOE-2, by giving the weather data, geographical features of building (i.e. elevation, longitude and latitude), period of simulation, building azimuth and tilt angle of roofing surface(s). Then by calling solar angles and using Eq. 3- 21 we can calculate the projected incident angle. Afterward, one can look up the relevant solar reflectance to the projected incident angle. Using the algorithms provided by Akbari and Touchaei (2014), a table of reflectance of DRM roof with respect to the zenith angles (or projected incident angles) was prepared as input to DOE-2.

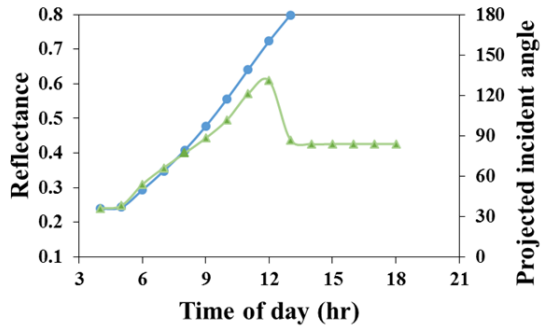
However, DOE-2.1E only considers the constant value for solar absorptance (or reflectances) of walls and roofs. Whereas we are looking to use mean hourly solar absorptances. As it was discussed in section 3.1.1, one of the advantages of DOE-2.1E is the capability of inserting input data which are not defined in the FORTRAN code of DOE-2. Functions can be used to input hourly solar absorptance to the calculations of LOAD subprogram. The function file is defined for each roof surface of building. This

function is finding the relevant solar absorptance from prepared table and calculated projected incident solar angle.

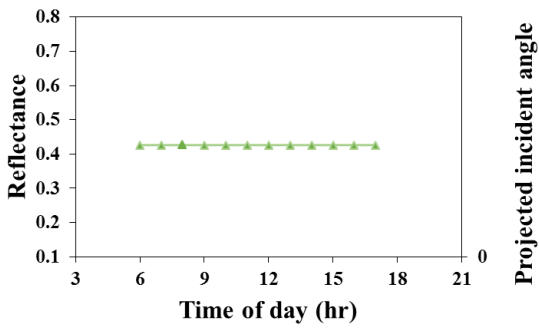
Fig.3-8 and Fig.3-9, demonstrate the variation of projected incident angle and looked up reflectance for a building with roof tilt angle of 45° at Houston (Latitude: 29.76° N and Longitude: -95.37 W). Here, the results for 21st of January and 21st of July are shown as examples.



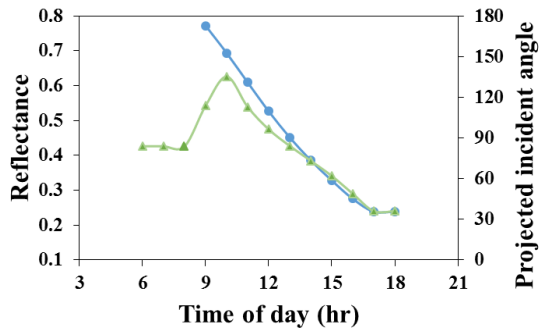
(a)



(b)

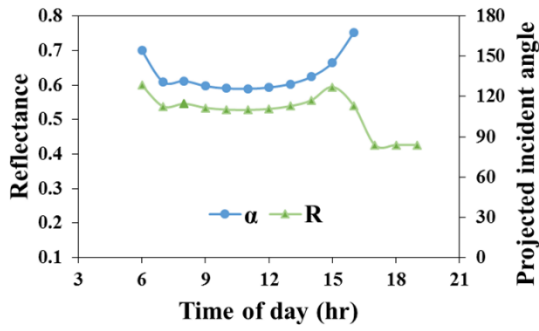


(c)

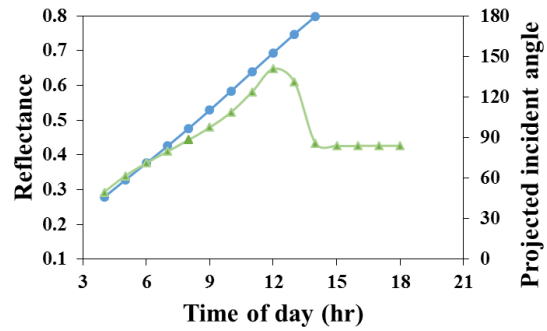


(d)

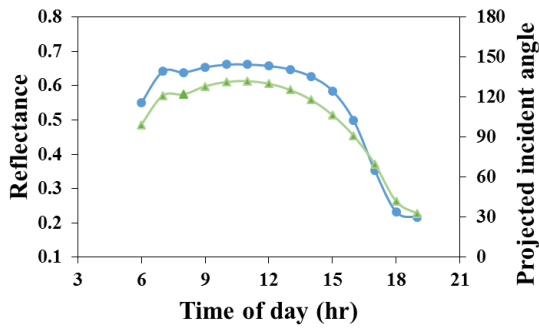
Fig.3-8. Variation of projected incident angle and solar reflectance for 45° tilted surface, 21st of January, Houston. Surfaces toward (a) South, (b) East, (c) North and (d) West



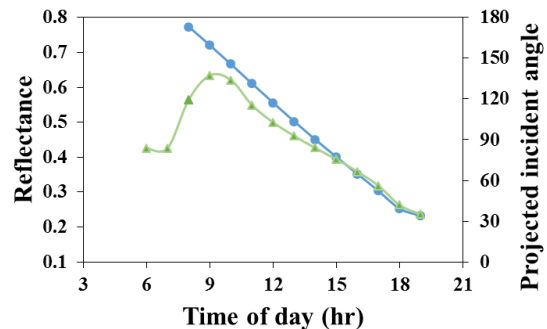
(a)



(b)



(c)

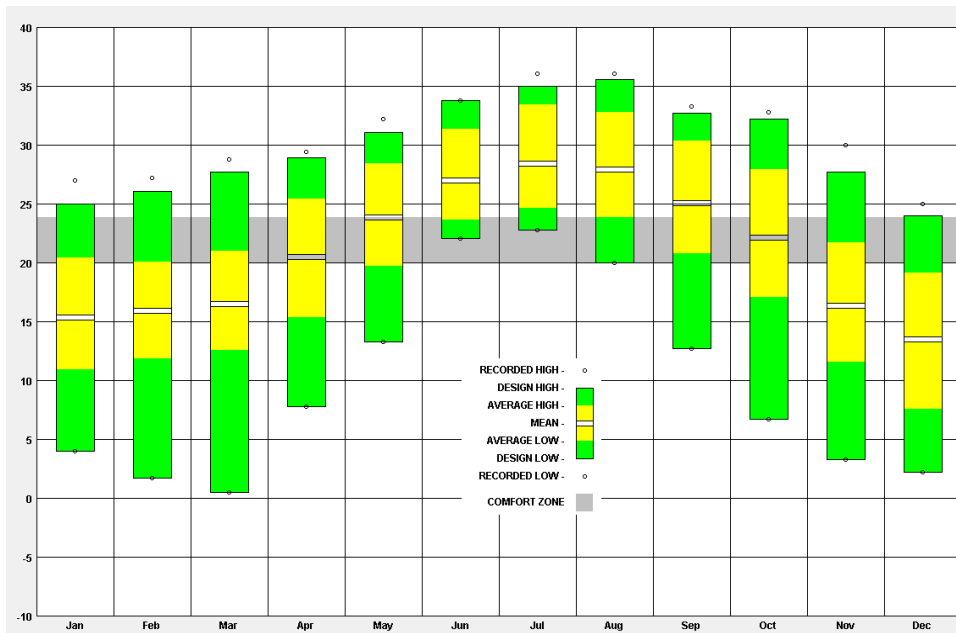


(d)

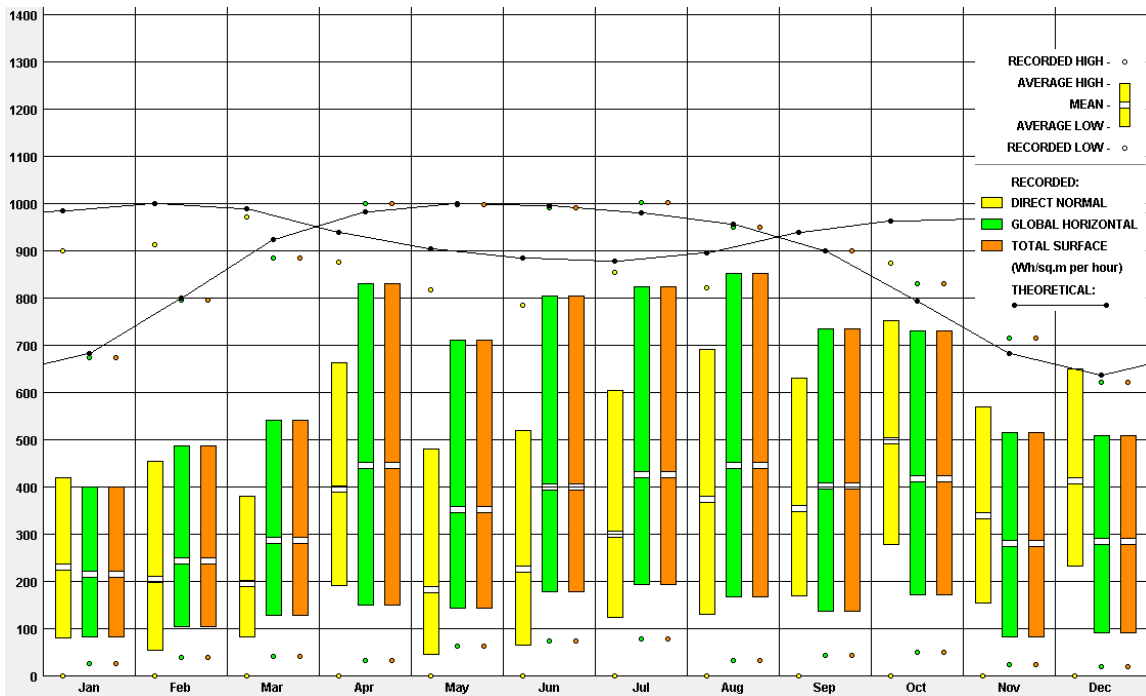
Fig.3-9. Variation of projected incident angle and solar reflectance for 45° tilted surface, 21st of July, Houston. Surfaces toward (a) South, (b) East, (c) North and (d) West

3.5 Outdoor climates

Three cities in different climate regions across U.S and Canada is selected: Houston, TX (hot and humid); Sacramento, CA (mild winters and hot, dry summers) and Montréal, QC (cold winter and humid summer). The solar radiation and meteorological elements for a 1-year period are obtained from latest version of typical meteorological year (TMY3) (Fig.3-10 and Fig. 3-11) and Canadian typical meteorological year (CTMY2).



(a)



(b)

Fig.3-10. Houston meteorological data from TMY3, (a) temperature range in degrees, (b) mean hourly solar radiation (Wh/m²) (Ligget & Milne, 2008)

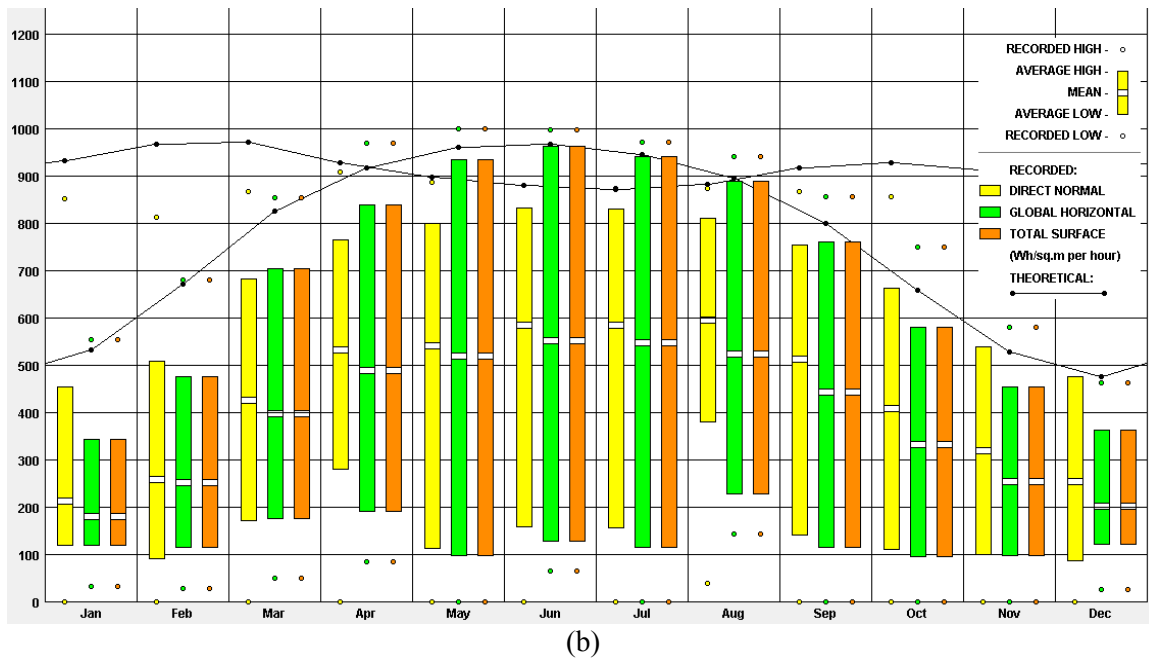
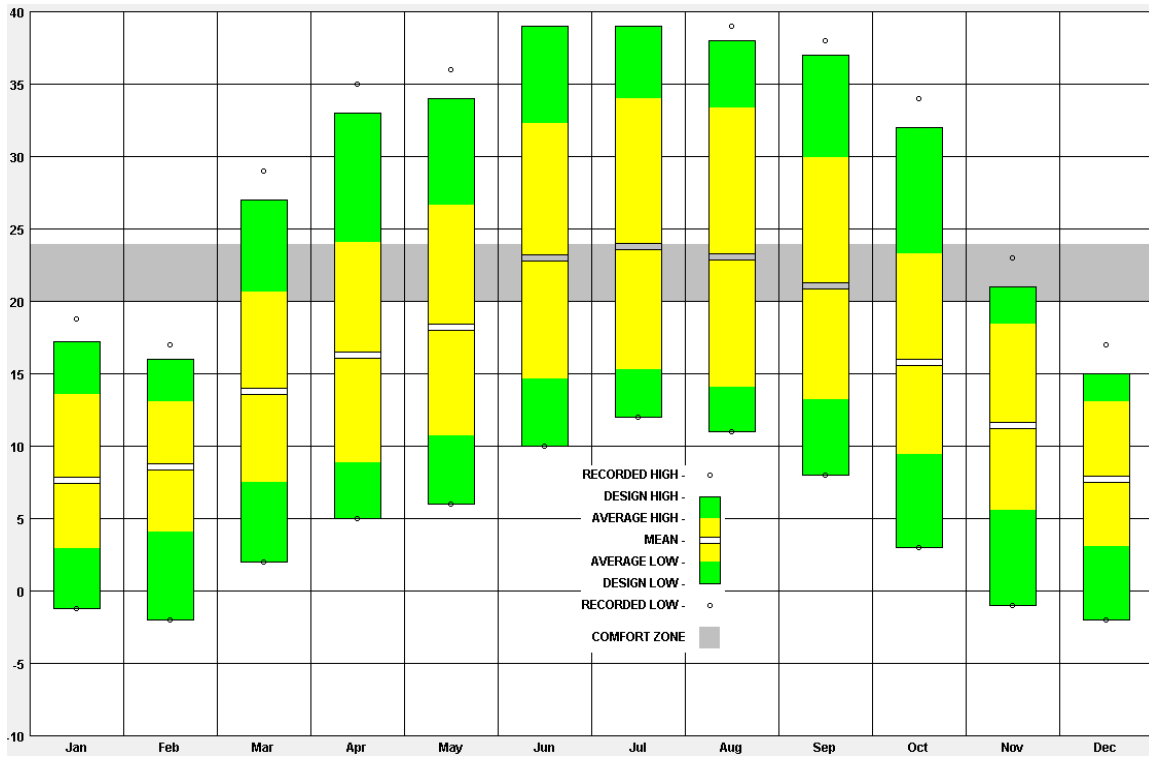


Fig. 3-11. Sacramento meteorological data from TMY3, (a) temperature range in degrees, (b) mean hourly solar radiation (Wh/m²) (Liggett & Milne, 2008)

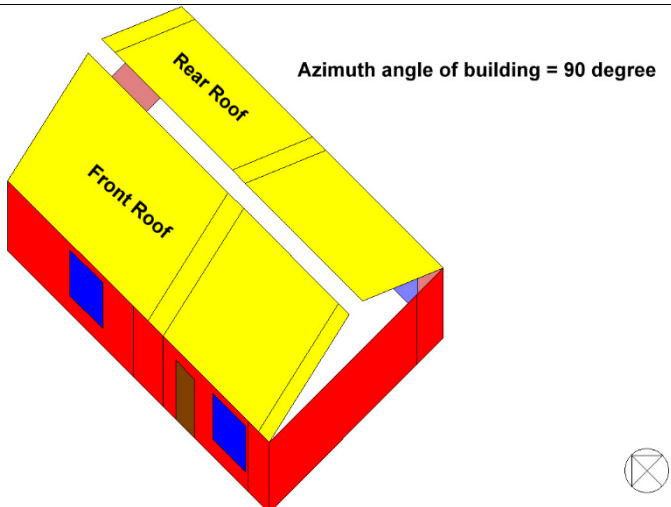
3.6 Prototypical building characteristics

Several sources are used to develop a single-family residential building prototype (110 m²). Old and new vintages with sloped roofs of 45° and 26.6° are considered for simulations. An old vintage assumed as the typical building based on the pre-1980 constructions. Konopacki et al. (1997) and Deru et al. (2011) are used to prepare the building envelop and HVAC system efficiencies of old prototype. The characteristics of a new prototype is obtained from residential prototypes provided by Pacific Northwest National Laboratory (PNNL) (2013) and single family residential building prototype from DOE-2.1E sample run book (1993).

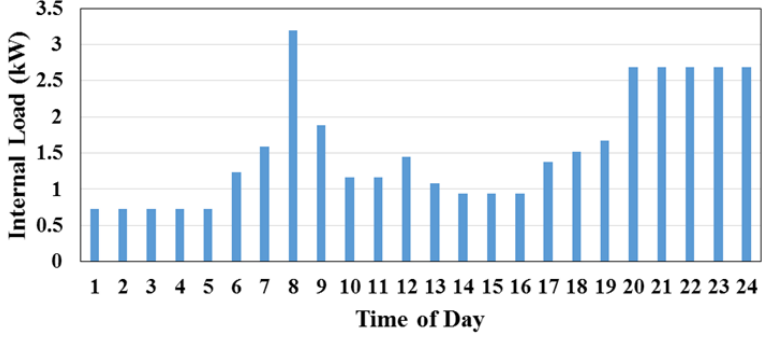
The features of prototypes are shown in Table 3-1. Energy simulations for each prototype in three building azimuth degrees are performs. The building azimuth angle of 0 degree is defined when the front and rear roofs are toward south and north, respectively. The direction of rotation is clockwise. Because of evenly distribution of windows in front and rear walls, the results of energy simulation in other 45 degree rotations of prototype must be equal to respective building azimuth of 0, 45 or 90 degrees. In addition, energy simulations of prototypes in Houston, Los Angeles and Montréal which they can represent cities in hot, moderate and cold climates, respectively, are performed.

A small single-family prototype is modelled as 2 zones: the living area and the sleeping quarters. The attic is not considered as a separate zone. The rear roof and front roof of each zone made from two parts: insulation and wood stud. So the function for pick up hourly solar reflectance is applied to each insulation and stud wood.

Table 3-1. New and old single-family residential prototype characteristics

Characteristics	New vintage	Old vintage
General		
Floor Area (m ²)	110	
Number of Floors	1	
Building Shape	 <p>Azimuth angle of building = 90 degree</p>	
Aspect Ratio	1.5	
Windows Fraction (Window-to-Wall Ratio)	16.4% for east and west facades	
Windows Position	Evenly distributed along two facades	
Envelope		
Exterior Walls		
Construction	Wood-Frame Walls (2x4 Stud) Aluminium Siding, ½ in Sheathing, Insulation, ½ in Drywall	
R-value of Insulation	R11 ¹	R7 (Konopacki S. A., 1997)
Average U-value (W/m ² K)	0.479	0.593

Roof		
Construction	Wood-Frame Roof (2x4 Stud) Asphalt Shingles, ½ in Plywood, Attic Air Space, Insulation, ½ in Drywall	
R-value of Insulation	R19 ¹	R11 (Konopacki S. A., 1997)
Tilt angle (Degrees)	26.6 and 45	
Average U-value (W/m ² K)	0.249	0.345
Window		
Dimensions	Punch Window, each 1.58 m high by 1.61 m wide	
Number of Panes	2 ²	1 (Konopacki S. A., 1997)
Shading Coefficient (Solar Heat Gain Coefficient)	0.43 (0.37) ²	0.62 (0.54) (Deru, 2011)
Center-of-Glass U-value (W/m ² K)	2.78	5.8
Frame width (m)	0.08	
Foundation		
Type	Slab-on-grade Floor (unheated)	
Construction	1 in Polystyrene ¹ , 4 in Concrete, Carpet and Pad	
U-value (W/m ² K)	0.676 (R 8.4)	
Interior Partition		
Construction	½ in Drywall, Wall Air Space, ½ in Drywall	
Infiltration	Using Residential Method of DOE-2.1E	

Internal Loads and Schedules¹	 <table border="1" data-bbox="625 262 1388 598"> <caption>Internal Load (kW) by Time of Day</caption> <thead> <tr> <th>Time of Day</th> <th>Internal Load (kW)</th> </tr> </thead> <tbody> <tr><td>1</td><td>0.7</td></tr> <tr><td>2</td><td>0.7</td></tr> <tr><td>3</td><td>0.7</td></tr> <tr><td>4</td><td>0.7</td></tr> <tr><td>5</td><td>0.7</td></tr> <tr><td>6</td><td>1.2</td></tr> <tr><td>7</td><td>1.6</td></tr> <tr><td>8</td><td>3.2</td></tr> <tr><td>9</td><td>1.8</td></tr> <tr><td>10</td><td>1.1</td></tr> <tr><td>11</td><td>1.1</td></tr> <tr><td>12</td><td>1.4</td></tr> <tr><td>13</td><td>1.0</td></tr> <tr><td>14</td><td>0.9</td></tr> <tr><td>15</td><td>0.9</td></tr> <tr><td>16</td><td>0.9</td></tr> <tr><td>17</td><td>1.3</td></tr> <tr><td>18</td><td>1.5</td></tr> <tr><td>19</td><td>1.6</td></tr> <tr><td>20</td><td>2.7</td></tr> <tr><td>21</td><td>2.7</td></tr> <tr><td>22</td><td>2.7</td></tr> <tr><td>23</td><td>2.7</td></tr> <tr><td>24</td><td>2.7</td></tr> </tbody> </table>		Time of Day	Internal Load (kW)	1	0.7	2	0.7	3	0.7	4	0.7	5	0.7	6	1.2	7	1.6	8	3.2	9	1.8	10	1.1	11	1.1	12	1.4	13	1.0	14	0.9	15	0.9	16	0.9	17	1.3	18	1.5	19	1.6	20	2.7	21	2.7	22	2.7	23	2.7	24	2.7
Time of Day	Internal Load (kW)																																																			
1	0.7																																																			
2	0.7																																																			
3	0.7																																																			
4	0.7																																																			
5	0.7																																																			
6	1.2																																																			
7	1.6																																																			
8	3.2																																																			
9	1.8																																																			
10	1.1																																																			
11	1.1																																																			
12	1.4																																																			
13	1.0																																																			
14	0.9																																																			
15	0.9																																																			
16	0.9																																																			
17	1.3																																																			
18	1.5																																																			
19	1.6																																																			
20	2.7																																																			
21	2.7																																																			
22	2.7																																																			
23	2.7																																																			
24	2.7																																																			
HVAC System																																																				
Type	Central On/Off (Air-to-Air) Heat Pump																																																			
Auxiliary Heat Source	Electric Baseboards																																																			
Schedule	24 hrs/7 days																																																			
Baseboard Capacity	1.5 kW																																																			
Fuel Type	Electricity																																																			
HVAC Efficiency																																																				
Heating COP (EIR)	3.3 (0.306) ¹	2.6 (0.385) (Deru, 2011)																																																		
Cooling COP (EIR)	2.9 (0.343) ¹	2.4 (0.416) (Deru, 2011)																																																		
HVAC Control																																																				
Thermostat Setpoint	Cooling 24°C / Heating 21°C																																																			
Supply Air Temperature	Maximum 40°C / Minimum 14°C																																																			
Economizers	No																																																			
Supply Fan (cfm) ¹	700																																																			

¹ (Lawrence Berkeley National Laboratory, 1993)

² (Pacific Northwest National Laboratory, 2013)

3.6.1 HVAC sizing procedure

DOE-2.1E automatically sizes the equipment based on the inputs (i.e. thermostat setpoints and supply air temperature) and the cooling load. At first, the HVAC system for each city and different scenarios (i.e. tilt angles, hourly reflectance or constant reflectance(s) from labelling approaches, old and new vintage) is sized by DOE-2.1E. Then, the maximum size of HVAC system is assigned for all the scenarios of each city.

Applying this procedure provides the capability to compare the results more accurately. Table 3-2, shows the given HVAC sizes for Houston, Sacramento and Montréal. HVAC system consists of central On/Off (Air-to-Air) heat pump and auxiliary heater (electric baseboard with capacity of 1.5 kW). The Auxiliary heat source is assumed constant in all cities.

<i>Table 3-2. Size of HVAC systems</i>		
	Cooling Capacity (tons)	Heating Capacity (kW)
Houston, TX	2.5	9.5
Sacramento, CA	1.6	6.1
Montréal, QC	1.4	5.4

3.7 Summary

Fig. 3-12 shows the steps that are introduced to calculate and add the hourly solar reflectance to the simulation algorithm of DOE-2.1E. Having roofing surface geometry and solar position is the first step to reach this purpose. At first, the geometry of building prototype was defined. Next the hourly solar angles from weather data were called. Then the projected incident solar angle was calculated. According to reflectance variation of DRM sample and zenith angle, the relevant solar reflectance was looked up. Inserting the hourly reflectance to DOE-2.1E is being proceed by using function capability of DOE-2.1E.

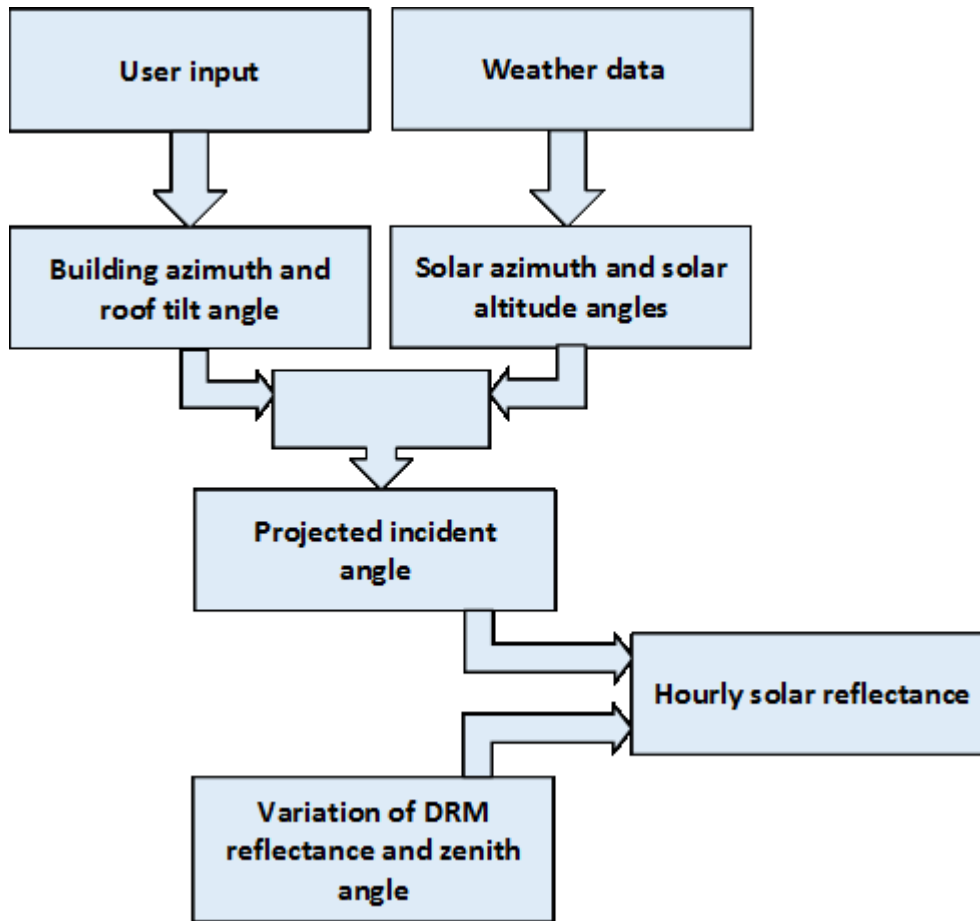


Fig. 3-12. The flowchart regarding to processes through DOE-2.1E to consider hourly solar reflectance of DRM sample

Finally I evaluate the accuracy of labelling approaches by comparing the results of HVAC energy consumption of hourly reflectance simulations and reflectances assigned by the approaches. I do the one year simulation with one reflectance according to M1, M2 and M3 labelling approaches. Also, the function for simulating the M4 and M5 approaches is defined. This function inserts the seasonal reflectance to the load calculation process of DOE-2.1E.

4 Simulated heating and cooling energy use

The simulations for a single family residential prototype building (110 m²) are carried out in 36 cases (Table 4-1). The selected prototype is simulated in three climates (i.e., hot: Houston, moderate: Sacramento, and cold: Montréal), for both new and old vintages, roof tilt angles of 26.6° and 45°, and three building azimuth degrees (i.e., 0°, 45° and 90°).

Building azimuth of zero degree represents the building which front roof faces south, and rear roof is toward north. The direction of rotation is clockwise, i.e., the direction of front roof is changed from south to west by rotating the building for 90°.

Table 4-1: The simulated cases of residential building

Cities	Vintage	Tilt angle (degrees)	Building azimuth (degrees) ¹
Houston Sacramento Montréal	New	26.6	0 (S-N)
			45
			90 (E-W)
		45	0
			45
			90
	Old	26.6	0
			45
			90
		45	0
			45
			90

1. Building azimuth of zero degree represents the building which front roof faces south, and rear roof is toward north. Also the direction of rotation is clockwise, e.g. after rotating the building azimuth for 90°, the direction of front roof is changed from south to west.

In this chapter, first the monthly and annually results of HVAC energy consumption are shown and discussed. The simulations are performed for six scenarios of solar reflectance. Five of the scenarios are based on the reflectances defined by the

labeling approaches. M1, M2 and M3 are constant throughout a year. M4 and M5 have three reflectances during a year; summer (May, June and July), winter (November, December and January) and swing seasons (other months) (Akbari & Touchaei, 2014). Finally, the building is simulated while the reflectance is calculated for each hour. The mean hourly solar reflectance of DRM (called Hourly R) is calculated based on the method introduced in section 3.3.1.

It is assumed that the simulation results of hourly R approach is the more accurate model for estimating thermal behaviour of DRMs through using DOE-2.1E. So, the accuracy of the labelling approaches are assessed by comparing the simulation results of each approach with hourly R . The annual, seasonal and monthly space cooling and heating energy consumption of HVAC system that are assessed by six reflectances scenarios are investigated.

4.1 Building HVAC energy consumption in Houston

Tables 4-2 to 4-7 show the annual energy consumption of HVAC system in twelve simulated cases of Houston. The annual energy consumption is the summation of space cooling and heating energy and their equipment (i.e., ventilation fan, pump and miscellaneous). Except the new vintages with 90° and 45° building azimuth degrees, M2 has the least annual energy estimation difference compared to M5.

Table 4-2: Annual energy consumption of HVAC system (kWh) in Houston, roof tilt angle of 26.6° and building azimuth of zero degree

Method	Vintage	Space Cooling	Space Heating	Pump & MISC.	Vent. Fan	Total
Hourly R	New	4857	355	35	168	5415
	Old	6505	736	34	289	7564
M1	New	4901	355	35	169	5460
	Old	6630	730	33	294	7687
M2	New	4865	358	35	168	5426
	Old	6579	736	33	291	7639
M3	New	4892	356	35	169	5452
	Old	6617	731	33	293	7674
M4	New	4891	355	35	169	5450
	Old	6617	729	33	293	7672
M5	New	4880	355	35	168	5438
	Old	6600	731	33	292	7656

Table 4-3: Annual energy consumption of HVAC system (kWh) in Houston, roof tilt angle of 26.6° and building azimuth of 45°

Method	Vintage	Space Cooling	Space Heating	Pump & MISC.	Vent. Fan	Total
Hourly R	New	5053	385	35	341	5814
	Old	6806	768	33	309	7916
M1	New	5085	382	35	179	5681
	Old	6910	769	33	313	8025
M2	New	5051	385	35	177	5648
	Old	6859	774	33	310	7976
M3	New	5077	383	35	178	5673
	Old	6898	770	33	312	8013
M4	New	5065	383	35	179	5662
	Old	6899	769	33	311	8012
M5	New	5067	384	35	178	5664
	Old	6899	769	33	312	8013

Table 4-4: Annual energy consumption of HVAC system (kWh) in Houston, roof tilt angle of 26.6° and building azimuth of 90°

Method	Vintage	Space Cooling	Space Heating	Pump & MISC.	Vent. Fan	Total
Hourly R	New	5206	364	35	185	5790
	Old	7037	728	34	323	8122
M1	New	5227	367	35	184	5813
	Old	7131	731	33	325	8220
M2	New	5191	369	35	183	5778
	Old	7081	737	33	322	8173
M3	New	5217	367	35	184	5803
	Old	7118	732	33	324	8207
M4	New	5218	366	35	184	5803
	Old	7119	731	33	324	8207
M5	New	5206	367	35	184	5792
	Old	7100	732	33	323	8188

Table 4-5: Annual energy consumption of HVAC system (kWh) in Houston, roof tilt angle of 45° and building azimuth of zero degree

Method	Vintage	Space Cooling	Space Heating	Pump & MISC.	Vent. Fan	Total
Hourly R	New	4832	352	36	168	5388
	Old	6438	709	34	284	7465
M1	New	4881	350	35	168	5434
	Old	6598	718	33	291	7640
M2	New	4850	353	35	167	5405
	Old	6550	722	33	289	7594
M3	New	4874	351	35	168	5428
	Old	6587	719	33	291	7630
M4	New	4873	350	35	167	5425
	Old	6586	718	33	291	7628
M5	New	4862	351	35	167	5415
	Old	6570	719	33	290	7612

Table 4-6: Annual energy consumption of HVAC system (kWh) in Houston, roof tilt angle of 45° and building azimuth of 45°

Method	Vintage	Space Cooling	Space Heating	Pump & MISC.	Vent. Fan	Total
Hourly R	New	5037	375	35	175	5622
	Old	6777	756	34	308	7875
M1	New	5072	377	35	178	5662
	Old	6890	756	33	312	7991
M2	New	5039	379	35	177	5630
	Old	6846	762	33	309	7950
M3	New	5064	377	35	178	5654
	Old	6880	757	33	311	7981
M4	New	5064	376	35	178	5653
	Old	6879	755	33	311	7978
M5	New	5053	377	35	177	5642
	Old	6863	757	0	312	7965

Table 4-7: Annual energy consumption of HVAC system (kWh) in Houston, roof tilt angle of 45° and building azimuth of 90°

Method	Vintage	Space Cooling	Space Heating	Pump & MISC.	Vent. Fan	Total
Hourly Reflectance	New	5182	362	35	184	5763
	Old	7010	719	34	321	8084
M1	New	5223	361	35	184	5803
	Old	7126	718	33	324	8201
M2	New	5188	364	35	183	5770
	Old	7078	725	33	322	8158
M3	New	5214	362	35	184	5795
	Old	7114	719	33	324	8190
M4	New	5215	361	35	184	5795
	Old	7115	717	33	324	8189
M5	New	5203	362	35	183	5783
	Old	7098	718	33	323	8172

The monthly results of simulated HVAC energy consumption is shown in Appendix C. Table 4-8 is the example of the monthly results. The monthly energy consumption in space cooling and heating of the new vintage with roof tilt angle of 26.6° and building azimuth of zero degree is shown in Table 4-8. The approaches M2

and M5 consider the same reflectance (R_{20}) during summer, and M1 and M5 has the equal reflectance (R_{avg}) during wintertime.

<i>Table 4-8: Monthly cooling and heating energy consumption of HVAC system (kWh), New vintage in Houston, roof tilt angle of 26.6° and building azimuth of zero degree</i>													
	Jan	Feb	Mar	Apr	May	Jun	Jul	Aug	Sep	Oct	Nov	Dec	Total
Space Heating													
Hourly R	58	73	74	2	0	0	0	0	0	4	38	106	355
M1	61	72	70	2	0	0	0	0	0	4	39	108	356
M2	61	72	71	2	0	0	0	0	0	4	39	108	357
M3	61	72	71	2	0	0	0	0	0	4	39	108	357
M4	61	72	70	2	0	0	0	0	0	4	39	107	355
M5	61	72	71	2	0	0	0	0	0	4	39	108	357
Space Cooling													
Hourly R	116	139	184	311	512	705	785	762	577	460	193	113	4857
M1	117	141	189	316	516	709	790	766	583	466	194	115	4902
M2	115	139	186	312	513	706	785	762	580	462	192	112	4864
M3	116	141	188	315	515	708	789	765	583	465	193	114	4892
M4	117	141	188	315	514	707	787	765	583	465	194	115	4891
M5	117	140	187	314	513	706	785	764	582	464	194	115	4881

Fig. 4-1 and Fig. 4-2 show the annual energy consumption of HVAC system for old and new vintages with different building azimuths. Additionally, the right axis presents the absolute value of estimation difference of the estimated energy consumption by HVAC system. $Q_{Hourly R}$ represents simulated energy consumption by applying hourly solar reflectance. The estimated energy consumption of HVAC system while the reflectances is calculated according to the labeling approaches is shown by Q_{Metric} . The estimation difference (%) is calculated as:

$$estimation\ difference\ \% = \frac{|Q_{Hourly R} - Q_{Metric}|}{Q_{Hourly R}} \times 100 \quad Eq. 4-1$$

Fig. 4-1 and Fig. 4-2 illustrate that higher R-value of roof insulation in new vintage can reduce the effect of the roof reflectance on energy consumption. Therefore, the estimation difference of the labelling approaches in predicting energy consumption of old vintages are higher than new vintages.

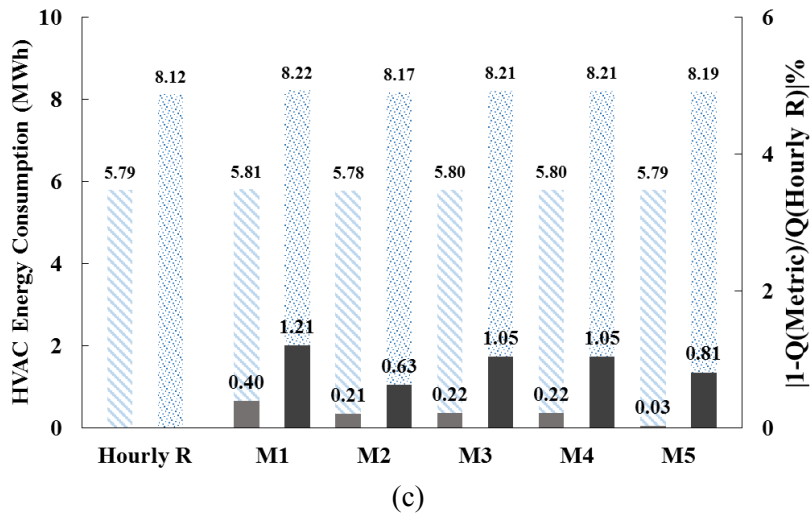
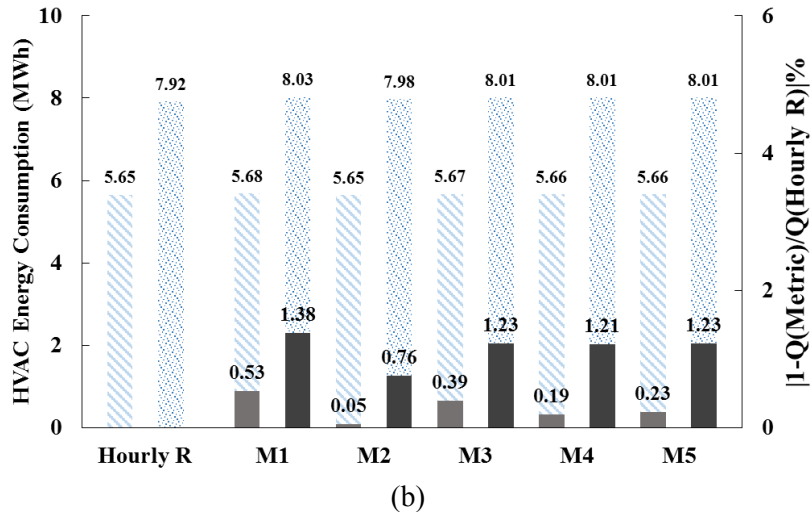
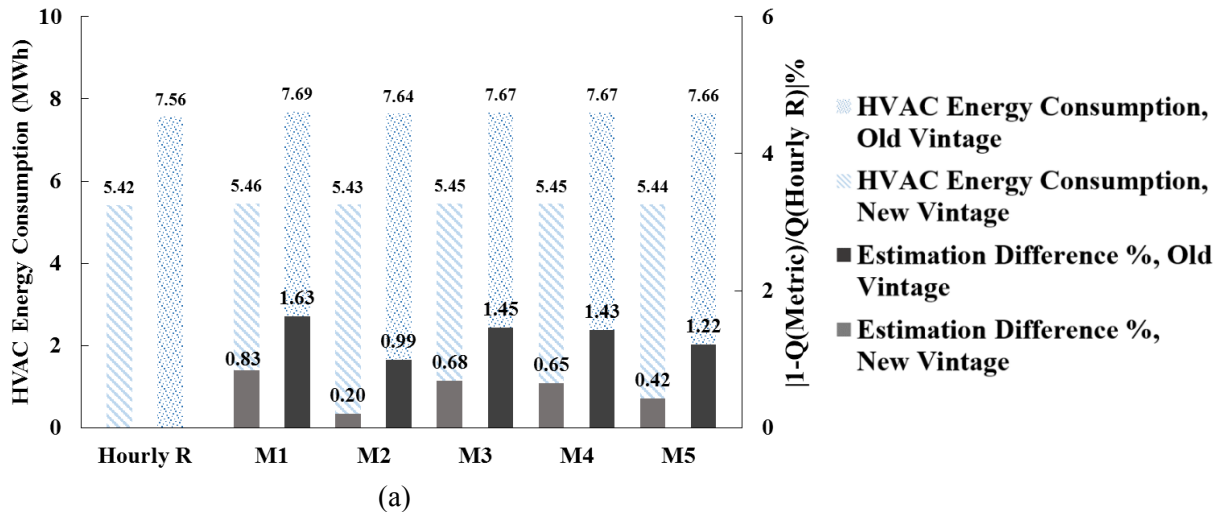


Fig. 4-1: Annual HVAC energy consumption and annually estimation difference of the labeling approaches (M1 to M5) to predict $Q_{Hourly R}$. The building is located in Houston with tilt angle of 26.6° ; building azimuth of (a) zero degree, (b) 45° and (c) 90° .

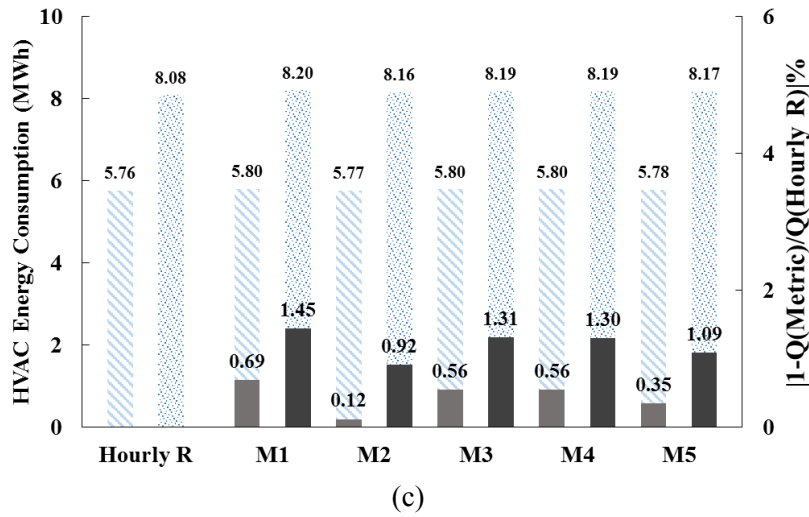
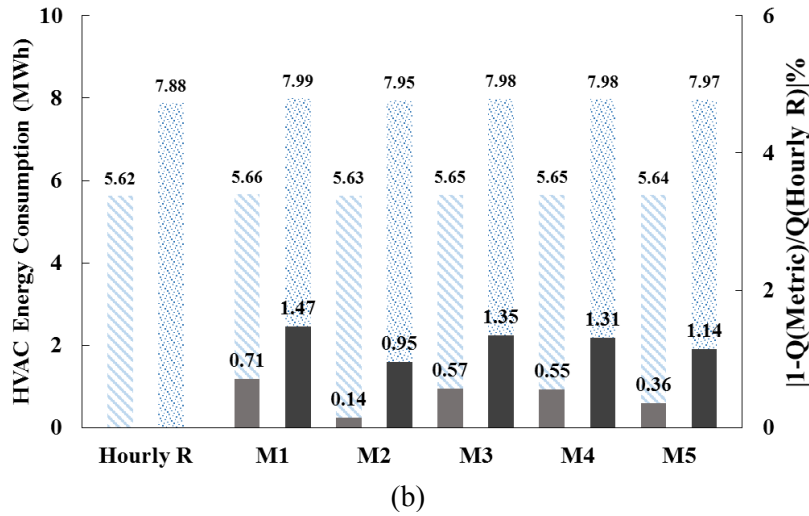
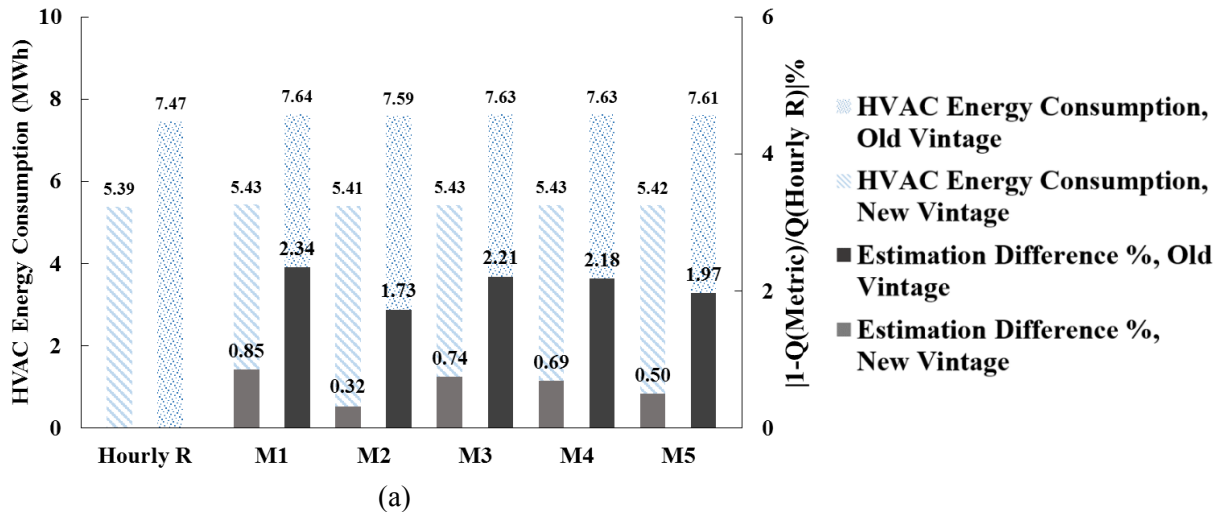


Fig. 4-2: Annual HVAC energy consumption and annually estimation difference of the labeling approaches (M1 to M5) to predict $Q_{Hourly R}$. The building is located in Houston with tilt angle of 45°; building azimuth of (a) zero degree, (b) 45° and (c) 90°.

Among the considered cities, Houston has the highest solar intensity and air temperature. Approximately 90% of annual consumption of HVAC system belongs to the cooling system (Table 4-8). Therefore, the effect of changing albedo (roof reflectance) would be more effective on cooling energy consumption compared to other cities. It can be concluded that the approach(es) with higher accuracy in modelling the reflectance of DRM during cooling season can more accurately estimate the thermal behaviour of roof and energy consumption of HVAC system.

M2 considers the R_{20} (summer reflectance) for whole of the year. For this reason, M2 can predict the energy consumptions in Houston significantly more accurate than other approaches. The approach M5 can estimate the cooling energy consumption during summertime with the same accuracy, but it is not accurate in swing season than does M2. The following paragraphs clarify this claim in detail.

Tables C.1 to C.4 from Appendix C.1 show the monthly space heating and cooling energy consumption of HVAC system. The results indicate M2 and M5 accurately predict the thermal performance of DRM over summer period (May, June and July). Table 4-9 illustrates the maximum estimation difference of the labeling approaches for summer, winter and swing season, individually. M2 and M5 overestimate mean hourly space cooling energy by up to 3.04 kJ/m^2 or 7.5%, during summer.

Table 4-9: Maximum estimation difference of the labeling approaches in estimating mean (hourly average) cooling and heating energy consumption in Houston

	Labeling approach	Summer	Winter	Swing season
Maximum estimation difference (%) and maximum mean hourly difference of estimating space heating ¹	M1	-	-3.6% -0.18 kJ/m ²	4.9% 0.32 kJ/m ²
	M2	-	-4.5% -0.22 kJ/m ²	4.2% 0.27 kJ/m ²
	M3	-	-4.5% -0.22 kJ/m ²	4.9% 0.32 kJ/m ²
	M4	-	-3.6% -0.18 kJ/m ²	4.9% 0.32 kJ/m ²
	M5	-	-3.6% -0.18 kJ/m ²	4.9% 0.32 kJ/m ²
Maximum estimation difference (%) and maximum mean hourly difference of estimating space cooling ²	M1	-8.1% -3.27 kJ/m ²	-	-3.1% -0.59 kJ/m ²
	M2	-7.5% -3.04 kJ/m ²	-	-1.9% -0.36 kJ/m ²
	M3	-7.9% -3.23 kJ/m ²	-	-2.9% -0.54 kJ/m ²
	M4	-7.7% -3.14 kJ/m ²	-	-2.9% -0.54 kJ/m ²
	M5	-7.5% -3.04 kJ/m ²	-	-2.7% -0.5 kJ/m ²

¹ The negative values of the estimation difference (%) shows that Q_{Metric} is higher than $Q_{HourlyR}$. It illustrates that the maximum estimation difference of the labeling approach is related to overestimations of the heat transfer through roof.

² The negative values of the estimation difference (%) shows that Q_{Metric} is higher than $Q_{HourlyR}$. It illustrates that the maximum estimation difference of the labeling approach is related to underestimation of the heat transfer through roof, during heating season.

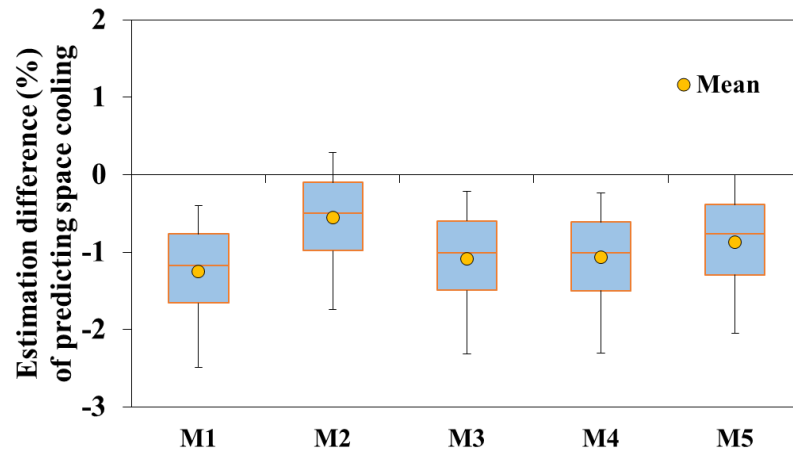
M2 uses one reflectance that is based on the summer solar reflectance of DRM (located in 37°N latitude). However, M5 uses the winter reflectance of DRM in U.S mainland during wintertime and the average of the winter and summer reflectances for swing season. During the swing seasons, M2 overestimates the cooling energy with less estimation difference than M5. Hence it has the minimum estimation difference in predicting cooling load as it illustrated in Fig. 4-3.

The maximum estimation difference of mean hourly HVAC energy consumption that is simulated during swing season by M2 is not more than 0.36 kJ/m² (1.9%). While M5 predictions is up to 0.5 kJ/m² (2.7%). Akbari & Touchaei (2014)

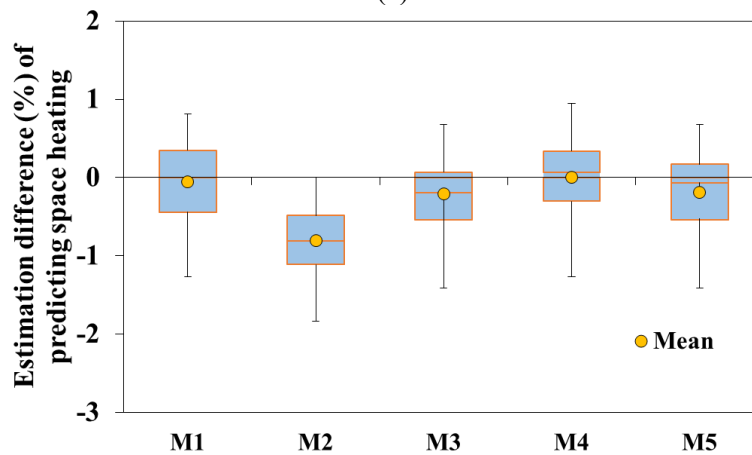
indicates that M2 can predict the heat absorption of roofs in lower latitudes slightly better than M5.

Fig. 4-3 shows the Box and Whisker Chart of the estimation differences (%) of the labeling approaches in estimating $Q_{\text{Hourly R}}$. Unlike previous figures that shown, the absolute values of estimation difference (%), hereinafter the estimation difference (%) is illustrated as $\frac{Q_{\text{Hourly R}} - Q_{\text{Metric}}}{Q_{\text{Hourly R}}}$. The vertical bars (whiskers) show the minimum and maximum values of estimation differences (%). The lower, middle and upper line of boxes display the 1st quartile, median and 3rd quartile, respectively. The circle marker presents the mean value of the estimation difference.

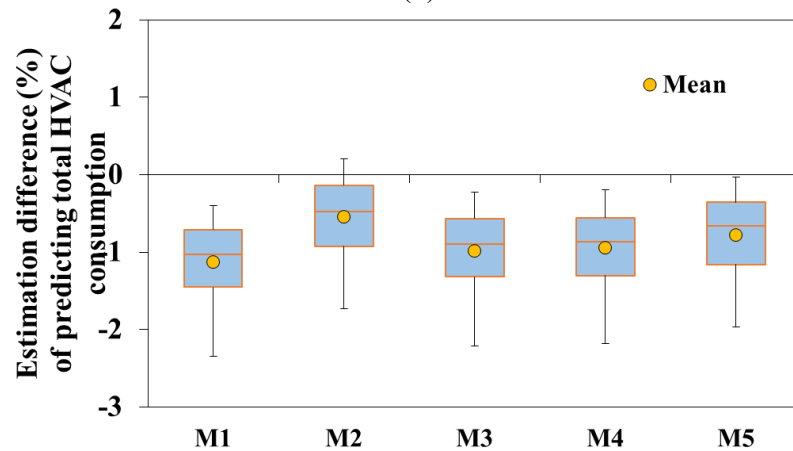
The negative value of estimation difference (%) shows that Q_{Metric} is higher than $Q_{\text{Hourly R}}$. For instance, Fig. 4-3.a indicates that all the approaches overestimate the annual absorbed heat of a roof except some cases of M2. These and monthly results (Table 4-9) indicate that assigned reflectances by the labelling approach is less than hourly reflectance during summer time. Accordingly, the approach with highest reflectance can predict cooling energy more accurately. M2 predicts the annual cooling energy consumption with the least median (-0.5% or 0.26 kWh/m²) and mean (-0.6% or 0.29 kWh/m²) estimation differences (%). The overestimation of annual space cooling energy by M2 is limited to 1.7% (0.92 kWh/m²). The mean and range of estimation difference (%) of other approaches are approximately the same and higher than M2_{estimation difference}.



(a)



(b)



(c)

Fig. 4-3: The estimation difference $\left(\frac{Q_{\text{Hourly R}} - Q_{\text{Metric}}}{Q_{\text{Hourly R}}}\right)\%$ of the labelling approaches in estimating annual HVAC energy consumption of (a) space cooling, (b) space heating and (c) total HVAC energy consumption in Houston. Minimum, 1st quartile, median, 3rd quartile and maximum amount of the estimation difference of the labelling approaches. The mean is shown as the circle marker.

As it is shown in Fig. 4-3.b, more accurate performance of M2 during summer, by considering high solar reflectance, has impact on space heating estimation during a heating season. The annual heating energy consumption estimated by M1, M3, M4 and M5 is much closer to $Q_{\text{Hourly R}}$ rather than M2 estimation.

The Approaches M2 and M3 overestimate the mean hourly heating energy consumption to within 0.22 kJ/m^2 (4.5%) during winter time (Table 4-9). Other approaches has the same maximum mean heating overestimation differences. Their estimation differences are limited to 0.18 kJ/m^2 (3.6%).

The space cooling energy is about ten times more than space heating energy in Houston. Consequently the approach with less estimation difference in predicting annual cooling energy can better characterize the reflectance of DRMs in low latitudes of US.

Fig. 4-3.c exhibits that all the approaches tend to overestimate energy consumption of heating system but not more than 2.3% or 1.6 kWh/m^2 , annually. Nevertheless, the approach M2 can more accurately estimate the annual HVAC energy to within median and mean estimation differences of 0.5% (0.3 kWh/m^2) and 0.5% (0.33 kWh/m^2), respectively. M2 overestimates the annual $Q_{\text{Hourly R}}$ by up to 1.7% (1.05 kWh/m^2). Using M5 instead of M2 can slightly increase the annual overestimation of heat flux from roof by no more than 0.3% (0.14 kWh/m^2).

The approaches M1, M3 and M4 predict total annual energy consumption ($Q_{\text{Hourly R}}$) by no more than 2.3% (1.43 kWh/m^2), 2.2% (1.34 kWh/m^2) and 2.2% (1.33 kWh/m^2) estimation differences. The average estimation differences of M1, M3 and M4 are twice the M2 and M5 estimation differences, approximately.

4.2 Building HVAC energy consumption in Sacramento

Sacramento is chosen as the city with mild weather condition. In addition, it is located at the latitude of 38°N . Hence, Sacramento can represent the location that the accuracy of the labelling approaches are investigated by Akbari & Touchaei (2014).

They propose using M2 for labelling DRMs based on their study on the performance of the approaches on mainland-US mean latitude of 37°N.

Table 4-10 to Table 4-15 present the annual energy consumption of HVAC system for residential building in Sacramento, CA. The annual energy consumption is the summation of the space cooling and the space heating energy and the HVAC equipment (i.e., ventilation fan, pump and miscellaneous). Nearly 60% of the annual HVAC energy consumption is used for space cooling.

Method	Vintage	Space Cooling	Space Heating	Pump & MISC.	Vent. Fan	Total
Hourly R	New	2354	1454	98	147	4053
	Old	3151	2327	88	183	5749
M1	New	2324	1439	100	193	4056
	Old	3237	2315	88	198	5838
M2	New	2360	1452	100	154	4066
	Old	3186	2330	88	196	5800
M3	New	2386	1443	100	155	4084
	Old	3224	2318	88	197	5827
M4	New	2383	1439	100	155	4077
	Old	3222	2315	88	197	5822
M5	New	2370	1442	100	154	4066
	Old	3204	2318	88	196	5806

Table 4-11: Annual energy consumption of HVAC system (kWh) in Sacramento, roof tilt angle of 26.6° and building azimuth of 45°

Method	Vintage	Space Cooling	Space Heating	Pump & MISC.	Vent. Fan	Total
Hourly R	New	2633	1488	98	165	4384
	Old	3581	2352	88	210	6231
M1	New	2660	1475	100	174	4409
	Old	3619	2343	88	219	6269
M2	New	2627	1488	100	172	4387
	Old	3570	2359	88	217	6234
M3	New	2652	1478	100	174	4404
	Old	3607	2347	88	218	6260
M4	New	2649	1474	100	173	4396
	Old	3604	2343	88	218	6253
M5	New	2637	1477	100	173	4387
	Old	3586	2347	88	217	6238

Table 4-12: Annual energy consumption of HVAC system (kWh) in Sacramento, roof tilt angle of 26.6° and building azimuth of 90°

Method	Vintage	Space Cooling	Space Heating	Pump & MISC.	Vent. Fan	Total
Hourly R	New	2796	1497	98	174	4565
	Old	3821	2334	89	220	6464
M1	New	2822	1484	100	184	4590
	Old	3860	2327	89	231	6507
M2	New	2788	1498	100	182	4568
	Old	3812	2344	89	229	6474
M3	New	2814	1488	100	183	4585
	Old	3848	2331	89	230	6498
M4	New	2811	1484	100	183	4578
	Old	3845	2327	89	230	6491
M5	New	2798	1487	100	182	4567
	Old	3827	2332	89	229	6477

Table 4-13: Annual energy consumption of HVAC system (kWh) in Sacramento, roof tilt angle of 45° and building azimuth of zero degree

Method	Vintage	Space Cooling	Space Heating	Pump & MISC.	Vent. Fan	Total
Hourly R	New	2321	1427	99	143	3990
	Old	3126	2295	89	182	5692
M1	New	2365	1421	100	153	4039
	Old	3191	2287	89	195	5762
M2	New	2336	1433	100	151	4020
	Old	3147	2301	89	192	5729
M3	New	2358	1424	100	153	4035
	Old	3180	2291	89	194	5754
M4	New	2356	1420	100	152	4028
	Old	3178	2288	89	194	5749
M5	New	2345	1424	100	153	4022
	Old	3162	2291	89	193	5735

Table 4-14: Annual energy consumption of HVAC system (kWh) in Sacramento, roof tilt angle of 45° and building azimuth of 45°

Method	Vintage	Space Cooling	Space Heating	Pump & MISC.	Vent. Fan	Total
Hourly R	New	2612	1468	98	164	4342
	Old	3549	2320	88	208	6165
M1	New	2641	1459	100	172	4372
	Old	3590	2318	89	217	6214
M2	New	2612	1471	100	171	4354
	Old	3546	2331	89	215	6181
M3	New	2634	1462	100	172	4368
	Old	3580	2321	89	216	6206
M4	New	2632	1459	100	172	4363
	Old	3576	2316	89	216	6197
M5	New	2621	1462	100	171	4354
	Old	3562	2321	89	215	6187

Table 4-15: Annual energy consumption of HVAC system (kWh) in Sacramento, roof tilt angle of 45° and building azimuth of 90°

Method	Vintage	Space Cooling	Space Heating	Pump & MISC.	Vent. Fan	Total
Hourly R	New	2612	1468	98	164	4342
	Old	3549	2320	88	208	6165
M1	New	2641	1459	100	172	4372
	Old	3590	2318	89	217	6214
M2	New	2612	1471	100	171	4354
	Old	3546	2331	89	215	6181
M3	New	2634	1462	100	172	4368
	Old	3580	2321	89	216	6206
M4	New	2632	1459	100	172	4363
	Old	3576	2316	89	216	6197
M5	New	2621	1462	100	171	4354
	Old	3562	2321	89	215	6187

Except the new and old vintages with 90° building azimuth degrees, M2 has the less or equal annual estimation difference compared to M5. In other words, $M2_{\text{estimation difference}}$ and $M5_{\text{estimation difference}}$ are the least in six and two cases out of twelve, respectively. In four remained cases both approaches have the least and same estimation differences (Figs. 4-4 and 4-5).

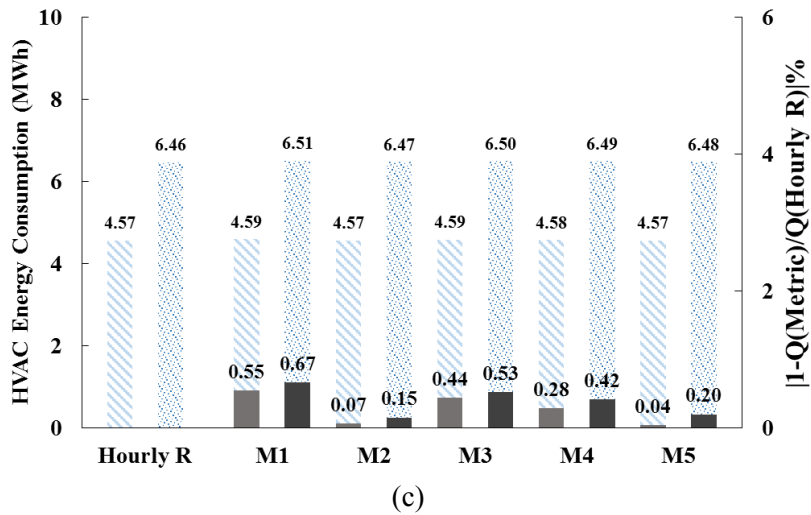
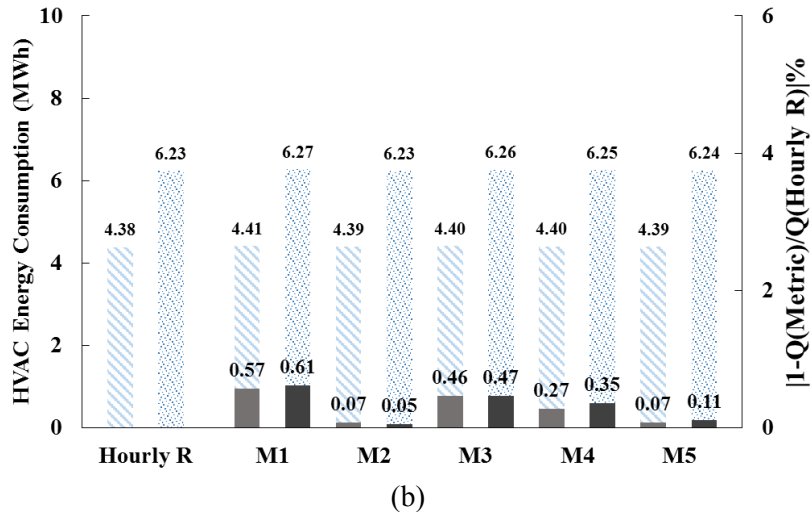
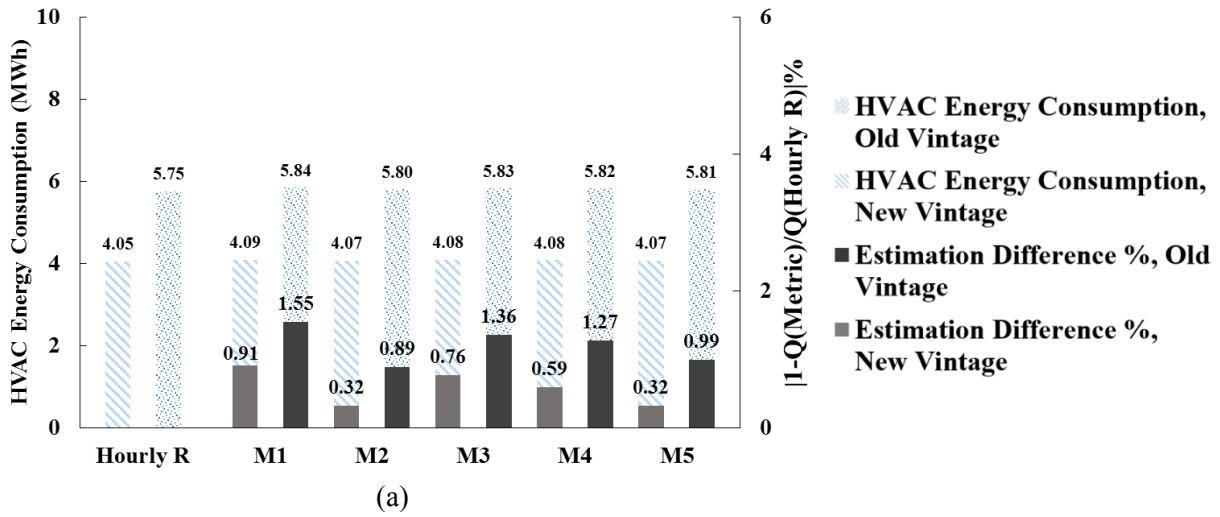


Fig. 4-4: Annual HVAC energy consumption and estimation difference between simulations with hourly reflectance and labeling approach reflectances (M1 to M5), for prototype in Sacramento with tilt angle of 26.6°; building azimuth of (a) zero degree, (b) 45° and (c) 90°.

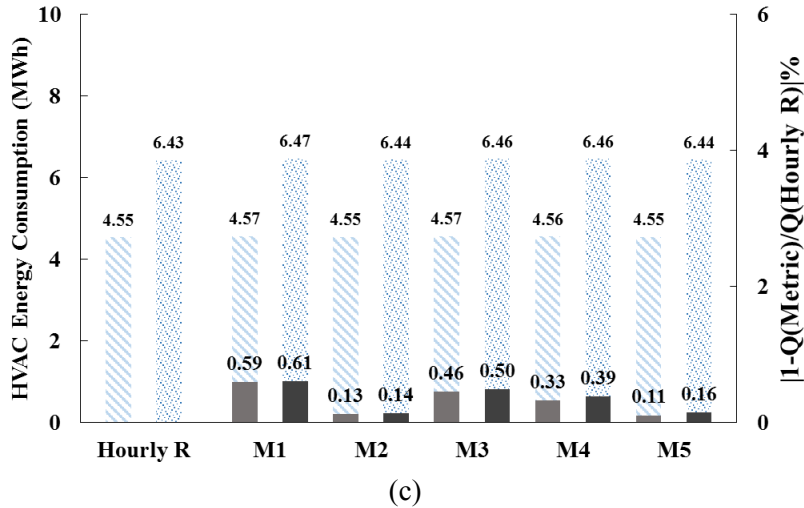
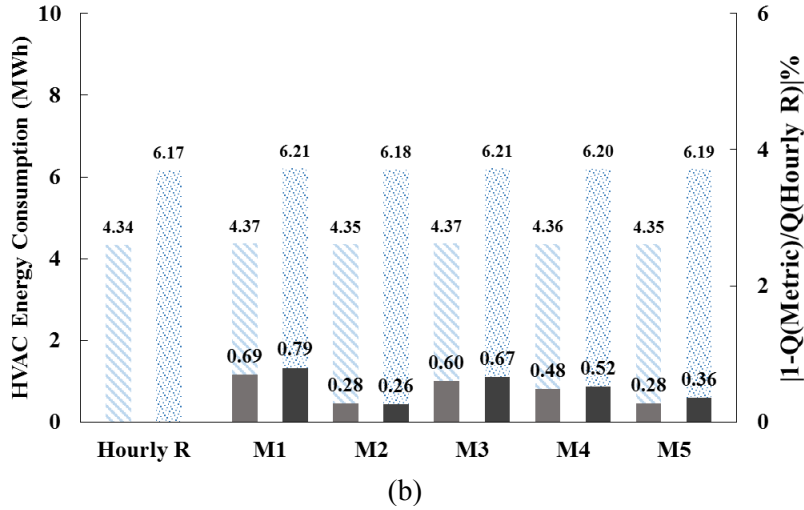
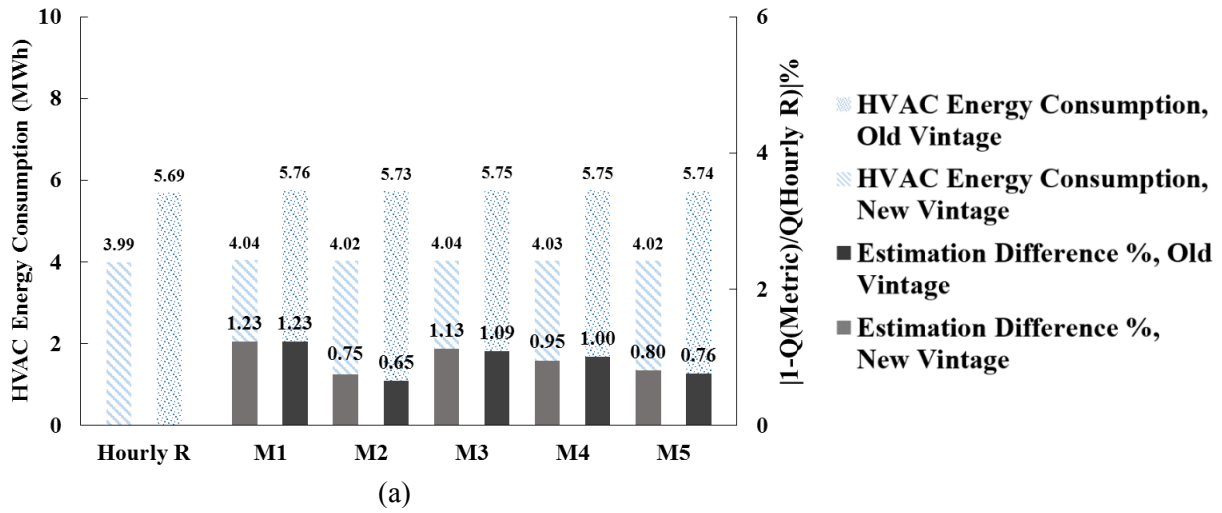


Fig. 4-5: Annual HVAC energy consumption and estimation difference between simulations with hourly reflectance and labeling approach reflectances (M1 to M5), for prototype in Sacramento with tilt angle of 45°; building azimuth of (a) zero degree, (b) 45° and (c) 90°.

Fig. 4-6 depicts the results for Sacramento. Fig. 4-6.a illustrates that all the approaches except some cases of M2 overestimate the heat absorption of DRM roof during warm days. Tables C.5 to C.8 from Appendix C.2 show the monthly space heating and cooling energy consumption of HVAC system. The results indicate M2 and M5 accurately predict the thermal performance of DRM over summer period (May, June and July).

Table 4-16 illustrates that the maximum estimation difference of the labelling approaches for summer, winter and swing seasons, individually. M2 and M5 overestimate mean hourly space cooling energy by up to 1.87 kJ/m² or 0.5%, during summer. However, implementing M2 can reduce the cooling overestimation of M5 for 1.33 kJ/m² during swing season. By comparing the performance of M5 and M2 it can be concluded that considering high solar reflectance during swing season reduce the estimation difference of predicted space cooling (Fig. 4-6.a). The mean of annual cooling energy estimation difference of M5 (-0.5%) is approximately 5 times higher than M2 (-0.1%).

The maximum estimation difference of the mean hourly space heating energy forecasted by M5 during winter is caused by underestimation of space heating (0.14 kJ/m²). However, this amount is less than maximum mean hourly space heating estimation difference of M2 (overestimation of 0.18 kJ/m²). But, the performance of M2 during annual energy consumption of heating system is significantly better than other approaches. According to Fig. 4-6.b, the median, mean and maximum estimation difference of annual heating energy consumption of M2 are 0.1% (-0.03 kWh/m²), 0.1% (-0.02 kWh/m²) and 1.1% (-0.3 kWh/m²).

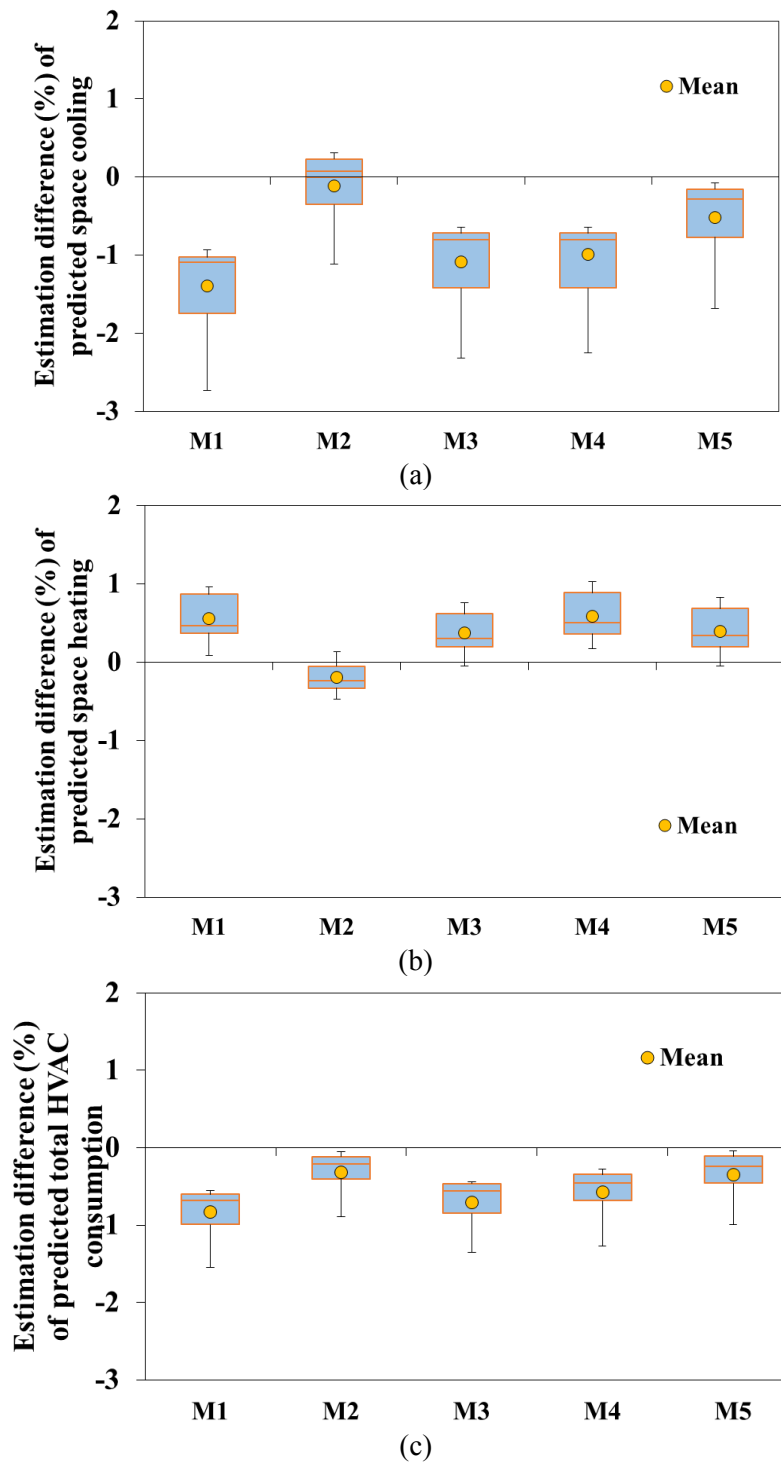


Fig. 4-6: The estimation difference ($\frac{Q_{\text{Hourly R}} - Q_{\text{Metric}}}{Q_{\text{Hourly R}}} \%$) of labeling approaches in estimating annual HVAC energy consumption of (a) space cooling and (b) space heating and (c) total HVAC energy consumption in Sacramento. Minimum, 1st quartile, median, 3rd quartile and maximum amount of estimation difference of each approach. The mean is shown as circle marker.

Table 4-16: Maximum estimation differences of the labeling approaches in estimating mean (hourly average) cooling and heating energy consumption in Sacramento

	Labeling approach	Summer	Winter	Swing season
Maximum estimation difference and maximum mean hourly difference of estimating space heating¹	M1	-	0.8% 0.14 kJ/m ²	0.9% 0.18 kJ/m ²
	M2	-	-0.7% -0.18 kJ/m ²	-1.0% -0.14 kJ/m ²
	M3	-	0.5% 0.10 kJ/m ²	0.7% 0.14 kJ/m ²
	M4	-	1.0% 0.18 kJ/m ²	1.3 % 0.18 kJ/m ²
	M5	-	0.8% 0.14 kJ/m ²	1.6 % 0.14 kJ/m ²
Maximum estimation difference and maximum mean hourly difference of estimating space cooling²	M1	-2.9% -0.77 kJ/m ²	-	-5.3% -0.54 kJ/m ²
	M2	-1.9% -0.50 kJ/m ²	-	-3.1% -0.32 kJ/m ²
	M3	-2.6% -0.68 kJ/m ²	-	-4.9% -0.50 kJ/m ²
	M4	-2.2% -0.60 kJ/m ²	-	-4.9% -0.50 kJ/m ²
	M5	-1.9% -0.50 kJ/m ²	-	-4.4% -0.45 kJ/m ²

¹ The negative values of the estimation difference shows that Q_{Metric} is higher than $Q_{Hourly R}$. It illustrates that the maximum estimation difference of the labeling approach is related to overestimations of the heat transfer through roof.

² The negative values of the estimation difference shows that Q_{Metric} is higher than $Q_{Hourly R}$. It illustrates that the maximum estimation difference of the labeling approach is related to underestimation of the heat transfer through roof, during heating season.

According to Fig. 4-6.c, the annual energy estimation difference of M2 and M5 are up to 0.9% (-0.42 kWh/m²) and 1.0% (-0.46 kWh/m²), respectively. M4 predicts annual $Q_{Hourly R}$ with a lower estimation difference in comparison with M1 and M3. M1, M3 and M4 predict annual $Q_{Hourly R}$ by no more than 1.6% (0.74 kWh/m²), 1.4% (-0.064 kWh/m²) and 1.3% (-0.6 kWh/m²) differences.

In summary, characterizing DRM by using summer reflectance (approach M2) has the least annual estimation difference (i.e. up to -0.3 kWh/m²) in predicting total HVAC energy consumption, in Sacramento. Therefore, it can more accurately predict heat transfer through the roof during entire of the year compared to other approaches.

Also, other approaches can estimate HVAC energy consumption by estimation differences no more than 1.55% (-81 kWh/m²).

4.3 Building HVAC energy consumption in Montréal

Montréal has the least sunny days among considered locations. Also, it has moderately sunny days during summer. In addition, Table 4-17 to Table 4-22 show that almost 15% of HVAC energy consumption is used to cool the space. This weather condition leads to reduce the effect of roof reflectance on HVAC energy consumption.

Table 4-17: Annual energy consumption of HVAC system (kWh) in Montréal, roof tilt angle of 26.6° and building azimuth of zero degree

Method	Vintage	Space Cooling	Space Heating	Pump & MISC.	Vent. Fan	Total
Hourly R	New	944	10112	100	336	11492
	Old	1237	14168	74	385	15864
M1	New	968	10093	101	341	11503
	Old	1281	14142	74	390	15887
M2	New	952	10119	100	340	11511
	Old	1254	14183	74	389	15900
M3	New	964	10099	100	341	11504
	Old	1274	14152	74	390	15890
M4	New	961	10093	101	340	11495
	Old	1270	14143	74	389	15876
M5	New	954	10101	100	340	11495
	Old	1259	14155	74	389	15877

Table 4-18: Annual energy consumption of HVAC system (kWh) in Montréal, roof tilt angle of 26.6° and building azimuth of 45°

Method	Vintage	Space Cooling	Space Heating	Pump & MISC.	Vent. Fan	Total
Hourly R	New	1097	10171	100	349	11717
	Old	1471	14204	77	396	16148
M1	New	1119	10156	101	354	11730
	Old	1499	14184	75	406	16164
M2	New	1101	10181	101	353	11736
	Old	1474	14224	75	405	16178
M3	New	1115	10162	101	353	11731
	Old	1494	14195	75	406	16170
M4	New	1112	10156	101	353	11722
	Old	1489	14184	75	405	16153
M5	New	1105	10163	101	353	11722
	Old	1479	14196	75	405	16155

Table 4-19: Annual energy consumption of HVAC system (kWh) in Montréal, roof tilt angle of 26.6° and building azimuth of 90°

Method	Vintage	Space Cooling	Space Heating	Pump & MISC.	Vent. Fan	Total
Hourly R	New	1199	10176	100	353	11828
	Old	1630	14135	77	404	16246
M1	New	1218	10158	102	358	11836
	Old	1662	14111	77	411	16261
M2	New	1202	10185	102	357	11846
	Old	1635	14150	76	410	16271
M3	New	1215	10165	102	357	11839
	Old	1656	14120	77	411	16264
M4	New	1212	10159	102	357	11830
	Old	1651	14111	77	410	16249
M5	New	1206	10167	102	357	11832
	Old	1641	14122	77	410	16250

Table 4-20: Annual energy consumption of HVAC system (kWh) in Montréal, roof tilt angle of 45° and building azimuth of zero degree

Method	Vintage	Space Cooling	Space Heating	Pump & MISC.	Vent. Fan	Total
Hourly R	New	926	10055	100	335	11416
	Old	1211	14116	72	388	15787
M1	New	953	10056	101	339	11449
	Old	1255	14085	75	388	15803
M2	New	938	10082	101	338	11459
	Old	1233	14125	74	387	15819
M3	New	949	10062	101	339	11451
	Old	1250	14095	74	387	15806
M4	New	946	10055	101	339	11441
	Old	1246	14085	74	387	15792
M5	New	941	10063	101	338	11443
	Old	1237	14097	74	387	15795

Table 4-21: Annual energy consumption of HVAC system (kWh) in Montréal, roof tilt angle of 45° and building azimuth of 45°

Method	Vintage	Space Cooling	Space Heating	Pump & MISC.	Vent. Fan	Total
Hourly R	New	1107	10121	100	348	11676
	Old	1482	14131	77	396	16086
M1	New	1111	10124	101	352	11688
	Old	1486	14134	75	405	16100
M2	New	1095	10149	101	352	11697
	Old	1463	14173	75	403	16114
M3	New	1107	10130	102	352	11691
	Old	1481	14145	75	404	16105
M4	New	1104	10124	101	352	11681
	Old	1477	14134	75	404	16090
M5	New	1098	10130	101	351	11680
	Old	1468	14145	0	403	16091

<i>Table 4-22: Annual energy consumption of HVAC system (kWh) in Montréal, roof tilt angle of 45° and building azimuth of 45°</i>						
Method	Vintage	Space Cooling	Space Heating	Pump & MISC.	Vent. Fan	Total
Hourly R	New	1213	10133	102	353	11801
	Old	1652	14069	77	401	16199
M1	New	1219	10131	102	357	11809
	Old	1658	14065	77	410	16210
M2	New	1201	10156	102	356	11815
	Old	1633	14103	77	409	16222
M3	New	1215	10137	102	357	11811
	Old	1653	14074	77	410	16214
M4	New	1212	10131	102	356	11801
	Old	1648	14065	77	410	16200
M5	New	1205	10138	102	356	11801
	Old	1638	14077	77	409	16201

Figs. 4-7 and 4-8 state that the maximum estimation differences of the labeling approaches are less than 0.4%. Unlike previous locations where M2 can predict the performance of DRM with least estimation difference, here it has the maximum difference. It occurs because of low solar elevation angles in high latitudes. For example, highest solar elevation at Montréal is 68°. Hence the annual total HVAC estimation difference of M2 is limited to 0.4% or 0.4 kWh/m² (Fig. 4-9).

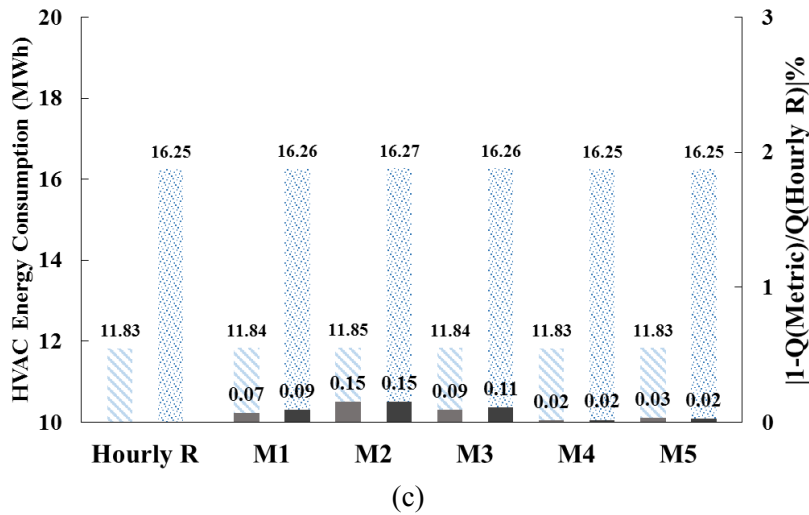
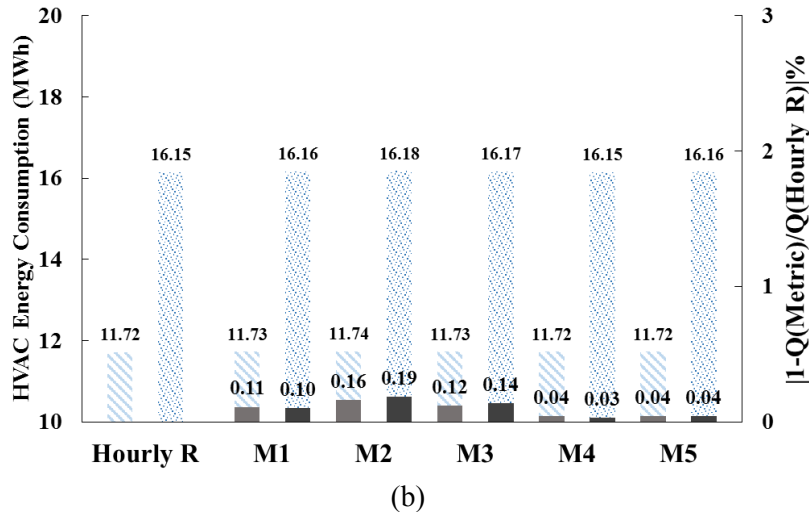
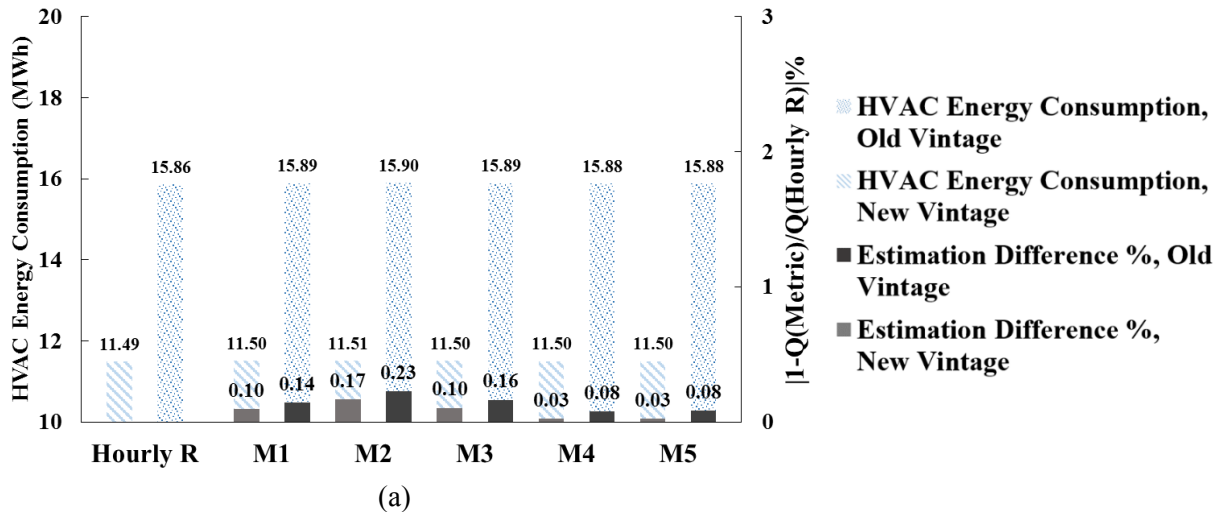


Fig. 4-7: Annual HVAC energy consumption and estimation difference between simulations with hourly reflectance and labeling approach reflectances (M1 to M5), for prototype in Montréal with tilt angle of 26.6°; building azimuth of (a) zero degree, (b) 45° and (c) 90°.

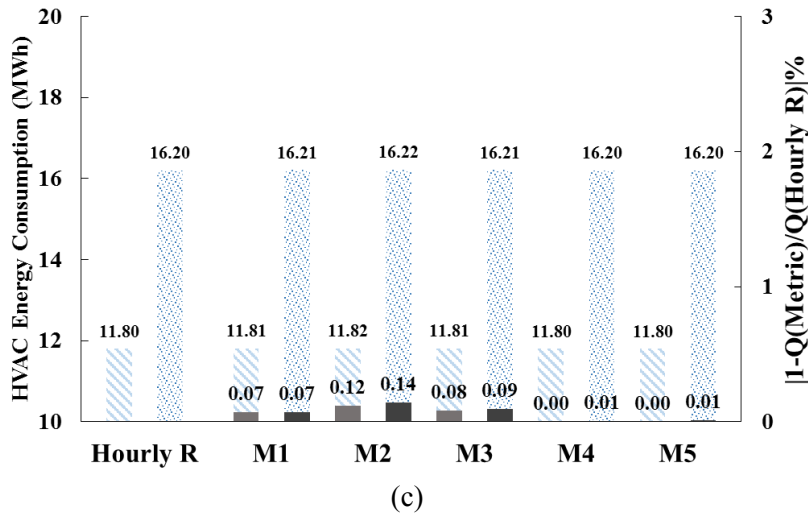
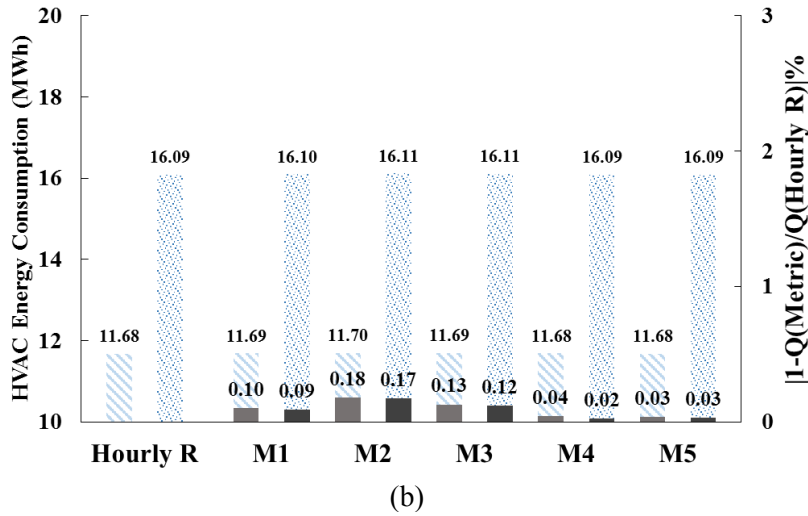
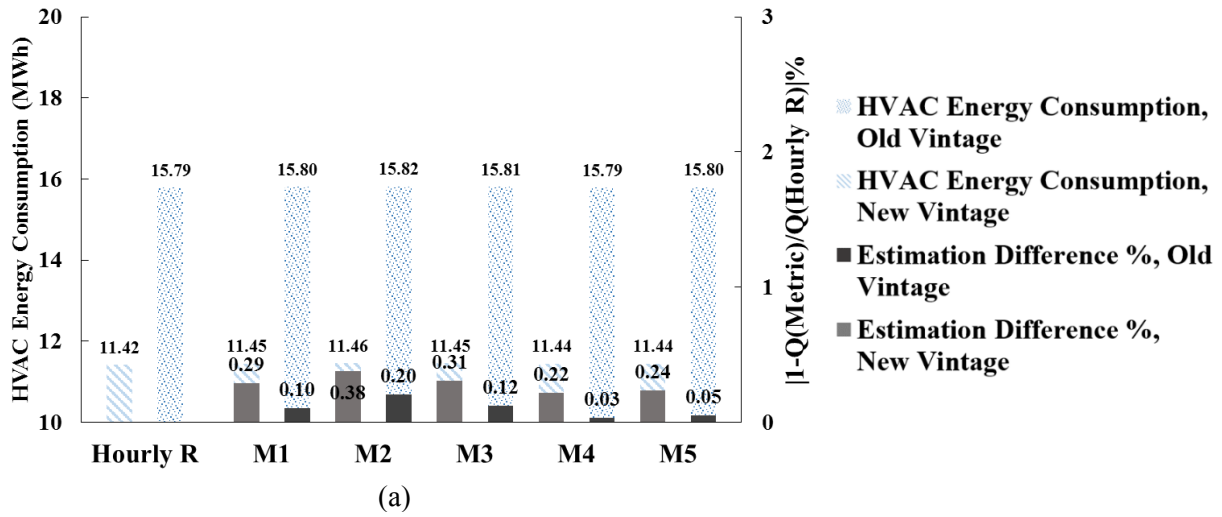


Fig. 4-8: Annual HVAC energy consumption and estimation difference between simulations with hourly reflectance and labeling approach reflectances (M1 to M5), for prototype in Montréal with tilt angle of 45°; building azimuth of (a) zero degree, (b) 45° and (c) 90°.

The range of estimation differences of the labeling approaches in predicting space cooling energy is around 3% (Fig. 4-9.a). This high estimation differences occur because of low cooling energy of Montréal (e.g., 20% of Sacramento cooling energy). So slightly difference in predicting $Q_{\text{Hourly R}}$ has high estimation differences. M2 has the least estimation difference of predicting annual space cooling energy by median and mean of 0.3% (0.03 kWh/m²) and 0.2% (0.02 kWh/m²). According to Table 4-23, M2 and M5 overestimate space cooling energy by no more than 0.59 kJ/m² or -3.7%. Other approaches has more maximum estimation differences up to -5.1% or -0.82 kJ/m². Results for cooling energy during swing season illustrate that the mean hourly reflectance is lower than R_{20} and higher than higher than R_{ave} . Hence M4 and M3, has the least maximum estimation difference in predicting the mean hourly cooling energy consumption during swing season (Table 4-23).

Table 4-23: Maximum estimation difference of the labeling approaches in estimating mean (hourly average) cooling and heating energy consumption in Sacramento

	Labeling approach	Summer	Winter	Swing season
Maximum estimation difference and maximum mean hourly difference of estimating space heating ¹	M1	-	-0.3% -0.41 kJ/m ²	0.3% 0.41 kJ/m ²
	M2	-	-0.4% -0.59 kJ/m ²	-0.6% -0.55 kJ/m ²
	M3	-	-0.3% -0.45 kJ/m ²	0.2% 0.32 kJ/m ²
	M4	-	-0.3% -0.36 kJ/m ²	0.4% 0.36 kJ/m ²
	M5	-	-0.3% -0.41 kJ/m ²	-0.4% -0.36 kJ/m ²
Maximum estimation difference and maximum mean hourly difference of estimating space cooling ²	M1	-5.1% -0.82 kJ/m ²	-	-2.7% -0.41 kJ/m ²
	M2	-3.7% -0.59 kJ/m ²	-	6.3% 0.45 kJ/m ²
	M3	-4.8% -0.77 kJ/m ²	-	-2.4% -0.36 kJ/m ²
	M4	-4.3% -0.68 kJ/m ²	-	-2.4% -0.36 kJ/m ²
	M5	-3.7% -0.59 kJ/m ²	-	5.0% 0.36 kJ/m ²

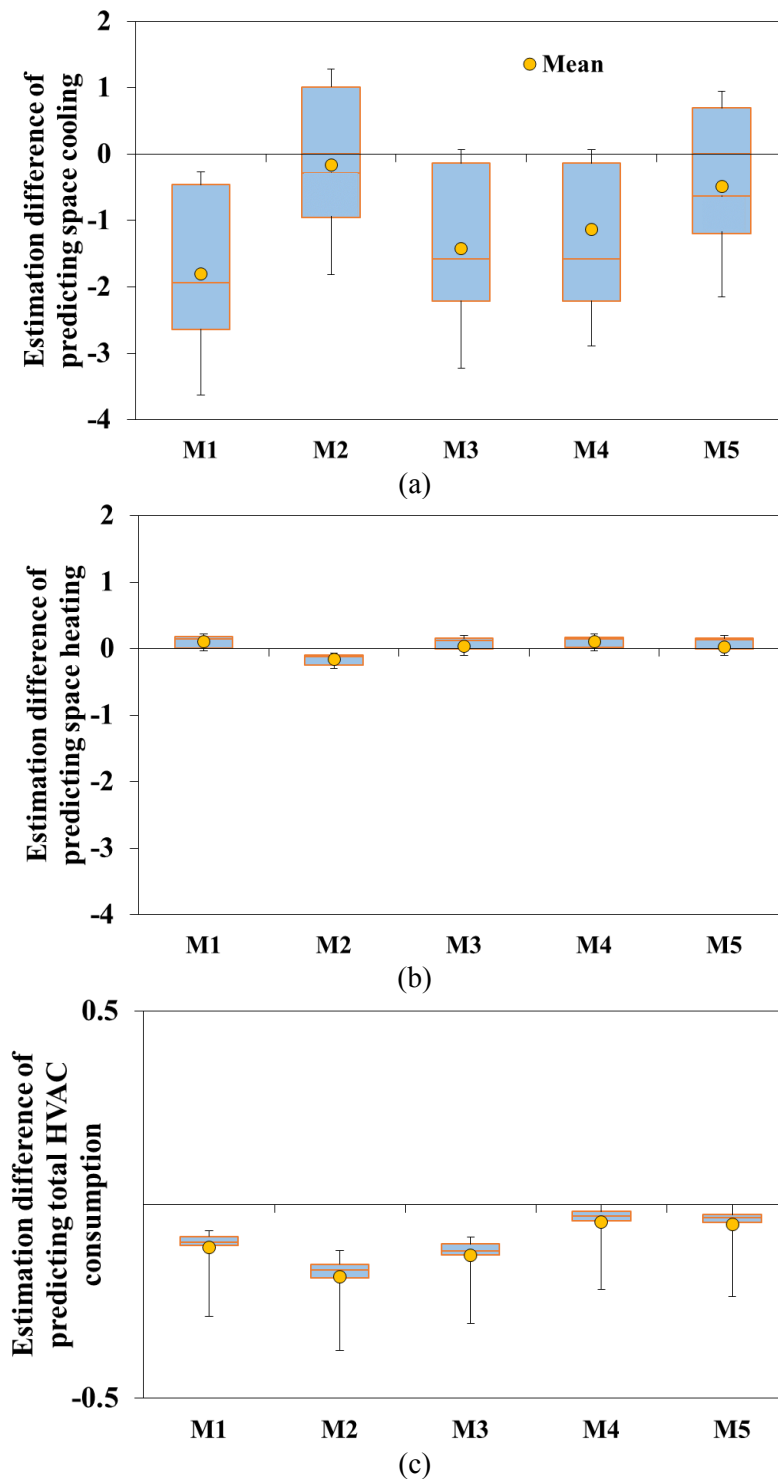


Fig. 4-9: The estimation difference ($\frac{Q_{Hourly R} - Q_{Metric}}{Q_{Hourly R}} \%$) of labeling approaches in predicting annual HVAC energy consumption of (a) space cooling and (b) space heating and (c) total HVAC energy consumption in Montréal. Minimum, 1st quartile, median, 3rd quartile and maximum amount of estimation differences of each approach. The mean is shown as circle marker.

As Fig. 4-9.b and Table 4-23 show the approach M2 underestimates the absorbed heat by roof during heating days. The annual and maximum mean hourly estimation difference of heating prediction by M2 are up to 0.3% (0.33 kWh/m²) and 0.45 kJ/m². Other approaches underestimate the annual heating energy by no more than 0.2% (0.24 kWh/m²). M5 has the least estimation difference of predicting annual heating energy by mean and maximum of 0.03 kWh/m² and 0.11 kWh/m² (0.1%), respectively.

Fig. 4-9.c demonstrates that all the approaches can predict solar heat gain through roof accurately. The maximum estimation difference of the annual total HVAC energy consumption of the approaches is up to 0.4% (0.47 kWh/m²) and it belongs to the M2. M4 has the best prediction of total HVAC energy consumption in Montréal by mean and maximum estimation difference of 0.0% (0.04 kWh/m²) and 0.2% (0.27 kWh/m²).

4.4 Peak demand estimation

All approaches can accurately predict the electricity peak demand. Table 4-24 shows the electricity peak demand of the prototype in Houston. As the table indicates, except May peak demand prediction of M1, the peak demand is precisely estimated by all the approaches. The results of peak load for all the simulated cases demonstrate that the peak load happens at either early morning (e.g. 8 AM) or late in the afternoon (e.g. 8 PM), when the irradiance is very small. Hence, the solar reflectance of roof has slightly effect on electricity peak demand. It can be concluded that the peak load in residential buildings is strongly dependent on the occupant schedule and miscellaneous equipment electricity consumption.

Table 4-24: Building electricity peak demand (kW) for new vintage in Houston with azimuth of zero degree and tilt angle of 45°

	Jan	Feb	Mar	Apr	May	Jun	Jul	Aug	Sep	Oct	Nov	Dec	Total
Day of a month	9	10	8	22	30	8	13	3	6	3	29	26	9
Time of a day	8	8	8	20	20	20	20	20	20	20	8	8	8
Hourly R	2.1	2.7	2.7	2.2	2.5	2.7	2.8	2.9	2.6	2.4	2.7	2.8	2.1
M1	2.1	2.7	2.7	2.2	2.6	2.7	2.8	2.9	2.6	2.4	2.7	2.8	2.1
M2	2.1	2.7	2.7	2.2	2.5	2.7	2.8	2.9	2.6	2.4	2.7	2.8	2.1
M3	2.1	2.7	2.7	2.2	2.5	2.7	2.8	2.9	2.6	2.4	2.7	2.8	2.1
M4	2.1	2.7	2.7	2.2	2.5	2.7	2.8	2.9	2.6	2.4	2.7	2.8	2.1
M5	2.1	2.7	2.7	2.2	2.5	2.7	2.8	2.9	2.6	2.4	2.7	2.8	2.1

4.5 Discussion

Simulations show that all the approaches can predict the annual energy consumption of HVAC system by up to 2.3% (1.43 kWh/m²) in Houston, 1.6% (0.74 kWh/m²) in Sacramento and 0.4% (0.47 kWh/m²) in Montréal.

The most accurate approach in predicting annual space cooling, space heating and total HVAC energy consumption in Houston and Sacramento is M2. It can accurately estimate the total annual energy consumption of HVAC system by no more than 1.7% (1.05 kWh/m²) and 0.9% (0.42 kWh/m²) in Houston and Sacramento, respectively.

The monthly results of HVAC energy consumption indicate M2 and M5 more accurately predict the thermal performance of DRM over summer period (May, June and July). M2 and M5 overestimate mean hourly space cooling energy during summer to within 3.04 kJ/m² and 1.87 kJ/m² in Houston and Sacramento, respectively. However, The Approaches M2 and M3 overestimate the mean hourly heating energy consumption to within 0.22 kJ/m² (4.5%) during winter time. Other approaches has the same maximum mean hourly heating overestimation. Their estimation differences are limited to 0.18 kJ/m² (3.6%).

The space cooling energy is more than space heating energy in Houston and Sacramento. Consequently, implementing summer reflectance (M2) can better

characterize the reflectance of DRMs in low latitudes and mid-mainland US. Using M2 in characterizing reflectance of DRMs can predict the annual space cooling energy by no more than 1.7% (0.92 kWh/m²) and 1.1% (0.3 kWh/m²) in Houston and Sacramento, respectively.

The effect of roof reflectance on HVAC energy consumption in mid-Northern America (e.g. Montréal) compared to mid-mainland US or lower latitudes, is much less. For example, Montréal has moderate sunny days during summer. Also it has short and typically cloudy days during winter while sun is low in the sky.

M4 has the best prediction of total HVAC energy consumption in Montréal by mean and maximum annual estimation differences of 0.0% (0.04 kWh/m²) and 0.2% (0.27 kWh/m²). Since M2 represents the summer solar reflectance, it accurately estimates the solar heat gain of roof during summer. However, using M2 to characterize the reflectance during heating season can exaggerate the annual space heating energy up to 0.3% (0.33 kWh/m²) in Montréal.

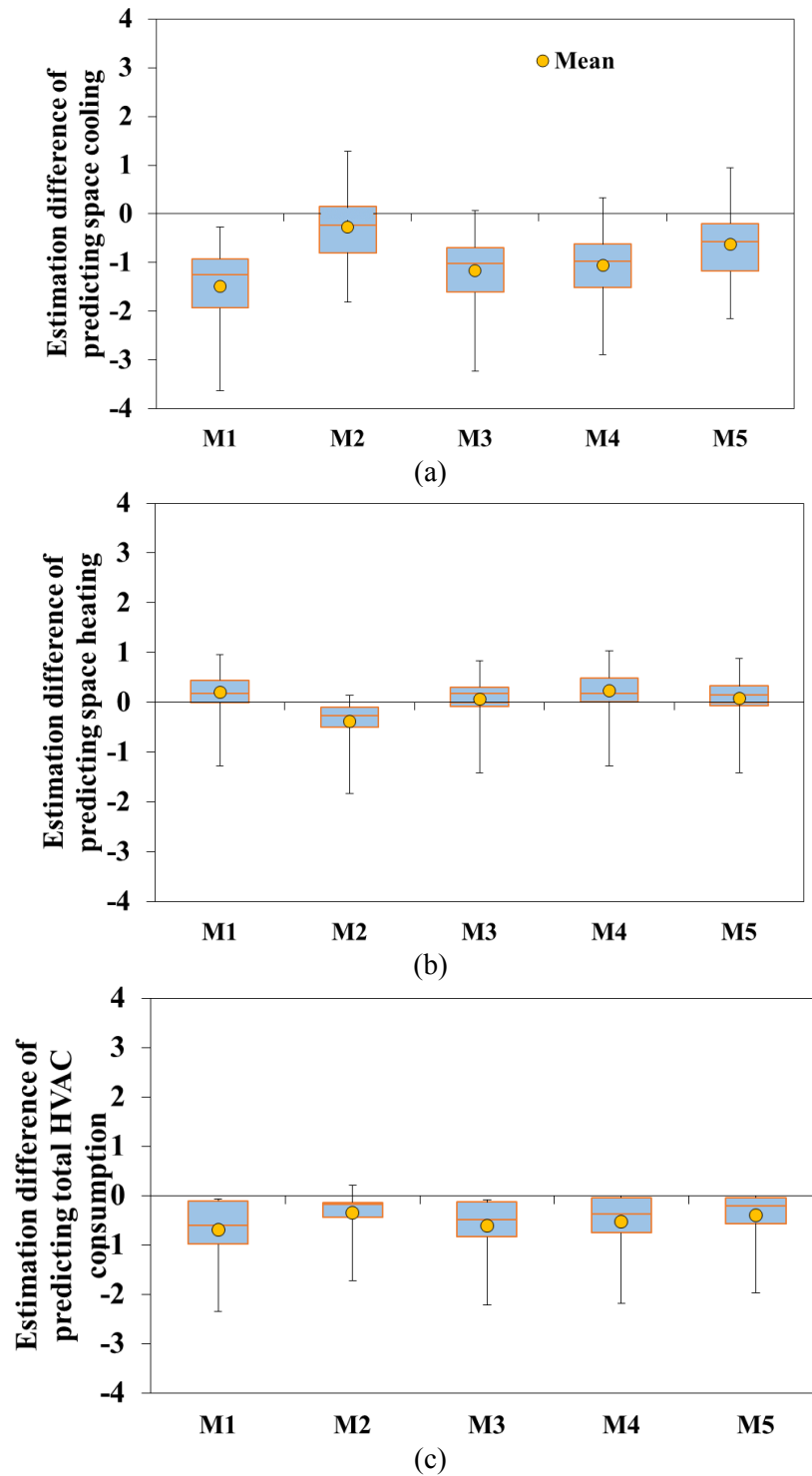


Fig. 4-10: Estimation difference $(\frac{Q_{Hourly R} - Q_{Metric}}{Q_{Hourly R}} \%)$ of labeling approaches in estimating annual HVAC energy consumption of (a) space cooling and (b) space heating and (c) total HVAC energy consumption in all the considered locations. Minimum, 1st quartile, median, 3rd quartile and maximum amount of estimation difference of each approach. The mean is shown as circle marker.

The estimation differences of considering the constant reflectance(s) of the labelling approaches for all the considered locations are assessed. The estimation differences in predicting the space cooling, heating and total HVAC energy consumption are illustrated in Fig. 4-10.

The approach M1 can estimate the space heating energy by no more than 1.2% estimation difference. However, M1 underestimates the reflectance of summer, because it overestimates the space cooling energy by median, mean and maximum of 1.2%, 1.5% and 3.6%.

M2 has the most accuracy in estimating space cooling energy by estimation difference no more than 1.8%. However, it overestimates the space heating energy by exaggerating reflectance of DRMs during winter-time. Since most of the HVAC energy consumption in Houston and Sacramento is related to space cooling, M2 is the most accurate approach to implement.

M3 and M4 consider a reflectance that it is more accurate in predicting annual space heating than space cooling. Therefore, they approximately have the same performance as M1. In addition, M4 has the best performance in predicting annual energy consumption in Montréal. M4 tends to overestimate the mean hourly heating space energy to within 0.36 kJ/m^2 . However, using M2 to characterize DRM reflectance in Montréal, rather than M4, can exaggerate the annual and mean hourly energy consumption by as much as 0.47 kWh/m^2 and 0.59 kJ/m^2 .

Using approach M5 instead of M2 can increase the mean and maximum estimation differences of space cooling from -0.3 and -1.8 to -0.6 and -2.1, respectively. (Fig. 4-10). Both approaches consider the same reflectance during summer. So the reason behind the higher estimation difference of M5 is related to the swing season reflectance. M5 consider the average of summer and winter reflectances for swing season that tends to overestimate the cooling energy.

M5 can estimate the annual heating energy better than does M2. Based on the analysis of all the simulations, the mean estimation difference of annual heating energy of M5 is 0.08% while M2 overestimates to within the mean of 0.39%.

To summarize, M2 is the most accurate model to be implemented for predicting the space cooling and total HVAC energy consumption of buildings. All approaches except M2 can accurately estimate the heating energy consumption. As it was expected, the mean and median of annual heating energy estimation differences of M1 is slightly lower than M3.

5 Summary and conclusion

The first objective of this research was to model DRMs incorporated with DOE-2.1E building energy analysis program. This model (called as hourly reflectance) is defined to simulate the energy consumption of HVAC system while reflectance of roof (DRM surface) is changed hourly.

Comparing the labelling approaches investigated by Akbari & Touchaei (2014) with hourly solar reflectance model was the second goal of this work. The comparison is based on the monthly and yearly results of HVAC energy consumption of the buildings simulated with DOE-2.1E. To meet these objectives, the following steps were taken.

First, a single family residential building prototype was selected from the DOE-2.1E sample run book (1993). Two vintages were considered for building prototype: old construction with old HVAC system (pre-1980) and new construction with new HVAC system. The data for modifying the building envelope and HVAC system of vintages were gathered from several sources.

Second, an algorithm was developed to calculate the solar incident angle on the perpendicular plane to DRM surface. Third, according to mean hourly solar incident angle, the reflectance of each simulation step (one hour) was looked up in the reflectance distribution of DRM.

Finally, energy consumption of the prototype building, while the reflectance was changing hourly ($Q_{\text{Hourly R}}$), was simulated using DOE-2.1E. Also, the simulations were performed while the reflectance was calculated based on the labeling approaches (Q_{Metric}). Then, the space cooling and heating, and the total HVAC energy consumptions were simulated. Finally, I compared the results by showing the estimation difference of the approach ($\frac{Q_{\text{Hourly R}} - Q_{\text{Metric}}}{Q_{\text{Hourly R}}} \%$). Simulations were performed for buildings with different azimuth and roof tilt angles in three cities across North America. Each location represents a specific climate region (i.e., hot, moderate and cold climates).

The approach M1 overestimates the annual space heating energy by no more than 1.2% (0.08 kWh/m²) in Houston and underestimates it to within 0.2% (0.28 kWh/m²) in Montréal. M1 underestimates the cooling energy consumption in all the cities up to 0.4 kWh/m².

M2 is the most accurate method in estimating annual space cooling energy by estimation difference no more than -1.7% (overestimation of 0.92 kWh/m²) in Houston, -1.1% (0.32 kWh/m²) in Sacramento and -1.8% (0.2 kWh/m²) in Montréal. According to monthly results, M2 overestimates mean hourly space cooling energy by up to 3.04 kJ/m² or 7.5%, during summer.

M2 overestimates the space heating energy by exaggerating reflectance of DRMs during winter. The approach M2 overestimates the annual space heating energy by as much as 1.8% (0.12 kWh/m²) in Houston, 0.5% (0.1 kWh/m²) in Sacramento and 0.3% (0.38 kWh/m²) in Montréal. The maximum mean hourly estimation difference of heating prediction by M2 is 0.45 kJ/m². Since most of the HVAC energy consumption in Houston and Sacramento is related to space cooling, M2 is the most accurate approach to implement.

M3 and M4 can predict annual space heating energy more accurately than space cooling energy. Therefore, they have approximately the same performance as M1. In addition, M4 has the best performance in predicting annual energy consumption in Montréal. M4 tends to overestimate the mean hourly heating space energy to within 0.36 kJ/m².

Using approach M5 instead of M2 can increase the maximum estimation difference of annual space cooling from -1.8% to -2.1%. Both approaches consider the same reflectance during summer. So the reason behind the higher estimation difference of M5 is related to the swing season reflectance. M5 consider the average of summer and winter reflectances for swing season that tends to overestimate the cooling energy. Assigning summer reflectance to swing season can significantly improve estimates of annual cooling energy use. For instance, the mean hourly estimation difference of the cooling energy predicted by M2 is not more than 0.36 kJ/m² (1.9%), in Houston. But

for the same location, maximum mean hourly estimation difference of the cooling energy predicted by M5 is 0.5 kJ/m^2 (2.7%).

Despite higher underestimation of annual heating energy, M2 can estimate total HVAC energy consumption in Houston and Sacramento much better than M5.

On the other hand, M5 can estimate the annual heating energy much more accurately than M2. The mean estimation difference of annual heating energy of M5 is 0.1% while M2 overestimates to within the mean of 0.4%. As it is expected, the M2 is more accurate than M5 in estimating annual total HVAC energy consumption. The mean, median and maximum estimation difference of predicting annual total HVAC system by M5 is -0.4%, -0.2% and -2%, respectively.

To summarize, M2 is the most accurate model to be implemented for predicting the space cooling and total HVAC energy consumption of buildings. Our results indicate that all the approaches except M2 can accurately estimate the heating energy consumption. However, M2 annual space heating estimation difference is limited to 0.38 kWh/m^2 .

5.1 Future work

In this study, the simulations for three cities across U.S mainland and southern of Canada were performed. Future work should consider more cities to more completely evaluate the performance of the labeling approaches. In addition, I propose investigating the accuracy of the labeling approaches in estimating thermal performance of DRMs on small commercial buildings (i.e. offices) with steep sloped roofs.

The accuracy of the labeling approaches in predicting electricity peak load can be further investigated by considering different occupancy schedule and building types (e.g. commercial buildings).

The effect of sunlight reflectance from surrounding buildings on energy consumption of building can be addressed in the developed algorithm (Appendix D).

Absence of the measured reflectances of DRM samples reasons us to use the tool prepared by Akbari & Touchaei (2014) to calculate hourly mean solar reflectance. This simulation tool is capable of applying different standard solar irradiances. In this study It was assumed that estimated reflectances by AM1GH standard solar irradiance condition (air mass 1 global horizontal) can represent the measured data in a laboratory (Levinson et al., 2010).

Further work should implement other solar radiation models to simulate the thermal performance of DRMs when they are exposed to the sunlight. For instance ASHRAE solar radiation algorithm (2007) propose a method with monthly variables for beam to diffuse ratio. Also using experimental solar radiation data from TMY3 can significantly improve the mean hourly estimated solar reflectance of DRMs, too.

5.2 Contribution

The algorithm can be used to simulate energy consumption of buildings with any type of roofs having variable solar reflectance. The solar reflectance of a roofing surface can be a function of solar incident angle and surface material. The developed algorithm is used to calculate the solar reflectance of a roof in each simulation time step. Results of this research advances the study of roofing surfaces having directional reflective materials.

5.3 Publications

The results of this thesis will be submitted to a peer-reviewed journal and 4th International Conference on Countermeasures to Urban Heat Island.

In addition to this thesis, the author investigated methods to improve the current standard of measuring solar reflectance of variegated roofing materials (CRRC, 2012), using Quasi-Monte Carlo techniques This study was presented in the Third International Conference on Countermeasures to Urban Heat Island, Venice 2014 (Hooshangi et al., 2014). The complete version of this paper is accepted for publishing in journal of Energy and Buildings, Elsevier (Hooshangi et al., 2015).

Finally, the author performed feasibility and sensitivity analysis of wind-diesel hybrid power system for remote communities of North of Quebec. This study presented in International Conference on Clean Energy (ICCE2013), Ottawa. Also, it was nominated by the conference scientific committee for publishing in Journal of Advances in Clean Energy (Hooshangi, 2014).

Bibliography

- Ahrab, M., & Akbari, H. (2013). Hygrothermal behaviour of flat cool and standard roofs on residential and commercial buildings in North America. *Building and Environment*, 60, 1-11.
- Akbari, H. (2005). Energy Saving Potentials and Air Quality Benefits of Urban Heat Island Mitigation. *Lawrence Berkeley National Laboratory*, No. LBNL--58285.
- Akbari, H., & Levinson, R. (2008). Evolution of Cool-Roof Standards in the US. *Advances in Building Energy Research*, 1-32.
- Akbari, H., & Taha, H. (1992). The impact of trees and white surfaces on residential heating and cooling energy use in four Canadian cities. *Energy*, 17(2), 141-149.
- Akbari, H., & Touchaei, A. (2013). The climate effects of increasing the albedo of roofs in a cold region. *34th AIVC Conference*. Athens.
- Akbari, H., & Touchaei, A. (2014). Modeling and labeling heterogeneous directional reflective roofing materials. *Solar Energy Materials and Solar Cells*, 124, 192-210.
- Akbari, H., Bretz, S., Hanford, J., Rosenfeld, A., Sailor, D., Taha, H., & Bos, W. (1992). *Monitoring peak power and cooling energy savings of shade trees and white surfaces in the Sacramento Municipal Utility District (SMUD) Project design and preliminary results*. CA (United States): Lawrence Berkeley Lab. (No. LBL--33342).
- Akbari, H., Levinson, R., & Berdahl, P. (2012). Cool materials rating instrumentation and testing. In D. Kolokotsa, M. Santamouris, & H. Akbari, *Advances in the development of cool* (pp. 174-194). Bentham Science Publishers.
- Akbari, H., Levinson, R., & Berdahl, P. (2012). Cool Materials Rating Instrumentation and Testing. In D. Kolokotsa, M. Santamouris, & H. Akbari, *Advances in the Development of Cool Materials for the Built Environment* (pp. 174-194).
- Akbari, H., Levinson, R., & Stern, S. (2008). Procedure for measuring the solar reflectance of flat or curved roofing assemblies. *Solar Energy* 82, 648–655.
- Akbari, H., Pomerantz, M., & Taha, H. (2001). Cool surfaces and shade trees to reduce energy use and improve air quality in urban areas. *Solar energy*, 70(3), 295-310.
- Akbari, H., Pomerantz, M., & Taha, H. (2001). Cool surfaces and shade trees to reduce energy use and improve air quality in urban areas. *Solar energy*, 70(3), 295-310.
- ASHRAE. (1999). ASHRAE Standard 90.1-1999: Energy Standard for Buildings Except Low-Rise Residential Buildings, SI Edition. *American Society of Heating, Refrigerating and Air-Conditioning Engineers, Atlanta, GA*.
- ASHRAE. (2001). ASHRAE Standard 90.1-2001: Energy Standard for Buildings Except Low-Rise Residential Buildings, SI Edition. *American Society of Heating, Refrigerating and Air-Conditioning Engineers, Atlanta, GA*.

- ASHRAE. (2004a). ASHRAE Standard 90.1-2004: Energy Standard for Buildings Except Low-Rise Residential Buildings, SI Edition. *American Society of Heating, Refrigerating and Air-Conditioning Engineers, Atlanta, GA.*
- ASHRAE. (2004b). ASHRAE Standard 90.2-2004: Energy-Efficient Design of Low-Rise Residential Buildings. *Society of Heating, Refrigerating and Air-Conditioning Engineers, Atlanta, GA.*
- ASHRAE. (2007). *ASHRAE HVAC Application, American Society of Heating Refrigerating and Air-Conditioning Engineers.* Atlanta (GA), US.
- ASHRAE. (2007). ASHRAE Standard 90.1-2007: Energy Standard for Buildings Except Low-Rise Residential Buildings, SI Edition. *American Society of Heating, Refrigerating and Air-Conditioning Engineers, Atlanta, GA.*
- ASHRAE. (2010). ASHRAE Standard 189.1, Standard for the Design of High-Performance Green Buildings Except Low-Rise Residential Buildings. *American Society of Heating, Refrigerating and Air-Conditioning Engineers, Atlanta, GA.*
- ASHRAE. (2010). ASHRAE Standard 90.1-2010: Energy Standard for Buildings Except Low-Rise Residential Buildings, SI Edition. *American Society of Heating, Refrigerating and Air-Conditioning Engineers, Atlanta, GA.*
- ASTM. (2006). ASTM E1918-06: Standard Test Method for Measuring Solar Reflectance of Horizontal and Low-Sloped Surfaces in the Field. *www.astm.org*, DOI: 10.1520/E1918-06.
- ASTM. (2009). ASTM C1549-09: Standard Test Method for Determination of Solar Reflectance near Ambient Temperature Using a Portable Solar Reflectometer, ASTM.
- ASTM. (2012). ASTM E903-12: Standard Test Method for Solar Absorptance, Reflectance, and Transmittance of Materials Using Integrating Spheres. *www.astm.org*, DOI: 10.1520/E0903-12.
- ASTM E903-12. (2012). Standard Test Method for Solar Absorptance, Reflectance, and Transmittance of Materials Using Integrating Spheres. *www.astm.org*, DOI: 10.1520/E0903-12.
- ASTM standard C1549-09. (2009). ASTM C 1549-09: Standard Test Method for Determination of Solar Reflectance Near Ambient Temperature Using a Portable Solar Reflectometer. *American Society for Testing and Materials.*
- Canada National Research Council. (May 1999). Performance Compliance for Buildings.
- CEC (California Energy Commission). (2008). Energy Efficiency Standards for Residential and Nonresidential Buildings. *California Energy Commission, Sacramento, CA.*
- Chicago. (2001, June 6). Amendment of Title 18 of Municipal Code of Chicago Concerning Energy Efficiency Requirements. *Journal of the City Council of Chicago*, p60939.
- Chicago. (2007). *City of Chicago Energy Conservation Code.* Chicago, IL: Index Publishing Corporation.

- Crawley, D., Hand, J., Kummert, M., & Griffith, B. (2008). Contrasting the capabilities of building energy performance simulation programs. *Building and environment*, 43(4), 661-673.
- CRRC. (2012). *CRRC-1 TEST METHOD #1: Standard Practice for Measuring Solar Reflectance of a Flat, Opaque, and Heterogeneous Surface Using a Portable Solar Reflectometer*. Retrieved from <http://www.coolroofs.org/>
- Deru, M. F. (2011). *US Department of Energy commercial reference building models of the national building stock*. Golden, CO: National Renewable Energy Laboratory.
- DOE official website-EnergyPlus. (n.d.). *About EnergyPlus*. Retrieved from EnergyPlus Energy Simulation Software: <http://apps1.eere.energy.gov/>
- DOE-2. (1980). *DOE-2 Refrence Manual, Part 1*. Lawrence Berkeley Laboratory.
- DOE-2. (1982). *DOE-2 Engineers Manual, version 2.1A*. Lawrence Berkeley Laboratory.
- DOE-2. (1991). *DOE-2 Basics, version 2.1E*. Lawrence Berkeley Laboratory LBL.
- DOE2 official website. (n.d.). Retrieved from DOE2: www.doe2.com
- Duffie, J., & Beckman, W. (2006). *Solar Engineering of Thermal Processes , third ed.* New Jersey: John Wiley and Sons, Inc.
- EN 14500. (2008). Blinds and Shutters – Thermal and Visual Comfort – Test and Calculation Methods. *BSI*.
- EPA (US Environmental Protection Agency). (2007). *Roof Products Criteria for US EPA Energy Star Program*. Retrieved from www.energystar.gov/index.cfm?c=roof_prods.pr_crit_roof_products
- Hooshangi, H. (2014). Feasibility study of wind-diesel hybrid power system for remote communities in north of Quebec. *Journal of Advances in Clean Energy*, 1, 84-95.
- Hooshangi, H., Akbari, H., & Touchaei, A. (2014). Measuring Solar Reflectance of Variegated Flat Roofing Materials Using Modified Monte Carlo Method. *Third International Conference on Countermeasures to Urban Heat Island*. Venice.
- Hooshangi, H., Akbari, H., & Touchaei, A. (2015). Measuring Solar Reflectance of Variegated Flat Roofing Materials Using Quasi-Monte Carlo Method. *Energy and Buildings*.
- Hosseini, M. (2014). *Cool Roofs Savings and Penalties in Cold Climates: the Effect of Snow Accumulation on roof*. Montreal: Concordia University.
- Hosseini, M., & Akbari, H. (2014). Heating energy penalties of cool roofs: the effect of snow accumulation on roofs. *Advances in Building Energy Research*, 8(1), 1-13.
- Islands, R. U. (2008). *Reducing Urban Heat Islands: Compendium of Strategies Cool Roofs*. Retrieved from <http://www.epa.gov/heatisland/resources/pdf/CoolRoofsCompendium.pdf>.
- Konopacki, S. A. (1997). *Cooling energy savings potential of light-colored roofs for residential and commercial buildings in 11 US metropolitan areas*. CA (United States): Lawrence Berkeley Lab.

- Konopacki, S., Gartland, L., Akbari, H., & Rainer, L. (1998). *Demonstration of Energy Savings of Cool Roofs*, . Berkeley, CA: Lawrence Berkeley National Laboratory.
- Kreider, J. (2000). *Handbook of heating, ventilation, and air conditioning*. CRC Press.
- Lawrence Berkeley National Laboratory. (1993). *Sample Run Book, version 2.1E*.
- Levinson, R., & Akbari, H. (2010). Potential benefits of cool roofs on commercial buildings: conserving energy, saving money, and reducing emission of greenhouse gases and air pollutants. *Energy Efficiency*, 3(1), 53-109.
- Levinson, R., Akbari, H., & Berdahl, P. (2010). Measuring solar reflectance—Part I: Defining a metric that accurately predicts solar heat gain. *Solar Energy*, 84(9), 1717-1744.
- Levinson, R., Akbari, H., & Reilly, J. (2007). Cooler tile-roofed buildings with near-infrared-reflective non-white coatings. *Building and Environment*, 42(7), 2591-2605.
- Levinson, R., Berdahl, P., Akbari, H., Miller, W., Joedicke, I., Reilly, J., . . . Vondran, M. (2007). Methods of creating solar-reflective nonwhite surfaces and their application to residential roofing materials. *Solar Energy Materials and Solar Cells*, 91(4), 304–314.
- Liggett, R., & Milne, M. (2008). Climate consultant 6. Los Angeles: : UCLA, Energy Design Tool Group.
- Masatoshi , N., Craig , F., Minako , N., & Masaki , N. (2013). Numerical study on specular solar reflectors aimed at increasing solar reflectivity of building envelope. *13th Conference of International Building Performance Simulation Association*. Chambéry, France.
- Pacific Northwest National Laboratory. (2013, July 11). *Building Energy Codes Program*. Retrieved from ENERGY.GOV: www.energycodes.gov
- Rose, W. (2007). White Roofs and Moisture in the US Desert Southwest. *Proceedings from ASHRAE Buildings X Conference*. Clearwater Beach, Florida.
- Sakai, H., Emura, K., Igawa, N., & Iyota, H. (2012). Reduction of reflected heat of the sun by retroreflective materials. *Journal of Heat Island Institute International*, Vol, 7, 2.
- Santamouris, M., Synnefa, A., & Karlessi, T. (2011). Using advanced cool materials in the urban built environment to mitigate heat islands and improve thermal comfort conditions. *Solar Energy*, 85(12), 3085-3102.
- Synnefa, A., Dandou, A., Santamouris, M., Tombrou, M., & Soulakellis, N. (2008). On the use of cool materials as a heat island mitigation strategy. *Journal of Applied Meteorology and Climatology*, 47(11), 2846-2856.
- Synnefa, A., Santamouris, M., & Akbari, H. (2007). Estimating the effect of using cool coatings on energy loads and thermal comfort in residential buildings in various climatic conditions. *Energy and Buildings*, 39(11), 1167-1174.
- Synnefa, A., Santamouris, M., & Apostolakis, K. (2007). On the development, optical properties and thermal performance of cool colored coatings for the urban environment. *Solar Energy*,, 81(4), 488-497.

- Taha, H., Konopacki, S., & Akbari, H. (1996). *Emission and Atmospheric Impacts of Reduced Urban Surface and Air Temperatures in the South Coast Air Basin*. Berkeley, CA: Lawrence Berkeley National Laboratory Report (LBL-39298).
- Winkelmann, F., Birdsall, B., Buhl, W., Ellington, K., Erdem, A., Hirsch, J., & Gates, S. (1993). *DOE-2 Supplement, Version 2.1E*. Springfield, Virginia National Technical Information Service.: Lawrence Berkeley Laboratory. .
- Yuan, J., Emura, K., & Sakai, H. (2012). Evaluation of the solar reflectance of highly reflective roofing sheets installed on building roofs. *Journal of Building Physics*, 37(2) 170–184.

Appendix A: Requirements of standards for cool roofs

The standards for cool roofs help owners to promote building energy efficiency and climate-appropriate use, and also stimulate the development of cool roof technology. Mostly two types of requirements defined by standard organizations: prescriptive and mandatory. Prescriptive compliance is the simplest path and requires (May 1999). Performance compliance is an option that permits to deviate from prescriptive requirements; however annual energy consumption by proposed design must be no greater than that of a reference case (by using computer software).

Appendix A.1: ASHRAE Standard 90.1

Mandatory and prescriptive requirements for buildings in USA are prescribed by American Society of Heating, Refrigerating and Air-Conditioning Engineers (ASHRAE). In 1999, ASHRAE Standard 90.1 (1999) credited cool roofs for high-rise residential and non-residential buildings for the first time (Akbari & Levinson, 2008). The prescriptive requirements for initial solar reflectance and thermal emittance of cool roofs assumed to be 0.70 and 0.75, respectively. Performance compliance of cool roofs for proposed building should have reflectance of at least 0.45.

The optionality and minimum requirements of cool roofs in ASHRAE 90.1-2001 (2001), ASHRAE 90.1-2004 (ASHRAE, 2004a) and ASHRAE 90.1-2007 (2007) is remained without any changes. In ASHRAE 90.1-2007, for proposed buildings in climate zones 1 through 3 with high albedo roofs, the roof insulation is allowed to be reduced. The ASHRAE 90.1-2010 (2010) has mandatory prescriptive requirements for roof solar reflectance and thermal emittance of proposed buildings in climate zones 1 through 3. A minimum three-year-aged solar reflectance and thermal emittance must be higher than 0.55 and 0.75, respectively.

ASTM C1549 or ASTM E1918, and, ASTM C1371 or ASTM E408 are accepted for testing solar reflectance and thermal emittance, respectively. However, many roof types, e.g. ballasted roofs, vegetated roofs etc., are excluded from this

compliances. It also states that measuring solar reflectance and thermal emittance shall be conducted by a laboratory accredited by a nationally recognized organization.

Appendix A.2: ASHRAE Standard 90.2

ASHRAE 90.2 is a residential energy standard that provide minimum requirements (both prescriptive and performance compliance by using DOE-2.1 simulation software) in low-rise residential buildings (single family to multi-family).

One of the ways of recognizing the coolness of a material is using Solar Reflectance Index (*SRI*). E1980 introduces *SRI* as Eq. A-1:

$$SRI = \frac{T_b - T_s}{T_b - T_w} \quad \text{Eq. (A-1)}$$

where T_b , T_s and T_w are the steady-state temperature of black, sample and white surfaces, respectively. For obtaining T_s we can use the Conservation Energy Law. Solar Reflectance Index of clean black surface ($S=0.05$ and $\varepsilon=0.90$) and clean white surface ($S=0.80$ and $\varepsilon=0.90$) are defined zero and 100.

In ASHRAE 90.2-2004 (2004b) a minimum solar reflectance and a minimum thermal emittance of cool roofs defined as 0.65 and 0.75, respectively. The compliance performance for cool and non-cool roofs is ambiguous. Also, the code for prescriptive compliance is related to the thermal transmittance of roof assembly. In other words, the minimum requirement of cool roofs in this code is adjusted by thermal transmittance of roof. In 2007 edition, minimum requirements are remained constant and it allows the residential building equipped with cool roofs to have a lower insulation.

Appendix A.3: International energy conservative code

The other primary organization, International Code Council (ICC) prepared the International Energy Conservative Code (IECC). IECC 2003, 2006 and 2009 editions referenced the ASHRAE 90.1 for minimum requirements of solar reflectance and thermal emittance of roofs. This code contains prescriptive and performance appliance for commercial and residential buildings. In version 2012, IECC added the minimum solar reflectance and thermal emittance of roofs in climate zones 1-3 that have a slope

less than 2 in 12 (Table A-3). This code separates requirements for three-year aged solar reflectance and thermal emittance of roofs which the initial values are unknown. Using the CRRC-1 standard is not referenced in this standard.

Appendix A.4: California energy commission's Title 24

Cool roofs have been considered by The California Energy Commission's Title 24 Energy Efficiency Standards for Residential and Non-residential Buildings since 2001. Cool roof materials in new constructions or major re-roofing projects are subjected by prescriptive requirements of California Title 24-2008 (2008). Table A-1 shows the minimum requirements based on types of the buildings.

According to section 10-113 of Title 24, solar reflectance (initial and three-year aged) and thermal emittance of cool roof products should be measured and labelled by the Cool Roof Rating Council (CRRC). For roofing materials which three-year aged solar reflectance of them are not tested by CRRC, the 3-year aged values must be derived from the following equation (Eq. A-2).

$$R_{aged} = [0.2 + 0.7(\rho_{initial} - 0.2)] \quad \text{Eq. (A-2)}$$

where $\rho_{initial}$ represents the initial solar reflectance. Also the asphalt shingles and all other roofing products which their CRRC tests are not available the default ratings for aged solar reflectance (and thermal emittance) assumed as 0.08 (0.75) for asphalt shingles and 0.10 (0.75) for all other type of roofing products. It should be noted that Title 24 consists of many exceptions to these roofing requirements.

Table A-1. Typical minimum cool roof requirements assumed by Title 24

Application	Roof type	Roof weight (lb/ft ²)	Climate zones	Solar reflectance [3-year aged]	Thermal emittance	SRI
Non-residential	Low slope	-	2-15	0.55	0.75	64
	Steep sloped	< 5	2-16	0.20	0.75	16
		>5 (& <25)	1-16	0.15	0.75	10
Low-rise residential	Low slope	<5	10-15	0.20	0.75	16
		>5	1-16	0.15	0.75	10
		-	13-15	0.55	0.75	64
	Steep slope	<5	10-15	0.2	0.75	16
		>5	1-16	0.15	0.75	10
	High-rise residential	Steep slope	-	10, 11, 13, 14, 15	0.55	0.75

Appendix A.5: Energy Star for roof products

Manufacturers can voluntarily participate in the Energy Star program. A product can qualify, if it meets the solar reflectance requirements expressed in Table A-2. For aesthetical aspects of buildings the minimum criteria for steep sloped is lower than low sloped roofs. The emissivity of products must be reported by manufacturers but this standard has not emissivity level requirement.

Table A-2. ENERGY STAR for roof products (Version 2.0) qualifying criteria (Islands, 2008)

Standard	Roof Type	Initial Solar Reflectance	Test Methods	3-year Aged Solar Reflectance	Test Methods
ENERGY STAR®	Low sloped (<9.5°)	0.65	ASTM E 903 or ASTM C 1549	0.50	ASTM E 1918 or ASTM C 1549
	Steep sloped (>9.5°)	0.25	ASTM E 903 or ASTM C 1549	0.15	ASTM C 1549

Appendix A.6: Cool-roof provisions in other standards and programmes

Other requirements for cool roofs such as ASHRAE Standard 189.1-2010 and Standard for the Design of High-Performance Green Buildings Except Low-Rise Residential Buildings (ASHRAE, 2010) and The U.S. Environmental Protection Agency’s (EPA) ENERGY STAR Reflective Roof Program (2007), Chicago (2001) (2007), are listed in Table A-3.

Table A- 3. Typical minimum cool roof requirements

Standard	Building Type	Roof Type	Initial Solar Reflectance	3-year Aged Solar Reflectance	Thermal Emittance [new or aged]	SRI [3-year aged]
Chicago, Illinois	-	Low sloped (<2:12)	0.65	0.50	-	-
		Medium-sloped (>2:12)	0.15	0.15	-	-
IECC (2012)	Commercial	Low sloped		0.55 (or initial 0.7)	0.75 (or initial 0.75)	64 (or initial 82)
ASHRAE Standard 189.1 (2010)	Except low-rise residential in climate zones 1-3	Low sloped		-	-	Initial 78
		Steep sloped		-	-	Initial 29

Appendix B. Cool roof solar reflectance measurement process

There are several instruments and test methods for measuring solar reflectance and thermal emittance of roof products. ASTM International has several test methods for measuring properties of materials (Table B-1). Also Cool Roof Rating Council (CRRC) has proposed a method (CRRC, 2012) for measuring the solar reflectance of variegated roof materials with portable solar reflectometer. The brief description of different standards for most common optical measurement instruments are shown in Table B-1 and the description of instruments are as follows:

i. Pyranometer is used for measuring solar reflectance of large flat or rough surfaces with area of 10m^2 . According to ASTM E1918-06 (2006), the global solar reflectance of horizontal or near horizontal surface (pitch $\leq 2:12$) should be measured in clear-sky where the angle between the solar beam and the surface normal (θ) is less than 45 degrees. Additionally, pyranometer is practical for tests on rough and/or variegated surfaces. Akbari et al. (2008) have proposed the development of “ASTM E1918” to measure reflectivity of samples whose areas are about 1 m^2 . However, need for clear sky and certain range of solar zenith angle ($z < 45$ based on method E1918) limited using pyranometer.

ii. The solar spectral (near-hemispherical) reflectance and transmittance of small samples (0.1 cm^2) can be measured by spectrophotometer equipped with an integrating sphere. The spectrophotometer projects light in the range of 250 to 2500 nm through several diffraction grating and mirrors. After striking lights on sample, the reflected lights from the sample are gathered in an integrated sphere and sensors measure the value of reflectance of opaque sample. Spectrophotometer accurately measures the flat and uniform samples. However, for flat, non-uniform, large sample, average of reflectance of non-overlapped spots can represent the mean reflectance of sample (Akbari et al., 2012). ASTM E903-12 (2012) and EN 14500 (2008) are methods for measuring specular and diffuse optical properties of samples by means of spectrophotometer.

iii. Portable reflectometer is quick and accurate instrument which is suitable for small area (2 cm^2) of uniform and homogenous samples. The radiation source of

reflectometer provides diffused radiations. This illumination is stroked at the sample port. Then the reflected radiation is detected by sensors which are installed in 20 degrees from normal. Measurements can be conducted based on ASTM C1549-09 (2009).

However, to measure solar reflectance of non-uniform flat and heterogeneous samples, Akbari et al. (2008) devised a statistical method C1549MC, also called CRRC-1 Test Method#1. This technique estimates the mean solar reflectance by measuring solar reflective of several random location (non-overlapping spots). CRRC propose this procedure for the reflectance measuring of the fiberglass asphalt shingle and other variegated samples.

Table B-1. Summary of standards for measuring solar reflectance

Standard	Instrument	Sample area	Measurements
ASTM E903	Integrating sphere spectrophotometer	0.1 cm ²	Solar spectral (near-hemispherical) reflectance and transmittance
ASTM C1549	Portable solar reflectometer	2 cm ²	Solar reflectance for AM 0, 1, 1.5 & 2. Accurate for opaque and uniform surfaces
ASTM E1918	Pyranometer	Large surfaces (10 m ²)	Global solar reflectance of horizontal and low-sloped surfaces, suitable for non-uniform and rough surfaces
C1549MC	Portable solar reflectometer	2 cm ²	Use for large and/or variegated surfaces

Appendix C. Monthly result of HVAC energy consumption

In this Appendix, the monthly results of the space cooling and space heating energy consumption of HVAC system are summarized. Table C-1 to Table C-4 show the monthly results for Houston. The results of Sacramento are listed in Table C-5 to Table C-8. Finally, the results related to prototypes in Montreal are detailed in Table C-9 to Table C-12.

Table C-1: Monthly cooling and heating energy consumption of HVAC system (kWh), old vintage in Houston, roof tilt angle of 26.6°

	Jan	Feb	Mar	Apr	May	Jun	Jul	Aug	Sep	Oct	Nov	Dec	Total
Building azimuth of zero degree													
Space Heating													
Hourly R	129	135	144	9	0	0	0	0	0	15	91	213	736
M1	129	135	137	8	1	0	0	0	0	15	91	213	729
M2	130	135	138	9	1	0	0	0	0	15	92	215	735
M3	130	135	137	8	1	0	0	0	0	15	91	213	730
M4	129	135	137	8	1	0	0	0	0	15	91	213	729
M5	129	135	137	9	1	0	0	0	0	15	91	213	730
Space Cooling													
Hourly R	153	186	242	424	693	904	1071	1029	777	615	254	157	6505
M1	151	189	248	432	700	970	1080	1035	786	623	257	159	6630
M2	148	187	245	427	695	965	1073	1029	781	619	254	156	6579
M3	151	188	247	431	699	969	1078	1034	785	622	256	158	6618
M4	151	189	248	431	697	967	1076	1034	785	622	257	160	6617
M5	151	188	247	429	695	965	1073	1032	784	621	257	159	6601
	Jan	Feb	Mar	Apr	May	Jun	Jul	Aug	Sep	Oct	Nov	Dec	Total
Building azimuth of 45°													
Space Heating													
Hourly R	137	138	139	7	0	0	0	0	0	16	98	233	768
M1	139	139	134	7	1	0	0	0	0	16	97	236	769
M2	139	140	136	7	1	0	0	0	0	16	98	237	774
M3	139	139	134	7	1	0	0	0	0	16	97	236	769
M4	138	139	134	7	1	0	0	0	0	16	97	236	768
M5	139	139	135	7	1	0	0	0	0	16	97	236	770
Space Cooling													
Hourly R	148	190	260	479	733	944	1132	1086	814	628	246	146	6806
M1	146	192	264	485	740	1011	1135	1092	819	632	246	147	6909
M2	145	190	259	480	734	1005	1129	1087	814	627	244	145	6859
M3	146	191	263	484	739	1010	1134	1091	818	631	246	146	6899
M4	147	191	264	484	737	1008	1132	1091	818	631	247	148	6898
M5	146	191	263	483	734	1005	1129	1090	817	630	246	147	6881
Building azimuth of 90°													
Space Heating													
Hourly R	130	136	138	5	0	0	0	0	0	14	88	217	728
M1	132	135	132	6	1	0	0	0	0	14	88	221	729

M2	133	136	134	6	1	0	0	0	0	14	90	222	736
M3	132	136	133	6	1	0	0	0	0	14	88	221	731
M4	132	136	133	6	1	0	0	0	0	14	88	221	731
M5	132	136	133	6	1	0	0	0	0	14	88	221	731
Space Cooling													
Hourly R	156	196	273	513	755	967	1153	1122	845	660	256	141	7037
M1	148	199	278	519	759	1032	1159	1127	851	663	257	138	7130
M2	146	197	274	514	754	1027	1153	1122	846	659	254	136	7082
M3	148	199	277	517	758	1031	1157	1126	850	662	256	137	7118
M4	148	199	277	518	757	1029	1155	1126	850	662	258	138	7117
M5	148	197	275	516	754	1027	1153	1125	849	661	257	138	7100

Table C-2: Monthly cooling and heating energy consumption of HVAC system (kWh), old vintage in Houston, roof tilt angle of 45°

	Jan	Feb	Mar	Apr	May	Jun	Jul	Aug	Sep	Oct	Nov	Dec	Total
Building azimuth of zero degree													
Space Heating													
Hourly R	126	134	142	9	0	0	0	0	0	14	88	206	719
M1	127	134	136	8	1	0	0	0	0	15	89	208	718
M2	127	135	137	8	1	0	0	0	0	15	89	209	721
M3	127	134	137	8	1	0	0	0	0	15	89	208	719
M4	127	134	137	8	1	0	0	0	0	15	89	208	719
M5	127	134	137	8	1	0	0	0	0	15	89	208	719
Space Cooling													
Hourly R	155	187	239	414	685	894	1062	1018	774	590	258	162	6438
M1	151	187	245	427	696	966	1075	1031	783	620	257	161	6599
M2	149	186	242	422	691	961	1069	1025	778	615	254	158	6550
M3	151	187	244	426	695	965	1073	1029	782	619	256	160	6587
M4	151	188	244	426	695	963	1071	1028	782	619	256	161	6584
M5	151	187	243	425	691	961	1069	1028	781	617	257	161	6571
Building azimuth of 45°													
Space Heating													
Hourly R	136	137	139	6	0	0	0	0	0	15	94	229	756
M1	136	137	134	7	1	0	0	0	0	16	95	231	757
M2	137	138	135	7	1	0	0	0	0	16	95	233	762
M3	136	138	134	7	1	0	0	0	0	16	95	231	758
M4	136	138	134	7	1	0	0	0	0	16	94	230	756
M5	136	138	135	7	1	0	0	0	0	16	95	231	759
Space Cooling													
Hourly R	148	189	258	475	729	938	1122	1083	812	630	248	145	6777
M1	146	191	262	482	737	1007	1132	1090	818	633	246	146	6890
M2	145	189	259	477	732	1003	1126	1085	813	629	244	144	6846
M3	146	191	262	481	735	1006	1131	1089	817	632	245	146	6881
M4	146	191	262	481	734	1005	1129	1089	817	633	246	146	6879
M5	146	190	261	479	732	1003	1126	1088	816	631	246	146	6864
Building azimuth of 90°													
Space Heating													
Hourly R	130	135	137	5	0	0	0	0	0	13	85	214	719
M1	130	135	132	6	1	0	0	0	0	13	85	216	718
M2	131	136	133	6	1	0	0	0	0	14	86	218	725

M3	130	135	132	6	1	0	0	0	0	14	85	216	719
M4	130	135	132	6	1	0	0	0	0	14	85	215	718
M5	130	135	132	6	1	0	0	0	0	14	85	216	719
Space Cooling													
Hourly R	150	197	272	511	750	964	1150	1120	845	661	255	135	7010
M1	149	200	277	517	757	1030	1157	1126	851	664	257	139	7124
M2	147	197	274	512	753	1025	1152	1121	846	660	255	136	7078
M3	149	199	277	516	756	1029	1156	1125	850	663	257	138	7115
M4	150	200	277	517	755	1027	1154	1126	850	664	258	139	7117
M5	149	199	275	514	753	1025	1152	1124	849	662	257	139	7098

Table C-3: Monthly cooling and heating energy consumption of HVAC system (kWh), new vintage in Houston, roof tilt angle of 26.6°

	Jan	Feb	Mar	Apr	May	Jun	Jul	Aug	Sep	Oct	Nov	Dec	Total
Building azimuth of zero degree													
Space Heating													
Hourly R	58	73	74	2	0	0	0	0	0	4	38	106	355
M1	61	72	70	2	0	0	0	0	0	4	39	108	356
M2	61	72	71	2	0	0	0	0	0	4	39	108	357
M3	61	72	71	2	0	0	0	0	0	4	39	108	357
M4	61	72	70	2	0	0	0	0	0	4	39	107	355
M5	61	72	71	2	0	0	0	0	0	4	39	108	357
Space Cooling													
Hourly R	116	139	184	311	512	705	785	762	577	460	193	113	4857
M1	117	141	189	316	516	709	790	766	583	466	194	115	4902
M2	115	139	186	312	513	706	785	762	580	462	192	112	4864
M3	116	141	188	315	515	708	789	765	583	465	193	114	4892
M4	117	141	188	315	514	707	787	765	583	465	194	115	4891
M5	117	140	187	314	513	706	785	764	582	464	194	115	4881
Building azimuth of 45°													
Space Heating													
Hourly R	66	76	74	1	0	0	0	0	0	5	42	121	385
M1	67	75	70	1	0	0	0	0	0	5	42	122	382
M2	68	76	71	1	0	0	0	0	0	5	42	123	386
M3	67	75	70	1	0	0	0	0	0	5	42	122	382
M4	67	75	70	1	0	0	0	0	0	5	42	122	382
M5	67	75	71	1	0	0	0	0	0	5	42	122	383
Space Cooling													
Hourly R	114	143	196	346	537	731	823	802	600	469	186	106	5053
M1	113	143	198	351	542	736	829	806	604	471	186	106	5085
M2	111	142	196	348	539	733	825	802	601	468	185	105	5055
M3	113	143	197	350	541	736	828	805	603	470	186	106	5078
M4	113	143	198	350	540	734	826	805	603	470	187	107	5076
M5	113	143	197	349	539	733	825	804	602	469	186	106	5065
Building azimuth of 90°													
Space Heating													
Hourly R	62	74	74	1	0	0	0	0	0	3	39	111	364
M1	64	74	69	1	0	0	0	0	0	3	40	115	366
M2	65	75	70	1	0	0	0	0	0	3	40	116	370

M3	64	75	69	1	0	0	0	0	0	3	40	116	368
M4	64	75	69	1	0	0	0	0	0	3	39	115	366
M5	64	75	70	1	0	0	0	0	0	3	40	115	368
Space Cooling													
Hourly R	118	146	205	369	551	748	843	827	619	486	193	101	5206
M1	114	146	208	372	554	752	847	830	623	489	194	99	5228
M2	111	145	205	369	551	748	842	826	619	486	192	97	5191
M3	113	146	207	371	553	751	846	829	622	488	193	98	5217
M4	114	147	207	371	552	750	844	829	622	489	194	99	5217
M5	114	146	206	370	551	748	842	828	621	488	194	99	5207

Table C-4: Monthly cooling and heating energy consumption of HVAC system (kWh), new vintage in Houston, roof tilt angle of 45°

	Jan	Feb	Mar	Apr	May	Jun	Jul	Aug	Sep	Oct	Nov	Dec	Total
Building azimuth of zero degree													
Space Heating													
Hourly R	58	72	74	2	0	0	0	0	0	4	38	104	352
M1	60	71	70	1	0	0	0	0	0	4	38	106	350
M2	60	72	71	2	0	0	0	0	0	4	38	106	353
M3	60	72	70	2	0	0	0	0	0	4	38	106	352
M4	60	72	70	1	0	0	0	0	0	4	38	106	351
M5	60	72	71	2	0	0	0	0	0	4	38	106	353
Space Cooling													
Hourly R	118	140	183	305	507	699	778	755	574	461	195	117	4832
M1	117	140	186	313	514	706	786	763	581	464	195	116	4881
M2	115	139	184	310	510	703	782	759	578	461	193	114	4848
M3	116	140	186	312	513	705	785	762	581	463	194	116	4873
M4	117	140	186	312	511	704	784	762	581	463	195	116	4871
M5	117	139	186	311	510	703	782	761	580	462	195	116	4862
Building azimuth of 45°													
Space Heating													
Hourly R	64	74	74	0	0	0	0	0	0	4	41	118	375
M1	66	75	70	1	0	0	0	0	0	4	41	120	377
M2	67	75	71	1	0	0	0	0	0	4	41	121	380
M3	66	75	70	1	0	0	0	0	0	4	41	120	377
M4	66	75	70	1	0	0	0	0	0	4	41	120	377
M5	66	75	70	1	0	0	0	0	0	4	41	120	377
Space Cooling													
Hourly R	114	143	195	344	534	728	818	798	599	468	188	108	5037
M1	113	143	197	349	540	734	826	803	603	471	186	107	5072
M2	111	142	195	346	537	731	822	800	600	468	185	105	5042
M3	112	143	197	348	539	733	825	802	602	470	186	106	5063
M4	113	143	197	348	538	732	824	803	602	470	187	107	5064
M5	113	143	196	347	537	731	822	802	601	469	186	107	5054
Building azimuth of 90°													
Space Heating													
Hourly R	62	73	73	1	0	0	0	0	0	3	39	111	362
M1	63	74	69	1	0	0	0	0	0	3	39	113	362
M2	63	74	70	1	0	0	0	0	0	3	39	114	364

M3	63	74	69	1	0	0	0	0	0	3	39	113	362
M4	63	74	69	1	0	0	0	0	0	3	39	113	362
M5	63	74	69	1	0	0	0	0	0	3	39	113	362
Space Cooling													
Hourly R	113	145	204	366	548	745	840	824	619	487	193	98	5182
M1	114	147	207	371	553	750	845	829	623	490	195	99	5223
M2	111	145	204	368	550	747	841	825	620	487	193	97	5188
M3	113	146	207	370	552	749	844	828	622	489	194	99	5213
M4	114	146	207	371	551	748	843	828	622	489	195	100	5214
M5	114	145	206	369	550	747	841	827	621	489	195	99	5203

Table C-5: Monthly cooling and heating energy consumption of HVAC system (kWh), old vintage in Sacramento, roof tilt angle of 26.6°

	Jan	Feb	Mar	Apr	May	Jun	Jul	Aug	Sep	Oct	Nov	Dec	Total
Building azimuth of zero degree													
Space Heating													
Hourly R	605	452	189	101	58	2	0	2	9	99	264	546	2327
M1	605	450	185	98	56	2	0	1	7	99	263	547	2313
M2	608	452	187	100	58	2	0	1	8	100	265	550	2331
M3	606	450	186	98	57	2	0	1	7	100	263	548	2318
M4	605	450	186	98	57	2	0	1	7	100	263	547	2316
M5	605	451	186	99	58	2	0	1	7	100	263	547	2319
Space Cooling													
Hourly R	12	10	159	235	322	550	604	569	430	212	64	12	3151
M1	12	11	167	244	330	554	614	571	440	217	65	12	3237
M2	10	10	163	238	324	547	607	565	435	213	62	10	3184
M3	12	11	166	243	329	552	612	570	439	216	64	11	3225
M4	12	11	166	243	327	550	610	570	439	217	66	12	3223
M5	12	11	165	241	324	547	607	568	437	215	65	12	3204
	Jan	Feb	Mar	Apr	May	Jun	Jul	Aug	Sep	Oct	Nov	Dec	Total
Building azimuth of 45°													
Space Heating													
Hourly R	616	465	186	83	41	1	0	1	6	103	286	564	2352
M1	617	463	185	81	40	1	0	0	5	103	285	564	2344
M2	619	465	187	83	42	1	0	0	5	104	287	567	2360
M3	617	464	185	82	41	1	0	0	5	103	286	565	2349
M4	616	464	185	81	41	1	0	0	5	103	285	564	2345
M5	617	464	185	82	42	1	0	0	5	103	285	564	2348
Space Cooling													
Hourly R	13	12	169	276	392	635	690	644	464	213	61	12	3581
M1	13	14	173	283	402	638	700	641	465	215	62	12	3618
M2	12	12	169	278	396	632	693	635	460	212	60	11	3570
M3	13	13	172	282	401	637	698	639	464	214	62	11	3606
M4	13	13	172	283	398	635	696	640	464	215	62	12	3603
M5	13	13	171	281	396	632	693	638	463	213	62	12	3587
	Jan	Feb	Mar	Apr	May	Jun	Jul	Aug	Sep	Oct	Nov	Dec	Total
Building azimuth of 90°													
Space Heating													
Hourly R	624	460	178	77	38	0	0	0	3	96	280	578	2334
M1	625	458	177	76	38	0	0	0	3	96	279	576	2328
M2	627	461	179	77	39	0	0	0	3	97	281	579	2343

M3	625	459	177	76	38	0	0	0	3	96	280	577	2331
M4	624	458	177	76	39	0	0	0	3	96	278	576	2327
M5	625	460	178	76	39	0	0	0	3	96	279	576	2332
Space Cooling													
Hourly R	6	9	189	317	434	670	731	690	500	227	46	2	3821
M1	6	9	192	323	441	680	741	687	501	229	49	3	3861
M2	5	8	188	317	435	673	734	681	496	226	46	3	3812
M3	6	8	192	321	440	678	739	685	500	228	47	3	3847
M4	6	9	192	322	438	676	737	686	500	229	49	3	3847
M5	6	8	190	320	435	673	735	684	499	227	49	3	3829

Table C-6: Monthly cooling and heating energy consumption of HVAC system (kWh), old vintage in Sacramento, roof tilt angle of 45°

	Jan	Feb	Mar	Apr	May	Jun	Jul	Aug	Sep	Oct	Nov	Dec	Total
Building azimuth of zero degree													
Space Heating													
Hourly R	600	447	184	101	59	2	0	1	8	97	258	538	2295
M1	600	446	184	98	56	2	0	1	7	98	258	539	2289
M2	602	449	186	99	57	2	0	1	7	98	259	542	2302
M3	601	447	184	98	56	2	0	1	7	98	258	539	2291
M4	600	447	184	98	57	2	0	1	7	98	257	538	2289
M5	600	448	185	98	57	2	0	1	7	98	258	539	2293
Space Cooling													
Hourly R	12	10	159	235	322	550	604	541	430	212	64	12	3151
M1	12	11	167	244	330	554	614	571	440	217	65	12	3237
M2	10	10	163	238	324	547	607	565	435	213	62	10	3184
M3	12	11	166	243	329	552	612	570	439	216	64	11	3225
M4	12	11	166	243	327	550	610	570	439	217	66	12	3223
M5	12	11	165	241	324	547	607	568	437	215	65	12	3204
	Jan	Feb	Mar	Apr	May	Jun	Jul	Aug	Sep	Oct	Nov	Dec	Total
Building azimuth of 45°													
Space Heating													
Hourly R	616	465	186	83	41	1	0	1	6	103	286	564	2352
M1	617	463	185	81	40	1	0	0	5	103	285	564	2344
M2	619	465	187	83	42	1	0	0	5	104	287	567	2360
M3	617	464	185	82	41	1	0	0	5	103	286	565	2349
M4	616	464	185	81	41	1	0	0	5	103	285	564	2345
M5	617	464	185	82	42	1	0	0	5	103	285	564	2348
Space Cooling													
Hourly R	14	12	166	273	386	629	681	639	462	213	62	12	3549
M1	13	13	170	279	397	634	695	637	464	215	62	12	3591
M2	12	12	167	275	391	628	689	632	459	211	60	11	3547
M3	13	13	170	278	395	632	693	636	463	214	61	11	3579
M4	13	13	170	279	393	630	691	636	463	214	62	12	3576
M5	13	12	169	277	391	628	689	634	462	213	62	12	3562
	Jan	Feb	Mar	Apr	May	Jun	Jul	Aug	Sep	Oct	Nov	Dec	Total
Building azimuth of 90°													
Space Heating													
Hourly R	621	459	175	74	38	0	0	0	3	94	275	573	2312
M1	621	455	174	73	38	0	0	0	3	93	274	572	2303
M2	623	459	176	75	39	0	0	0	3	94	275	575	2319

M3	622	456	174	74	38	0	0	0	3	93	274	573	2307
M4	621	456	174	74	38	0	0	0	3	93	273	571	2303
M5	621	457	175	74	38	0	0	0	3	93	274	572	2307
Space Cooling													
Hourly R	6	8	187	315	431	675	727	688	499	227	46	2	3811
M1	5	8	191	321	439	677	738	686	502	229	48	3	3847
M2	5	8	188	316	433	671	733	680	497	226	46	3	3806
M3	5	8	191	320	438	676	737	685	500	228	48	3	3839
M4	6	8	191	320	436	674	735	685	501	229	48	3	3836
M5	5	8	189	319	433	671	733	683	499	228	48	3	3819

Table C-7: Monthly cooling and heating energy consumption of HVAC system (kWh), New vintage in Sacramento, roof tilt angle of 26.6°

	Jan	Feb	Mar	Apr	May	Jun	Jul	Aug	Sep	Oct	Nov	Dec	Total
Building azimuth of zero degree													
Space Heating													
Hourly R	414	307	107	46	21	0	0	0	3	38	154	364	1454
M1	413	303	104	44	19	0	0	0	1	38	153	365	1440
M2	415	306	106	44	20	0	0	0	1	39	154	368	1453
M3	414	304	105	44	19	0	0	0	1	38	153	366	1444
M4	413	303	105	44	20	0	0	0	1	38	152	365	1441
M5	413	304	105	44	20	0	0	0	1	38	153	365	1443
Space Cooling													
Hourly R	4	4	114	167	237	412	457	429	327	161	40	2	2354
M1	4	5	119	174	242	416	461	432	334	163	40	3	2393
M2	4	5	117	170	238	411	456	427	331	161	39	2	2361
M3	4	5	119	173	241	415	460	431	334	162	40	3	2387
M4	4	5	119	173	240	413	459	431	334	163	41	3	2385
M5	4	5	118	172	238	411	457	430	333	162	40	3	2373
	Jan	Feb	Mar	Apr	May	Jun	Jul	Aug	Sep	Oct	Nov	Dec	Total
Building azimuth of 45°													
Space Heating													
Hourly R	422	317	108	34	14	0	0	0	3	41	170	379	1488
M1	422	314	107	32	12	0	0	0	0	41	168	378	1474
M2	424	317	109	33	13	0	0	0	0	42	170	381	1489
M3	422	315	107	32	12	0	0	0	0	41	169	379	1477
M4	421	314	107	32	12	0	0	0	0	41	168	378	1473
M5	422	315	108	33	13	0	0	0	0	41	168	378	1478
Space Cooling													
Hourly R	6	7	121	198	285	472	514	481	350	159	37	3	2633
M1	5	6	124	201	291	474	520	482	354	160	38	4	2659
M2	5	6	121	198	287	470	515	478	350	158	36	3	2627
M3	5	6	123	201	290	473	518	481	353	160	37	4	2651
M4	5	6	123	201	289	472	517	481	354	160	38	4	2650
M5	5	6	122	200	287	470	515	480	352	159	38	4	2638
	Jan	Feb	Mar	Apr	May	Jun	Jul	Aug	Sep	Oct	Nov	Dec	Total
Building azimuth of 90°													
Space Heating													
Hourly R	433	319	102	30	13	0	0	0	0	36	168	396	1497
M1	432	315	101	28	11	0	0	0	0	36	167	393	1483

M2	434	319	103	29	11	0	0	0	0	37	168	396	1497
M3	433	316	102	29	11	0	0	0	0	36	167	394	1488
M4	432	315	101	28	11	0	0	0	0	36	167	392	1482
M5	432	317	102	29	11	0	0	0	0	36	167	393	1487
Space Cooling													
Hourly R	2	4	131	223	312	501	545	510	374	168	25	1	2796
M1	2	5	134	226	318	502	550	512	378	169	27	1	2824
M2	1	4	131	223	314	497	545	507	374	166	26	1	2789
M3	2	4	134	225	317	501	548	510	377	168	27	1	2814
M4	2	4	134	225	315	500	547	511	377	168	28	1	2812
M5	2	4	133	224	314	497	545	509	376	167	27	1	2799

Table C-8: Monthly cooling and heating energy consumption of HVAC system (kWh), New vintage in Sacramento, roof tilt angle of 45°

	Jan	Feb	Mar	Apr	May	Jun	Jul	Aug	Sep	Oct	Nov	Dec	Total
Building azimuth of zero degree													
Space Heating													
Hourly R	414	307	107	46	21	0	0	0	3	38	154	364	1454
M1	413	303	104	44	19	0	0	0	1	38	153	365	1440
M2	415	306	106	44	20	0	0	0	1	39	154	368	1453
M3	414	304	105	44	19	0	0	0	1	38	153	366	1444
M4	413	303	105	44	20	0	0	0	1	38	152	365	1441
M5	413	304	105	44	20	0	0	0	1	38	153	365	1443
Space Cooling													
Hourly R	5	5	115	162	229	403	448	421	327	162	42	2	2321
M1	5	5	117	170	238	411	456	427	331	162	42	3	2367
M2	4	5	114	166	234	406	452	423	329	160	41	3	2337
M3	4	5	116	169	237	410	455	426	331	161	42	3	2359
M4	5	5	116	169	236	408	454	426	331	161	42	3	2356
M5	5	5	116	168	234	406	452	425	330	161	42	3	2347
	Jan	Feb	Mar	Apr	May	Jun	Jul	Aug	Sep	Oct	Nov	Dec	Total
Building azimuth of 45°													
Space Heating													
Hourly R	420	314	107	33	14	0	0	0	0	40	165	375	1468
M1	419	313	106	31	12	0	0	0	0	40	165	374	1460
M2	420	315	107	33	13	0	0	0	0	40	166	376	1470
M3	419	313	106	32	12	0	0	0	0	40	166	374	1462
M4	418	312	106	32	12	0	0	0	0	40	165	373	1458
M5	419	314	107	32	13	0	0	0	0	40	165	374	1464
Space Cooling													
Hourly R	6	6	120	195	281	468	509	477	351	159	37	3	2612
M1	5	6	122	199	288	471	516	479	354	160	38	4	2642
M2	5	6	120	196	284	467	511	475	350	158	36	3	2611
M3	5	6	122	199	287	470	515	478	353	159	37	3	2634
M4	6	6	122	199	286	469	513	478	353	160	38	4	2634
M5	5	6	121	198	284	467	511	477	352	159	38	4	2622
	Jan	Feb	Mar	Apr	May	Jun	Jul	Aug	Sep	Oct	Nov	Dec	Total
Building azimuth of 90°													
Space Heating													
Hourly R	432	317	100	29	13	0	0	0	0	36	165	393	1485
M1	430	314	100	27	11	0	0	0	0	35	164	390	1471
M2	432	317	101	28	11	0	0	0	0	36	165	393	1483

M3	431	315	100	28	11	0	0	0	0	35	164	391	1475
M4	429	315	100	28	11	0	0	0	0	35	163	390	1471
M5	430	315	100	28	11	0	0	0	0	35	164	390	1473
Space Cooling													
Hourly R	2	4	131	221	311	498	542	509	374	169	26	1	2788
M1	1	4	135	225	317	500	548	511	378	170	27	1	2817
M2	1	4	132	222	313	496	543	506	375	168	26	1	2787
M3	1	4	134	225	315	499	547	510	377	169	27	1	2809
M4	2	4	134	225	314	498	545	510	377	170	28	1	2808
M5	1	4	133	224	313	496	543	509	376	169	27	1	2796

Table C-9: Monthly cooling and heating energy consumption of HVAC system (kWh), Old vintage in Montréal, roof tilt angle of 26.6°

	Jan	Feb	Mar	Apr	May	Jun	Jul	Aug	Sep	Oct	Nov	Dec	Total
Building azimuth of zero degree													
Space Heating													
Hourly R	3600	3025	1938	720	221	29	6	14	109	461	1109	2936	14168
M1	3605	3019	1930	711	216	27	7	13	108	457	1110	2939	14142
M2	3610	3026	1938	716	219	28	7	14	109	460	1113	2943	14183
M3	3607	3021	1932	713	217	27	7	13	109	458	1111	2940	14155
M4	3604	3020	1932	712	218	28	7	13	108	457	1110	2938	14147
M5	3605	3023	1934	714	219	28	7	13	109	458	1110	2939	14159
Space Cooling													
Hourly R	0	0	1	19	106	266	360	336	137	12	0	0	1237
M1	0	0	1	21	114	271	376	345	141	12	0	0	1281
M2	0	0	1	20	110	266	370	340	138	11	0	0	1256
M3	0	0	1	21	113	270	374	344	140	12	0	0	1275
M4	0	0	1	21	112	269	373	344	140	12	0	0	1272
M5	0	0	1	20	110	266	370	342	139	11	0	0	1259
	Jan	Feb	Mar	Apr	May	Jun	Jul	Aug	Sep	Oct	Nov	Dec	Total
Building azimuth of 45°													
Space Heating													
Hourly R	3644	3049	1918	688	197	21	4	10	101	472	1131	2969	14204
M1	3646	3043	1914	684	192	20	4	9	101	468	1132	2971	14184
M2	3651	3051	1922	689	194	21	5	9	103	471	1134	2975	14225
M3	3648	3046	1916	685	192	19	4	9	101	469	1133	2972	14194
M4	3645	3045	1915	685	193	20	4	9	101	469	1131	2970	14187
M5	3646	3047	1918	687	194	21	5	9	102	469	1132	2971	14201
Space Cooling													
Hourly R	0	0	2	28	141	320	421	392	153	14	0	0	1471
M1	0	0	2	29	147	324	432	396	153	14	0	0	1497
M2	0	0	2	28	143	319	427	392	149	13	0	0	1473
M3	0	0	2	29	147	323	431	395	152	14	0	0	1493
M4	0	0	2	29	145	321	430	395	153	14	0	0	1489
M5	0	0	2	28	143	319	428	394	152	14	0	0	1480
	Jan	Feb	Mar	Apr	May	Jun	Jul	Aug	Sep	Oct	Nov	Dec	Total
Building azimuth of 90°													
Space Heating													
Hourly R	3657	3040	1869	671	189	19	3	9	91	466	1134	2987	14135
M1	3658	3033	1866	667	184	18	4	8	91	463	1132	2985	14109
M2	3663	3041	1874	671	187	19	4	8	93	467	1135	2989	14151

M3	3659	3035	1868	668	185	18	4	8	92	464	1133	2986	14120
M4	3657	3034	1868	668	186	18	4	8	92	464	1132	2984	14115
M5	3658	3037	1870	669	187	19	4	8	92	465	1132	2985	14126
Space Cooling													
Hourly R	0	0	2	36	168	358	453	426	178	9	0	0	1630
M1	0	0	2	38	174	361	467	431	180	9	0	0	1662
M2	0	0	2	36	170	355	462	426	176	8	0	0	1635
M3	0	0	2	38	173	359	466	430	179	9	0	0	1656
M4	0	0	2	38	172	358	464	430	179	9	0	0	1652
M5	0	0	2	37	170	355	462	429	178	9	0	0	1642

Table C-10: Monthly cooling and heating energy consumption of HVAC system (kWh), Old vintage in Montréal, roof tilt angle of 45°

	Jan	Feb	Mar	Apr	May	Jun	Jul	Aug	Sep	Oct	Nov	Dec	Total
Building azimuth of zero degree													
Space Heating													
Hourly R	3583	3007	1927	719	223	28	6	13	107	453	1129	2921	14116
M1	3588	3007	1932	713	216	26	6	13	106	452	1102	2924	14085
M2	3594	3014	1939	717	218	27	6	13	108	454	1104	2929	14123
M3	3590	3008	1934	714	216	26	6	13	106	453	1102	2925	14093
M4	3587	3008	1933	714	217	27	6	13	106	452	1101	2923	14087
M5	3588	3010	1935	715	218	27	6	13	107	453	1102	2924	14098
Space Cooling													
Hourly R	0	0	1	18	102	257	353	331	135	14	0	0	1211
M1	0	0	1	19	108	266	371	340	137	12	0	0	1254
M2	0	0	1	18	105	262	366	336	135	11	0	0	1233
M3	0	0	1	19	108	265	370	339	136	12	0	0	1250
M4	0	0	1	19	107	264	368	339	137	12	0	0	1247
M5	0	0	1	19	105	262	366	338	136	12	0	0	1239
	Jan	Feb	Mar	Apr	May	Jun	Jul	Aug	Sep	Oct	Nov	Dec	Total
Building azimuth of 45°													
Space Heating													
Hourly R	3632	3039	1912	687	195	21	3	9	97	463	1122	2951	14131
M1	3635	3035	1911	683	191	19	4	9	99	464	1126	2960	14136
M2	3640	3042	1919	687	192	20	4	9	100	467	1128	2964	14172
M3	3637	3037	1913	684	191	19	4	9	99	465	1126	2961	14145
M4	3634	3036	1913	684	192	19	4	9	99	465	1125	2959	14139
M5	3635	3038	1915	685	192	20	4	9	99	465	1126	2960	14148
Space Cooling													
Hourly R	0	0	2	26	137	316	428	399	159	15	0	0	1482
M1	0	0	2	28	144	321	430	395	153	14	0	0	1487
M2	0	0	2	26	140	316	425	391	149	13	0	0	1462
M3	0	0	2	27	143	320	429	394	152	13	0	0	1480
M4	0	0	2	28	142	318	427	394	152	14	0	0	1477
M5	0	0	2	27	140	316	425	393	151	13	0	0	1467
	Jan	Feb	Mar	Apr	May	Jun	Jul	Aug	Sep	Oct	Nov	Dec	Total
Building azimuth of 90°													
Space Heating													
Hourly R	3649	3035	1865	668	186	18	3	8	86	457	1123	2971	14069
M1	3649	3026	1862	665	182	18	3	8	89	459	1127	2977	14065
M2	3654	3033	1870	668	185	18	3	8	91	462	1130	2981	14103

M3	3650	3028	1864	666	183	18	3	8	90	460	1128	2978	14076
M4	3648	3027	1864	666	184	18	3	8	89	460	1127	2976	14070
M5	3649	3029	1866	667	185	18	3	8	90	461	1127	2977	14080
Space Cooling													
Hourly R	0	0	2	36	166	356	461	435	185	11	0	0	1652
M1	0	0	2	37	174	360	466	432	180	9	0	0	1660
M2	0	0	2	35	169	354	461	427	176	8	0	0	1632
M3	0	0	2	37	172	358	465	431	179	9	0	0	1653
M4	0	0	2	37	171	356	463	431	179	9	0	0	1648
M5	0	0	2	36	169	354	461	430	178	9	0	0	1639

Table C-11: Monthly cooling and heating energy consumption of HVAC system (kWh), New vintage in Montréal, roof tilt angle of 26.6°

	Jan	Feb	Mar	Apr	May	Jun	Jul	Aug	Sep	Oct	Nov	Dec	Total
Building azimuth of zero degree													
Space Heating													
Hourly R	2682	2282	1335	486	140	10	1	4	56	294	732	2090	10112
M1	2685	2276	1330	481	135	9	1	4	55	291	733	2092	10092
M2	2689	2280	1335	485	137	10	1	4	56	293	735	2095	10120
M3	2686	2277	1332	482	135	10	1	4	55	291	734	2092	10099
M4	2685	2276	1331	482	136	10	1	4	55	291	733	2091	10095
M5	2685	2278	1333	483	137	10	1	4	56	292	733	2092	10104
Space Cooling													
Hourly R	0	0	0	11	75	200	283	262	107	6	0	0	944
M1	0	0	0	13	80	203	289	269	109	6	0	0	969
M2	0	0	0	12	77	200	285	266	106	6	0	0	952
M3	0	0	0	12	79	202	288	268	108	6	0	0	963
M4	0	0	0	12	78	201	287	268	108	6	0	0	960
M5	0	0	0	12	77	200	285	267	107	6	0	0	954
	Jan	Feb	Mar	Apr	May	Jun	Jul	Aug	Sep	Oct	Nov	Dec	Total
Building azimuth of 45°													
Space Heating													
Hourly R	2716	2304	1327	470	125	6	0	2	53	303	748	2117	10171
M1	2719	2297	1325	467	120	5	0	2	53	300	748	2118	10154
M2	2723	2302	1330	470	122	6	0	2	54	301	750	2120	10180
M3	2720	2298	1326	468	121	5	0	2	53	300	749	2118	10160
M4	2718	2298	1326	468	122	6	0	2	53	300	748	2117	10158
M5	2719	2300	1328	469	122	6	0	2	54	300	748	2118	10166
Space Cooling													
Hourly R	0	0	1	17	98	237	320	300	117	7	0	0	1097
M1	0	0	1	18	102	240	327	305	119	8	0	0	1120
M2	0	0	1	17	100	236	324	301	117	7	0	0	1103
M3	0	0	1	17	102	239	327	304	118	7	0	0	1115
M4	0	0	1	18	101	237	326	304	118	8	0	0	1113
M5	0	0	1	17	100	236	324	303	118	7	0	0	1106
	Jan	Feb	Mar	Apr	May	Jun	Jul	Aug	Sep	Oct	Nov	Dec	Total
Building azimuth of 90°													
Space Heating													
Hourly R	2736	2307	1306	463	118	4	0	2	47	305	754	2134	10176
M1	2737	2298	1305	461	115	5	0	2	47	301	753	2134	10158
M2	2741	2303	1310	464	116	5	0	2	48	305	755	2137	10186

M3	2738	2300	1306	462	115	5	0	2	47	302	753	2135	10165
M4	2736	2299	1306	462	116	5	0	2	47	302	752	2133	10160
M5	2737	2301	1307	462	116	5	0	2	47	303	753	2134	10167
Space Cooling													
Hourly R	0	0	1	20	113	260	343	323	132	7	0	0	1199
M1	0	0	1	22	118	263	350	327	133	5	0	0	1219
M2	0	0	1	21	115	260	347	324	131	5	0	0	1204
M3	0	0	1	22	118	262	349	326	133	5	0	0	1216
M4	0	0	1	22	117	261	348	326	133	5	0	0	1213
M5	0	0	1	21	115	260	347	325	132	5	0	0	1206

Table C-12: Monthly cooling and heating energy consumption of HVAC system (kWh), New vintage in Montréal, roof tilt angle of 45°

	Jan	Feb	Mar	Apr	May	Jun	Jul	Aug	Sep	Oct	Nov	Dec	Total
Building azimuth of zero degree													
Space Heating													
Hourly R	2669	2269	1327	488	140	10	1	2	55	288	727	2079	10055
M1	2673	2267	1331	484	135	9	1	4	55	288	728	2082	10057
M2	2678	2272	1336	486	137	10	1	4	55	290	729	2085	10083
M3	2674	2268	1332	484	136	9	1	4	55	288	728	2082	10061
M4	2672	2267	1332	484	136	9	1	4	55	288	728	2081	10057
M5	2673	2269	1333	485	137	10	1	4	55	289	728	2082	10066
Space Cooling													
Hourly R	0	0	0	10	72	194	277	260	106	7	0	0	926
M1	0	0	0	12	77	200	286	266	106	6	0	0	953
M2	0	0	0	11	74	197	283	263	105	6	0	0	939
M3	0	0	0	11	76	199	285	265	106	6	0	0	948
M4	0	0	0	11	76	198	284	266	106	6	0	0	947
M5	0	0	0	11	74	197	283	265	106	6	0	0	942
	Jan	Feb	Mar	Apr	May	Jun	Jul	Aug	Sep	Oct	Nov	Dec	Total
Building azimuth of 45°													
Space Heating													
Hourly R	2709	2296	1323	469	124	6	0	2	50	297	741	2104	10121
M1	2711	2291	1323	467	120	5	0	2	52	297	745	2110	10123
M2	2715	2296	1328	469	122	5	0	2	53	299	746	2113	10148
M3	2712	2292	1324	468	120	5	0	2	52	297	745	2111	10128
M4	2711	2292	1324	468	121	5	0	2	52	297	745	2109	10126
M5	2711	2294	1325	468	122	5	0	2	52	298	745	2110	10132
Space Cooling													
Hourly R	0	0	0	16	96	235	325	305	122	8	0	0	1107
M1	0	0	1	17	101	238	326	304	119	7	0	0	1113
M2	0	0	0	16	98	234	323	301	116	7	0	0	1095
M3	0	0	1	16	100	237	325	303	118	7	0	0	1107
M4	0	0	1	16	99	235	324	303	118	7	0	0	1103
M5	0	0	0	16	98	234	323	302	117	7	0	0	1097
	Jan	Feb	Mar	Apr	May	Jun	Jul	Aug	Sep	Oct	Nov	Dec	Total
Building azimuth of 90°													
Space Heating													
Hourly R	2730	2302	1304	462	116	4	0	2	44	299	746	2124	10133
M1	2731	2293	1302	460	114	4	0	2	46	299	750	2128	10129
M2	2735	2298	1308	462	115	5	0	2	46	302	751	2131	10155

M3	2732	2295	1304	461	114	4	0	2	46	300	750	2129	10137
M4	2731	2294	1304	461	115	5	0	2	46	300	750	2128	10136
M5	2731	2296	1305	461	115	5	0	2	46	301	750	2128	10140
Space Cooling													
Hourly R	0	0	0	20	112	260	349	329	138	5	0	0	1213
M1	0	0	1	21	118	263	350	327	134	5	0	0	1219
M2	0	0	1	20	115	259	346	324	132	4	0	0	1201
M3	0	0	1	21	117	262	349	327	134	5	0	0	1216
M4	0	0	1	21	116	261	348	327	134	5	0	0	1213
M5	0	0	1	21	115	259	346	326	133	5	0	0	1206

Appendix D. The FORTRAN code for finding hourly projected incident solar angle on the roofing surface

The developed algorithm to find a solar angles respect to the Directional Reflective roofing surface is shown below. This code calls the calculated azimuth and altitude angles which is define as PHSUND and THSNHR from DOE-2. Knowing the roof tilt angle (t1) and roof azimuth angle (t3), the code calculate the projected incident angle on the surface perpendicular to the DRM corrugations.

```
real t1      !rotation about x axis (~tilt)
real t2      !rotation about y axis
real t3      !rotation about z axis (~azimuth)
real R(3,3)  !rotation matrix
real z       !zenith angle
real s       !azimuth angle
real b
real c
real o       !incident angle
real ol

t1 = -22.62
t2 = 0
t3 = 180
t1 = t1*pi/180
t2 = t2*pi/180
t3 = t3*pi/180

R(1,1) = cos(t2)*cos(t3)
R(1,2) = -cos(t1)*sin(t3)+sin(t1)*sin(t2)*cos(t3)
R(1,3) = sin(t3)*sin(t1)+cos(t3)*sin(t2)*cos(t1)
R(2,1) = cos(t2)*sin(t3)
R(2,2) = sin(t1)*sin(t2)*sin(t3)+cos(t1)*cos(t3)
R(2,3) = -cos(t3)*sin(t1)+cos(t1)*sin(t2)*sin(t3)
R(3,1) = -sin(t2)
R(3,2) = cos(t2)*sin(t1)
R(3,3) = cos(t2)*cos(t1)

fbw = (cos(N)/cos(M)+1-((cos(N)/cos(M))^2+1-2*(cos(N)/cos(M))*cos(M+N))^0.5)/2
fwb = (cos(M)/cos(N)+1-((cos(M)/cos(N))^2+1-2*(cos(M)/cos(N))*cos(M+N))^0.5)/2
fsw = 1-fbw;
```

```
fsb = 1-fwb;
```

```
z1 = 90-PHSUND
```

```
s1 = THSNHR
```

```
z = z1*pi/180
```

```
s = s1*pi/180
```

```
ni(1)=sin(z)*sin(s)
```

```
ni(2)=sin(z)*cos(s)
```

```
ni(3)=cos(z)
```

```
ni_new(1)=ni(1)*R(1,1)+ni(2)*R(2,1)+ni(3)*R(3,1)
```

```
ni_new(2)=ni(1)*R(1,2)+ni(2)*R(2,2)+ni(3)*R(3,2)
```

```
ni_new(3)=ni(1)*R(1,3)+ni(2)*R(2,3)+ni(3)*R(3,3)
```

```
c=ni_new(3)/norm(ni_new,2)
```

```
b=ni_new(2)/norm(ni_new,2)
```

```
o=atan(b/c)
```

```
o1=atan(c/b)
```

```
end
```